SCHOOL OF CIVIL ENGINEERING

JOINT HIGHWAY RESEARCH PROJECT

JHRP-78-16

EFFECT OF BINDER CHARACTERISTICS ON TENSILE PROPERTIES OF BITUMINOUS MIXTURES

N. P. Khosla

PURDUE UNIVERSITY
INDIANA STATE HIGHWAY COMMISSION

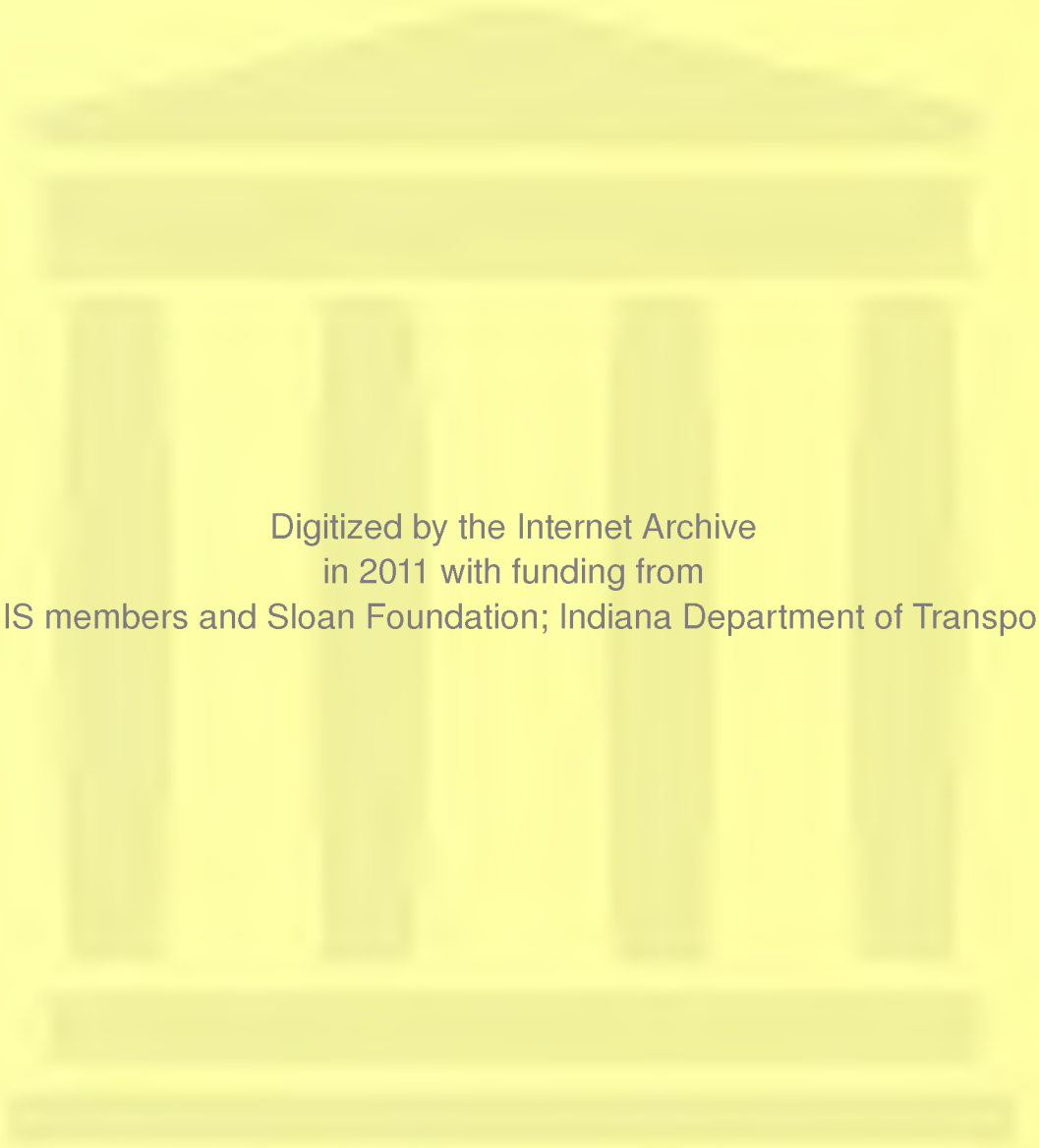

78-16

Final Report

EFFECT OF BINDER CHARACTERISTICS ON TENSILE PROPERTIES OF BITUMINOUS MIXTURES

TO: Harold L. Michael, Director
Joint Highway Research Project

August 2, 1978

File: 2-4-31

FROM: W. H. Goetz, Research Engineer
Joint Highway Research Project

Project: C-36-6EE

The attached Final Report is submitted on the JHRP research study of similar title. This Report is titled "Effect of Binder Characteristics on Tensile Properties of Bituminous Mixtures" and has been authored by N. P. Khosla, Graduate Instructor in Research on our staff under the direction of Professor W. H. Goetz.

Experiments for this study were conducted on bituminous mixtures in indirect tension to measure tensile properties for use as indices of performance of mixtures containing conventional and modified binders with varying temperature susceptible characteristics. The tests were monitored using acoustic emission techniques. Parameters for this study included a single aggregate of 100 percent crushed limestone at one gradation, four binder types, eight temperatures and variable testing speed. Regression equations are presented that relate significant variables to limiting strain and limiting stiffness.

The Report is presented to the Board as fulfillment of the objectives of the Study.

Respectfully submitted,

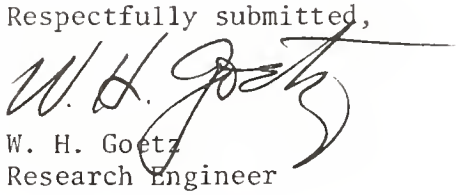

W. H. Goetz
Research Engineer

WHG:ms

cc: A. G. Altschaeffl
W. L. Dolch
R. L. Eskew
G. D. Gibson
W. H. Goetz
M. J. Gutzwiller
G. K. Hallock
D. E. Hancher
K. R. Hoover
J. F. McLaughlin
R. F. Marsh
R. D. Miles
P. L. Owens
G. T. Satterly
C. F. Scholer
M. B. Scott
K. C. Sinha
C. A. Venable
L. E. Wood
E. J. Yoder
S. R. Yoder

Final Report

EFFECT OF BINDER CHARACTERISTICS ON TENSILE PROPERTIES OF BITUMINOUS MIXTURES

by

Narendra P. Khosla
Graduate Instructor in Research

Joint Highway Research Project

Project No.: C-36-6EE

File No.: 2-4-31

Prepared as Part of an Investigation

Conducted by

Joint Highway Research Project
Engineering Experiment Station
Purdue University

in cooperation with the

Indiana State Highway Commission

Purdue University
West Lafayette, Indiana
August 2, 1978

ACKNOWLEDGMENTS

The author is indebted to his major advisor, Professor W.H. Goetz, for the advice, guidance, constructive criticism and continuous encouragement through the course of this study and for his critical review of the manuscript.

The interest and time to time suggestions and advice of Dr. M.E. Harr and Dr. E.C. Ting are gratefully appreciated.

The time and effort rendered by Dr. V.L. Anderson in statistical experimental designs and data analysis is gratefully acknowledged.

The author wishes to thank Dr. W.L. Dolch for his suggestions and help in viscosity measurements at low temperatures.

Sincere thanks are extended to K.E. McConnaughay, Inc., for supplying the asphalt emulsion.

Grateful acknowledgement also is made to the authorities of the Joint Highway Research Project, Engineering Experiment Station, Purdue University for the sponsorship of this research.

Sincere thanks are extended to the authorities at the Central Road Research Institute, New Delhi, India, for the opportunity of pursuing the advanced degree.

Finally, special thanks go to the author's wife whose support, patience and understanding greatly aided the successful completion of this investigation.

TABLE OF CONTENTS

LIST OF TABLES

LIST OF FIGURES

ABSTRACT

Khosla, Narendra Prakash. Ph.D., Purdue University, August 1978. Effect of Binder Characteristics on Tensile Properties of Bituminous Mixtures. Major Professor: Prof. W.H. Goetz.

Experiments were conducted on bituminous mixtures in indirect tension to measure tensile properties for use as indices of performance of mixtures containing conventional and modified binders with varying temperature susceptible characteristics. The tests were monitored using acoustic emission techniques.

Parameters for this study included a single aggregate of 100 percent crushed limestone at one gradation, four binder types, eight temperatures and variable testing speed. Regression equations are presented that relate significant variables to limiting strain and limiting stiffness.

The most significant parameter in this study is temperature. A small change in temperature changes the limiting stiffness much more than a similar change in any other parameter.

The results provide strong evidence to support the postulation that the tensile characteristics of a bituminous mixture can be controlled by controlling the characteristics of the binder. In this regard, this study utilized three binders with nominal penetration grade of 85-100 and a soft

binder with nominal penetration grade of 200-250. The three 85-100 penetration grade binders included a highly temperature susceptible asphalt, high float emulsion residue and a partially air blown asphalt. The results show that the soft asphalt, in comparison with all of the 85-100 penetration materials, produces lower stiffness values of mixtures at low as well as at high temperatures. Emulsification and air blowing are shown to be very viable methods for improving the temperature susceptibility of asphalt binders. As compared to the highly temperature susceptible Canadian asphalt, the high float emulsion residue made from the Canadian asphalt and the partially air blown asphalt produce lower stiffness values at lower temperatures and higher stiffness values at higher temperatures, thus providing improved performance at both ends of the temperature scale.

Acoustic emission experiments showed that this technique is very effective in detecting crack initiation and is useful in defining the failure point of bituminous mixtures at low temperatures.

INTRODUCTION

Cracking of bituminous pavements is a serious problem in some areas today. It impairs the riding quality and shortens the life of the pavement thus causing increased maintenance and cost. Often, beginning as a hairline crack, it slowly extends and permits the ingress of water which in turn weakens the underlying layers, thus manifesting itself in the form of a structural failure. This form of cracking has been reported in several studies (1, 2, 3, 4, 5, 6). The importance of the problem has further been demonstrated (7, 8, 9) by an attempt to define, observe, and correlate factors involved therein. One of the possible solutions is to use softer grades of asphalt and modified binders. Failure by cracking will occur when fatigue capacity of the material is exceeded or when strains within the bituminous concrete exceed some limiting value (10). Considerable information is available that enables prediction of stress field within the mixture from imposed load or non-load conditions. Strain response for the bitumen to imposed load can be calculated by using stiffness values generated by Van der Poel (11, 12).

Purpose

Pavlovich (16), using a direct tension test, has established failure criteria for different conditions of time

of loading, temperature as encountered during pavement service, and common mixture variables. The purpose of this study was to determine the degree to which the tensile characteristics of a bituminous mixture can be controlled by controlling the characteristics of the binder. In view of the complexity of direct tension testing and the large quantities of materials necessary to perform these tests, there appeared to be a need for some quick and easy means for such an evaluation. The tensile splitting test is considered to be promising, and is a comparatively easy and efficient test method with which to obtain the tensile characteristics of bituminous mixtures. From a theoretical point of view, the tensile splitting test is not considered to be as sound as the uniaxial tension test. For the tensile splitting test, a biaxial state of stress is assumed in the calculations. However, because of the wide application and popularity of the tensile splitting test, an attempt was made to correlate the tensile properties as measured by the direct tension test and the tensile splitting test.

Discs, sawed from the test specimens used in the previous study which utilized direct tension (16), were subjected to the tensile splitting test. These tests were performed on specimens more than one year old. It was determined that due to the age hardening of the discs and due to the degradation of aggregate during compaction of the specimens, one to one correlation did not exist between the tensile properties as measured by these two tests. However, enough

correlation did exist to conclude that the tensile splitting test measures essentially the same properties as the direct tension test. Moreover, unlike the tensile splitting test, direct tension test results had a large variability. In fact the coefficient of variation of the data in direct tension test was so high that it limited the evaluation of some important factors in the study. It was against this background that the tension splitting test was selected to determine tensile properties for use as the indices of performance of mixtures containing conventional and modified binders with varying temperature susceptible characteristics.

Review of Literature

Cracking of bituminous pavements has been an active topic in the literature since 1930. Rader (17), Brown and Steinbaugh (18), and Busby and Rader (19) demcnstrated that the mixture should be designed to have a high modulus of rupture to ensure adequate tensile strength but a low stiffness modulus so that the mixture would be pliable rather than stiff and brittle. It has been emphasized (17, 19, 20, 21, 22) that the use of softer asphalt cements is a practical solution to the problem of low temperature cracking.

Hughes and Faris (23) conducted laboratory tests to determine deformation as related to asphalt types. Asphalt beams were made to fail in flexture and it was concluded that, for fast rates of loading, asphalt source, asphalt penetration and temperature (below $32^{o}F$) have little effect on deformation

or failure strain. Slow rate of loading, however, showed that source, penetration, and temperature have an effect. Van der Poel's work on asphalts (11, 12) generally supported these findings but it was not until later that mixtures were considered. Vallerga (24) emphasized the need for relating properties of bituminous mixtures to performance. Hass and Anderson (25) have mentioned the following as the possible causes of low temperature cracking:

1. An exceeding of the tensile strength or tolerable strain of the bituminous surface by thermally induced stresses and strains,

   a) Without considering traffic loads

   b) Added to traffic imposed stresses and strains

2. Freezing, cracking and shrinkage of the subgrade, and propagation through the bituminous surface.

In a discussion for a symposium (7) on non-traffic load associated cracking of asphalt pavements, Hills and O'Brien provided theoretical equations to predict the temperature at which cracking will occur for a bituminous mixture of given tensile strength and stiffness modulus. Methods have been developed (13, 14, 15) to predict stresses and, hence, strains for viscoelastic systems.

The literature contains many suggestions and methods to determine stiffness of a bituminous material and from this to predict bituminous mixture stiffness. Van der Poel's method (12) has further been modified by Heukelom and Klomp (26) and Heukelom (27) to estimate mixture stiffness

as a function of bitumen stiffness from the following semi-empirical formula,

$$S_{mix}\ (t,\ T) = S_{bit}\ (t,\ T) \left[1 + \frac{2.5}{n} \frac{C_v}{1-C_v} \right]^n$$

where,

S_{mix} = stiffness modulus of the mixture at a particular loading time, t and temperature, T

S_{bit} = stiffness modulus of the binder for the same t and T

$$n = 0.83 \log \frac{4 \times 10^5}{S_{bit}}$$

C_v = volume concentration of the aggregate,

$$= \frac{\text{Volume of aggregate}}{\text{Volume of (aggregate + asphalt)}}$$

$$= \frac{100 - \%\ \text{VMA}}{100 - \%\ \text{Air Voids}}$$

VMA = Voids in mineral aggregate

The equation was originally developed for well-compacted mixtures with about 3% air voids and C_v values between about 0.7 and 0.9. For mixtures with air voids greater than 3%, a "corrected" C_v value, developed by Van Draat and Sommer (28) should be substituted.

McLeod (22) has suggested a method for finding stiffness of bitumens and bituminous mixtures. The major difference between the McLeod and the Heukelom method is that McLeod has presented an alternative to the P.I. (penetration index) method of measuring temperature susceptibility of an asphalt. McLeod utilizes a Pen-Vis number which is based on the

relationship between viscosity at 275°F and penetration at 77°F. Lefebvre (29) has further investigated this approach, using a number of Canadian asphalts and has recommended its use. McLeod (22) has suggested norms for eliminating low temperature pavement cracking and has proposed the limiting stiffness value of 5×10^5 psi at -40°F.

Pavlovich (16) presented the effect of mixture variables and environmental and loading conditions on limiting tensile strain values as determined by a direct tension test. High, as well as low viscosity asphalt cements within nominal penetration grades of 60 - 70, 85 - 100, and 120 - 150 were used as binders in this study; one of the striking findings was that within the range investigated, asphalt type had no effect on limiting strain.

Use of acoustic emission signals has been recommended (31, 32, 33, 34) as a technique to detect cracking in metals. Pavlovich (16) has further demonstrated its usefulness in the determination of the failure of bituminous mixtures at low temperatures. Acoustic emission signals are detected by a lead-zirconate-titanate (PZT) transducer. The signals go to a pair of counters that record the rate of emission and total counts. Plastic limit or yield point is accompanied by a peaking of count rate followed by immediate decay. Failure by fracture is indicated by a sharp increase in cumulative counts. Unfortunately, the use of acoustic emission is restricted to low temperatures, because at elevated temperatures the transmitted wave is of so low a

strength that it can not activate the transducer. However, cracking is mainly associated with low temperature conditions, and hence this equipment is useful in this region.

Research Approach

One of the main reasons for bituminous pavement cracking is its brittle behavior at low temperatures and/or when the asphalt it contains becomes hard. Hardening of the asphalt with aging or use of asphalt with low penetration increases the susceptibility of the pavement to low temperature strain and cracking. Thus, bituminous paving mixtures exhibit both plastic and elastic properties depending on the temperature to which the mixtures are subjected and the viscosity of the asphalt in the mixture. In the past, stability has been a major concern, and rightly so. However, the importance of stability often has been overemphasized, and asphaltic mixtures of excessively high stability have been used. Where high stability was obtained at the expense of pliancy by using low penetration asphalt, mixtures frequently demonstrated poor resistance to cracking, especially at low temperature. At present, specifications do not include any criteria for controlling the behavior of asphaltic mixtures at low temperature. Resistance to cracking should be a consideration in designing paving mixtures.

The above review of the literature indicates that for satisfactory performance bituminous mixtures at low temperatures should have adequate tensile strength and a low stiffness

modulus, accompanied with high failure strain. The need for low temperature design modifications in some regions was recognized by Rader (17) over 35 years ago. The appreciation of this need seems to have lain relatively dormant until the markedly increased attention given to low temperature cracking during the last few years. Although, based on field studies in Canada, it has been postulated that the use of softer grades of binders can be a potential solution to the problem of low temperature cracking, a laboratory evaluation to corroborate and quantify this effect has had little attention.

The performance of a bituminous mixture is dependent upon the type and character of its constituents. Tensile strength, strain at failure, and stiffness are temperature dependent characteristics of a bituminous mixture, and variations in these characteristics are ascribed to the known variations of the asphalt binder. At the low temperature extreme, it is desirable to obtain as low a stiffness as possible. However, this can, in turn, result in too low a stiffness over the medium to high temperature range for fatigue and permanent deformation requirements. Ideally, a mix should have temperature susceptible characteristics that will satisfy both ends of the temperature performance scale. The solution does not lie only in the use of proper grades of binders, but should also involve consideration of temperature susceptible characteristics. Based on this reasoning, a harder grade with low temperature susceptibility perhaps can perform as well at low temperature as a softer grade with high temperature

susceptibility. Also, the harder grade with low temperature susceptibility will result in a better performance of the bituminous mixture at medium to high temperatures. The requirement of better performance of the bituminous mixture thus requires the proper selection of the binder with suitable temperature susceptible characteristics.

Air blowing and emulsification, amongst many, are the feasible means to modify temperature susceptibility of the binders. Emulsification of the base asphalt is a viable method for providing a residue with improved temperature susceptible characteristics. In this regard, the use of high float emulsions has been common in Indiana and elsewhere. The major emphasis of improved temperature susceptible characteristics of the high float emulsions, however, has been on the dividends with respect to stability at high ambient temperatures. The recognition of the impact of their improved temperature susceptibility on low temperature characteristics of bituminous mixtures has remained relatively dormant. Moreover, there has been no attempt to corroborate the benefits accruing from improved temperature susceptibility of high float emulsions by any quantitative laboratory evaluation. It was thus considered plausible to examine the effects of such a modification in the bituminous mixture.

With regard to modification by the use of air-blowing, a recent field study (30) indicates promising potential in this approach. However, it should be borne in mind that if

air-blowing is carried too far, this can result in a serious loss of ductility, and the adhesion between aggregate and asphalt cement may be detrimentally affected. Hence, it was considered worthwhile to evaluate the partially air-blown asphalts as incorporated in the bituminous mixture.

Two test methods for measuring the tensile properties of bituminous mixtures are the following:

1. Direct, uniaxial tension test
2. Tensile splitting test

The direct tension test consists of applying an axial tensile force directly to the specimen and measuring the stress-strain characteristics of the material. Although this test seems simple in theory and principle, serious difficulties have been encountered in its practical application. Besides the difficulties of additional bending stresses due to alignment problems and gripping of the specimen, the test set-up is complex and time consuming and involves large quantities of the materials. The tensile splitting test was developed in 1953 by Carneiro and Barcellos of Brazil and Akazawa of Japan, working independently. This test was developed with a view towards simplicity of specimen preparation and testing procedure. Hveem or Marshall test specimens can be used by loading across a diameter in a compression testing frame. Tensile stresses induced in the direction of a diameter at right angles to the compressive loading eventually result in fracture of the specimen. Horizontal deformation is measured along the face of the specimen, in the direction of the

principal tensile stresses.

Statement of Problem

In light of the foregoing remarks, it was decided that the focus of this study would be to justify the postulation that the stiffness and failure strain of a bituminous mixture can be controlled by controlling the characteristics of the binder. For this purpose, binders with varying characteristics as such, as well as with suitable modifications with regard to their temperature susceptibility, e.g. emulsification and air-blowing, were incorporated into the mixtures.

In view of the practical advantages of the tensile splitting test, it was decided to use this test for the purpose of evaluating the tensile characteristics of the mixtures. The compacted specimens with the above mentioned binders were prepared and subjected to the tensile splitting test and the response was evaluated in terms of stiffness and failure strain as measured by this test.

In conjunction with the above, acoustic emission was used to detect cracking and thus to better define the failure mechanism in bituminous mixtures. In this regard, the load-cumulative count rate was used to define more precisely the limiting strain and limiting load at which failure occurred.

In the sections that follow, this pre-view is amplified to include a detailed description and execution of different facets of this study.

MATERIALS AND MIXTURE PROPERTIES

In this section, the material used for this investigation and their source and properties are presented, and the mixtures and their design are described.

Aggregate

Aggregate for this study consisted of 100 percent crushed limestone obtained from the Erie Stone Company of Huntington, Indiana. This producer is listed as quarry number 58 by the Indiana State Highway Commission (35). Geological setting for this material is the Louisville limestone formation of the Silurian period (36).

Materials for this study originated from quarry stockpiles accepted by the Indiana State Highway Commission Bureau of Materials and Tests. These sources were designated as size Nos. 9 and 14-2. Filler was minus No. 200 screenings from the 14-2 size.

Aggregates were transported to the Purdue Bituminous Materials Laboratory where they were resized to logarithmic sieve series, washed, dried and stored.

The following physical properties were measured in strict conformance with applicable ASTM Standards:

A. Los Angeles Abrasion (percent wear), (ASTM C 131)

Percent wear values in the Los Angeles Abrasion Test

are given below:

Grading	Wear after 100 rev., %	Wear after 500 rev., %
B	9.1	40.2
C	8.9	39.8
D	9.2	40.5

B. Specific Gravity and Absorption (ASTM C 127, C 128)

The specific gravity and absorption values are given below:

Size Fraction	G_{Bulk}	G_{BSSD}	G_{APP}	%ABS.
Coarse Agg.	2.602	2.648	2.725	1.72
Fine Agg.	2.749	2.778	2.831	1.05
Filler	-	-	2.809	-

Binders

Four binders were used for this study. These materials included three asphalt cements and one high float emulsion residue, designated as M1, M2, M3 and M4. The type and identification, nominal penetration, ductility and softening point data for these materials are given below:

Type and Identification	Nominal Penetration, 77°F	Ductility 5cm/min., 77°F	Ductility 1cm/min., 39.2°F	Softening Point (°F)
Canadian asphalt (M1)	85-100	100^+	16	113
Partially air-blown asphalt (M2)	85-100	100^+	8	123
Soft asphalt (M3)	200-250	100^+	100^+	107
HF emulsion residue (M4)	85-100	100^+	15	204

The Canadian asphalt, M1, was provided by Pounder Emulsion, Ltd., Winnepeg, Canada, the partially air-blown asphalt, M2, by Asphalt Materials, Inc., Indianapolis, Indiana, and the soft asphalt, M3, by the American Oil Company of Whiting, Indiana. The high float emulsion, M4, with the Canadian asphalt as the base asphalt, was formulated in and supplied by the K.E. McConnaughay Laboratory, Lafayette, Indiana. All asphalt cements were stored after arrival until used in the experiment in a walk-in refrigerator at a temperature of approximately 23°F (-5°C). Asphalt required for testing or specimen fabrication was chipped from the container at this temperature without removal from the refrigerator. In order to insure uniform quality and avoid any spoilage due to storage, the emulsion was formulated as and when needed for the fabrication of the specimens.

Tests for Physical Properties

A. Penetration

Penetration tests for the binders were performed under loads of 50g., 100 g. and 200g., at temperatures of 39.2°F and 77°F and for periods of 5, 15, 30, 45 and 60 seconds. The data accruing from these tests are given in Table 1 and plotted in Figures 1 and 2. The penetration values for different periods of loading and at different temperatures were used in calculating the viscosity values. The details of penetration - viscosity conversion are given in the section dealing with "viscosity".

TABLE 1

Penetration Values of the Binders

Binder	Penetration (dmm) 5 sec.	15 sec.	30 sec.	45 sec.	60 sec.
			50g., 77°F		
M1	-	-	-	-	-
M2	-	-	-	-	-
M3	170	275	370	445	-
M4	-	-	-	-	-
			100g., 77°F		
M1	105	175	240	285	-
M2	85	130	170	200	-
M3	231	-	-	-	-
M4	80	122	162	190	-
			200g., 39.2°F		
M1	14	19	24	-	29
M2	26	34	39	-	46
M3	31	50	70	-	93
M4	21	27	32	-	38

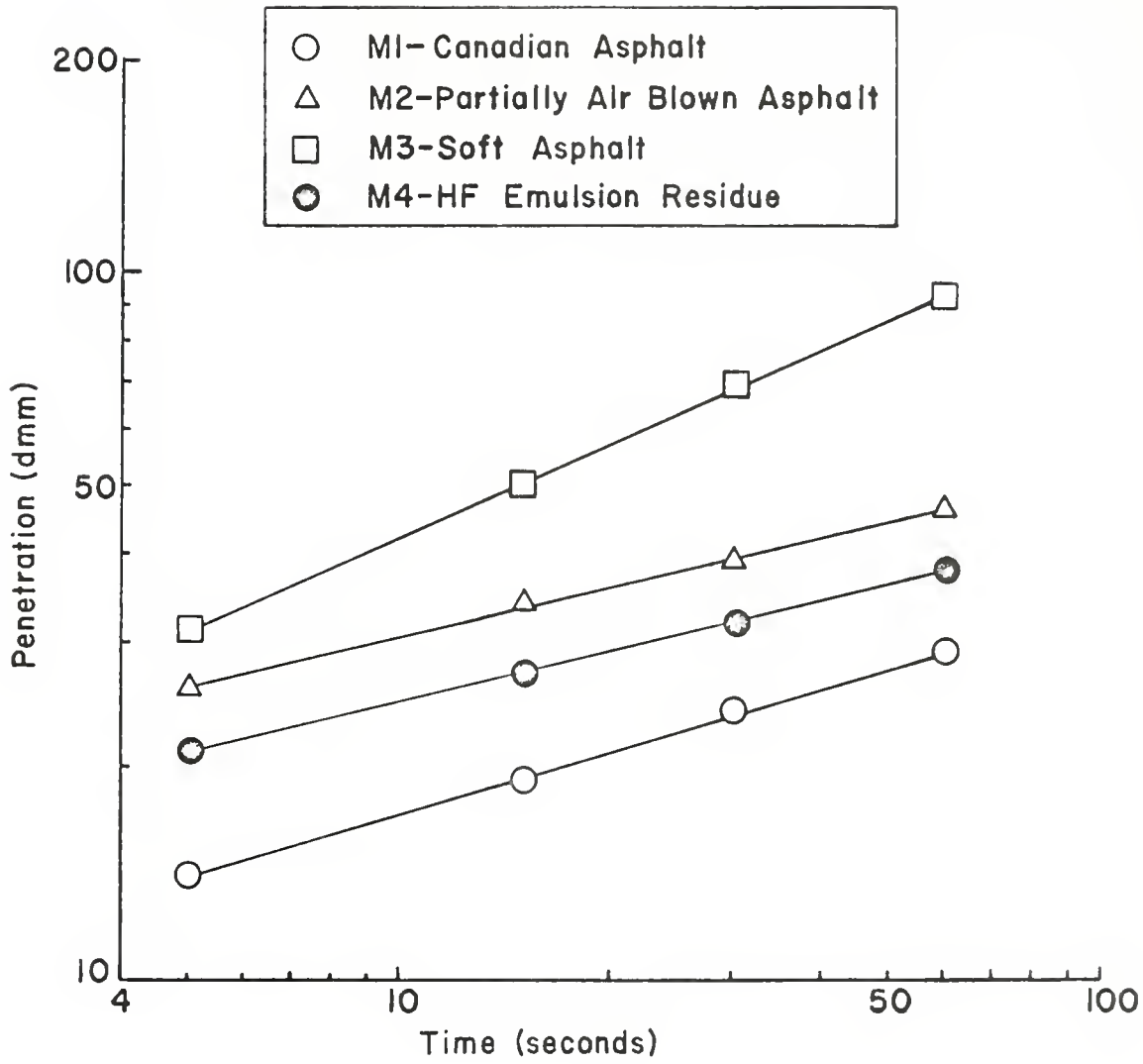

FIGURE 1 PENETRATION VS. TIME AT 39.2° F FOR BINDERS M1, M2, M3, M4

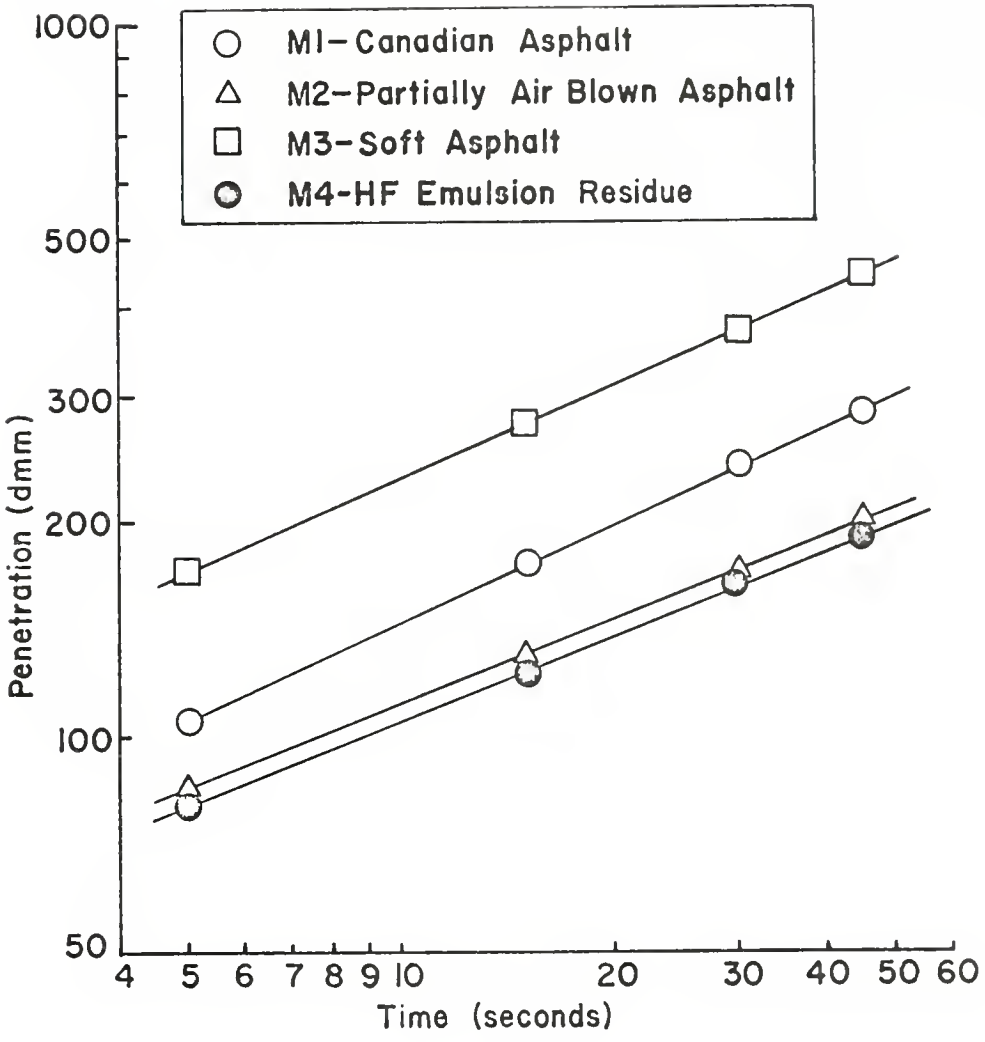

FIGURE 2 PENETRATION VS. TIME AT 77°F FOR BINDERS M1, M2, M3, M4

B. Viscosity

Various means were employed for measuring viscosity at different temperatures. At 39.2°F and 77°F viscosity values were calculated by converting penetration values to viscosity using Pendleton equations. The details of the method of such conversions are given in Appendix A. Absolute viscosity values for the binders at -10°F and 0°F were measured by a Ball Penetrometer. A detailed illustration of this method is given in Appendix B. Absolute viscosity at 140°F was measured by using Asphalt Institute vacuum capillary viscometers. Kinematic viscosity at 275°F for M1, M2 and M3 was measured by Zeitfuchs Cross-Arm viscometers. Kinematic viscosity for M4 could not be measured due to the fact that this material did not flow at 275°F under atmospheric pressure. The measured values of absolute and kinematic viscosities are given in Table 2. Also, see section C under "Temperature Susceptible Characteristics" for additional discussion on measurement of viscosity.

TABLE 2

Viscosity Values of the Binders

Binder	Absolute (Poises)					Kinematic (cSt)
	-10°F	0°F	39.2°F	77°F	140°F	275°F
M1	8.67×10^{10}	1.58×10^{10}	9.8×10^{7}	5.9×10^{5}	430	155
M2	4.45×10^{10}	4.47×10^{9}	2.8×10^{7}	9.5×10^{5}	2350	457
M3	1.78×10^{10}	6.31×10^{9}	1.8×10^{7}	1.3×10^{5}	275	133
M4	2.69×10^{10}	8.41×10^{9}	4.5×10^{7}	1.07×10^{6}	2500	-

Temperature Susceptible Characteristics

The various indices characterizing the temperature susceptibility of the binders are described in this section.

A. Penetration Index

Penetration Index of the binders was calculated according to Pfeiffer and Van Doormal (27). They define the index as:

$$PI = \frac{30}{1+90PTS} - 10$$

where PI = penetration index

PTS = penetration temperature susceptibility

$$= \frac{\log_{10} 800 - \log_{10} P}{T_{R\&B} - T_P}$$

where P = penetration at $77^{\circ}F$ ($25^{\circ}C$) 100 g., 5 seconds

$T_{R\&B}$ = ring and ball softening point in $^{\circ}F$

T_P = temperature where penetration is determined, $77^{\circ}F$ for this case

Penetration indices of -2 to +2 correspond with "normal" residual asphalts whereas indices of less than -2 indicate highly temperature susceptible pitch types and indices above +2 are found for low susceptibility blown materials.

Penetration indices for the binders are shown in Table 3.

TABLE 3

Penetration Indices of Binders

Binder	Pen. @ 77°F	PI
M1	105	-0.62
M2	85	+0.35
M3	231	+1.45
M4	80	+7.55

The penetration index is based on the concept that the penetration of an asphalt at its softening point is 800. This assumption has been questioned by many investigators. The validity of the penetration index is further open to doubt as all the bituminous materials at their softening point are not simple liquids and do not possess the same viscosity. The viscosities of bituminous materials at their ring and ball softening points have been shown (37, 38) to vary from 8000 to 30,000 poises. The fact that the viscosity is not constant at the ring and ball temperature would be expected from a consideration of the physics of the test. To begin with, the ring and ball method combines the principles of a falling ball viscometer and those of the falling coaxial cylinder viscometer since the ball falls through the material and at the same time moves the mass of the binder in a shearing action similar to the falling coaxial cylinder apparatus. Also, the rate of shear varies in the ring and ball method and any

variation in the rate of shear will affect the numerical value of the viscosity for a non-Newtonian liquid. This is particularly true for high float emulsion residues. While it may be argued that most asphalts at the ring and ball temperature are essentially liquids, it is, nevertheless, true that at the start of this test the binder is subjected to shear at temperatures where the viscosity is many times greater than that at the ring and ball temperature and at which the material may possess definite non-Newtonian characteristics.

B. Pen-Vis Number

In view of the shortcomings of penetration index as proposed by Pfeiffer and Van Doormal, McLeod (22) has presented an alternative method of showing the temperature susceptibility of a binder in terms of Pen-Vis number. It is based on the relationship between viscosity at 275°F (or 140°F) and penetration at 77°F. Lefebvre (29) has further investigated this approach, using a number of Canadian asphalts and has recommended its use. Pen-Vis numbers for the binders used in this study are shown in Table 4.

TABLE 4

Binder Pen-Vis Numbers

Binder	Pen @ 77°F	Absolute Viscosity (poises) @ 140°F	Kinematic Viscosity (cSt) @ 275°F	Pen-Vis Number
M1	105	430	155	-1.7
M2	85	2350	457	-0.17
M3	231	275	133	-1.0
M4	80	2500	-	-0.14

C. Viscosity

Many investigators have suggested that the slope of the viscosity vs. temperature curve be used as an index of temperature susceptibility. Above their softening points bituminous materials possess different rheological and colloidal properties than at temperatures below the softening point. Thus, at these two temperature levels, the materials will have different temperature-viscosity relationships and no simple index can be expected to apply over a wide temperature span. The relationship of viscosity to temperature is complicated and confused by the changes in colloidal properties of bituminous materials occurring with changes in temperature. At high temperatures the asphalt cements are essentially sol-type materials possessing Newtonian flow characteristics as shown in Figure 3, while the high float emulsion residue certainly exhibits non-Newtonian characteristics as depicted

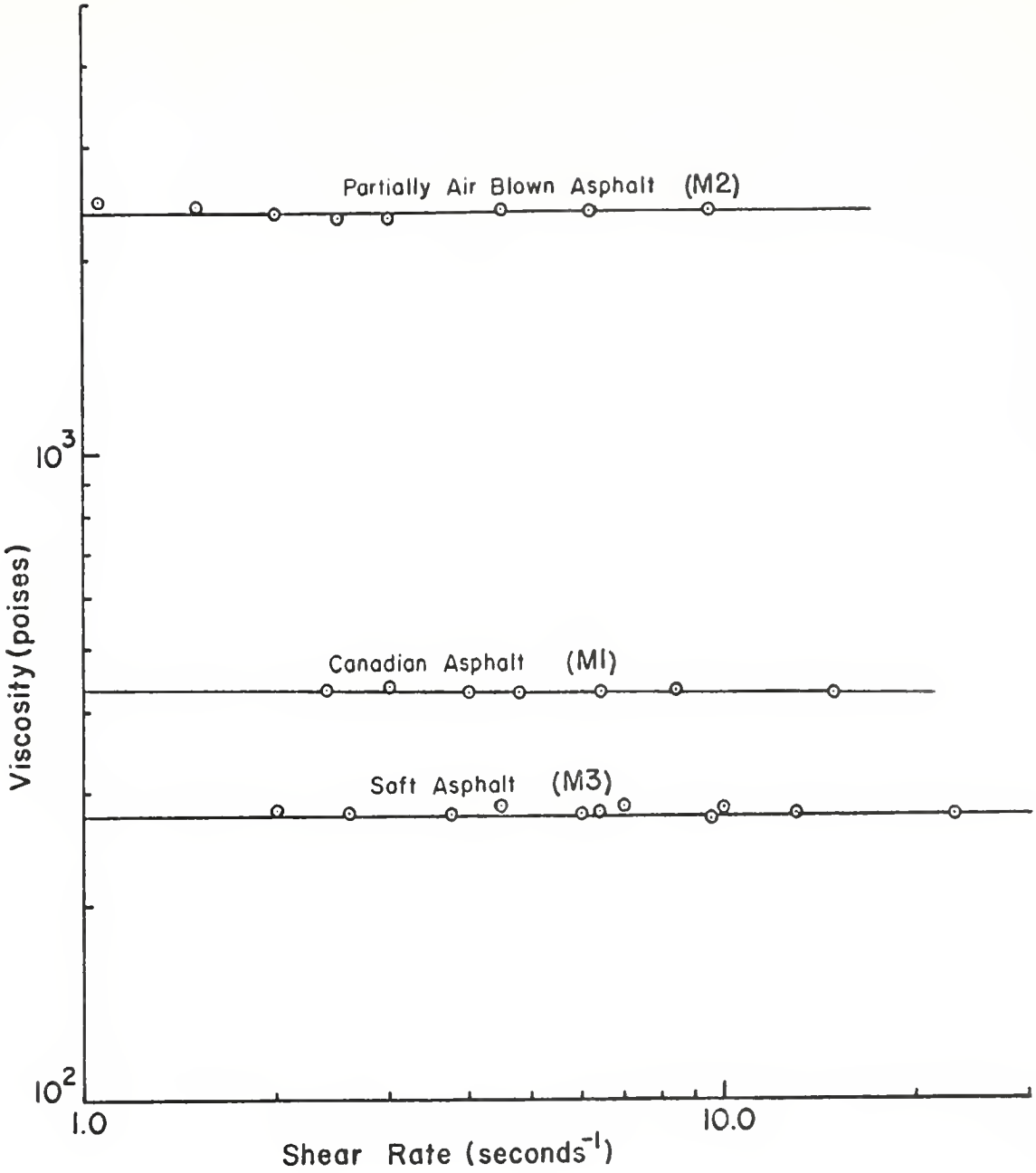

FIGURE 3 VISCOSITY VS. SHEAR RATE AT 140°F FOR ASPHALTS MI, M2, M3

in Figure 4. At lower temperatures all the binders may manifest non-Newtonian flow to varying degrees. The viscosity-temperature curve, as such, can be useful in comparing rheological behavior of the binders. The viscosity-temperature relationships for the binders used in this study are shown in Figure 5.

The viscosity measurements of the asphalt cements at 140°F were made by means of Nos. 50, 100 and 200 Asphalt Institute vacuum capillary viscometers. Shear rates were varied by varying the size of the viscometers and the vacuum, and the corresponding viscosities were measured and reported as shown in Figure 3. In the case of the emulsion residue, a No. 400 Asphalt Institute vacuum capillary viscometer was used to measure viscosity at 140°F and the vacuum was varied to generate different shear rates. In Figure 4 is shown the set of viscosity-shear rate curves for different bulbs in the viscometer tube. As the material is pulled up the viscometer tube, the viscosity, for the same shear rate, decreases. Such intriguing behavior of the high float emulsion residue could be ascribed to its non-Newtonian complex flow as is indicated by its shear susceptibility value (39) of 0.23. The material is sheared to some extent before it reaches the next bulb and owing to its complex flow its behavior in any given bulb largely depends on the preceding shear history.

Simple instruments capable of measuring viscosities of the binders at the required low temperatures are not available and, thus, some indirect methods were employed for this

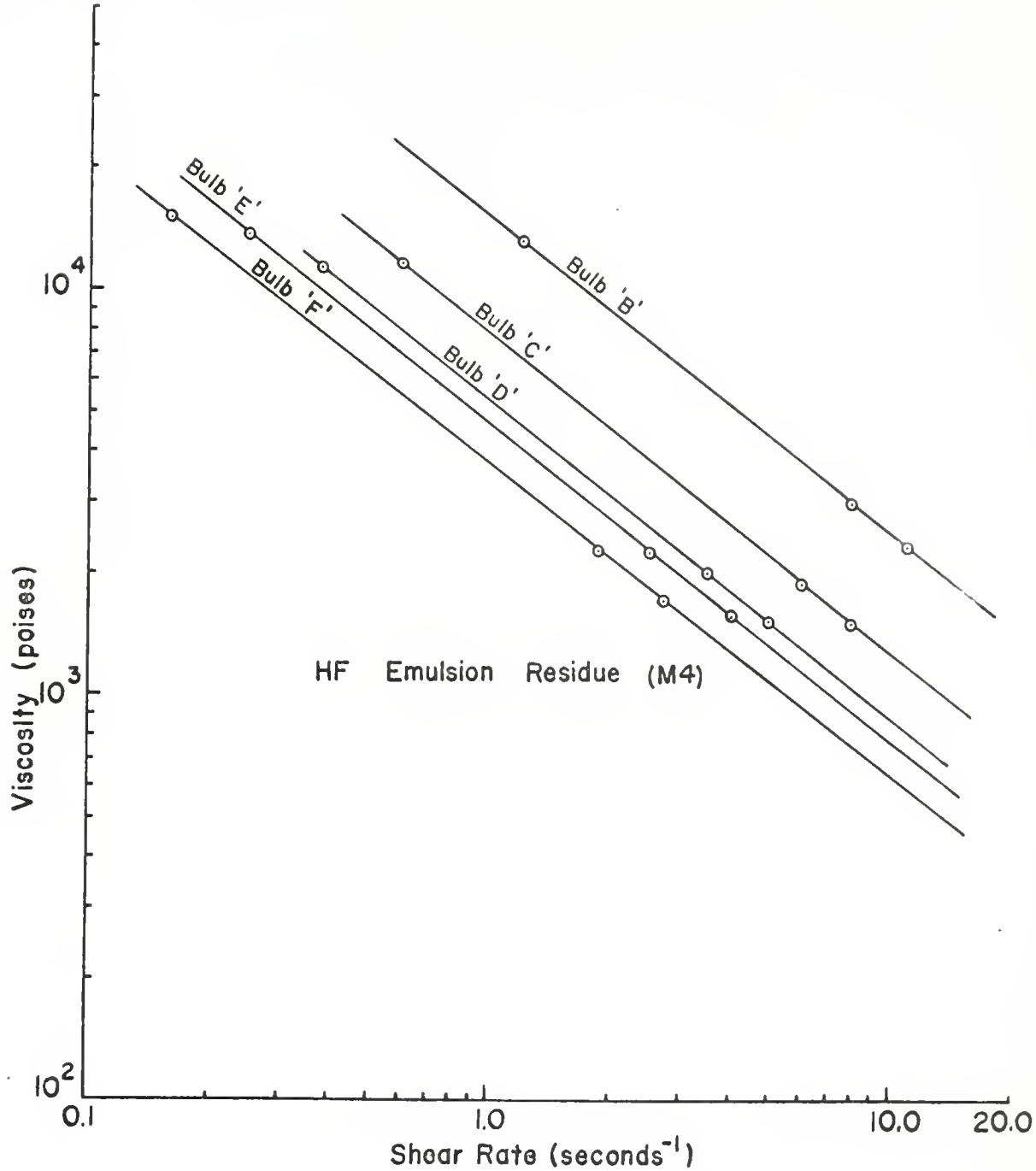

FIGURE 4 VISCOSITY VS. SHEAR RATE AT 140° F FOR EMULSION RESIDUE M4

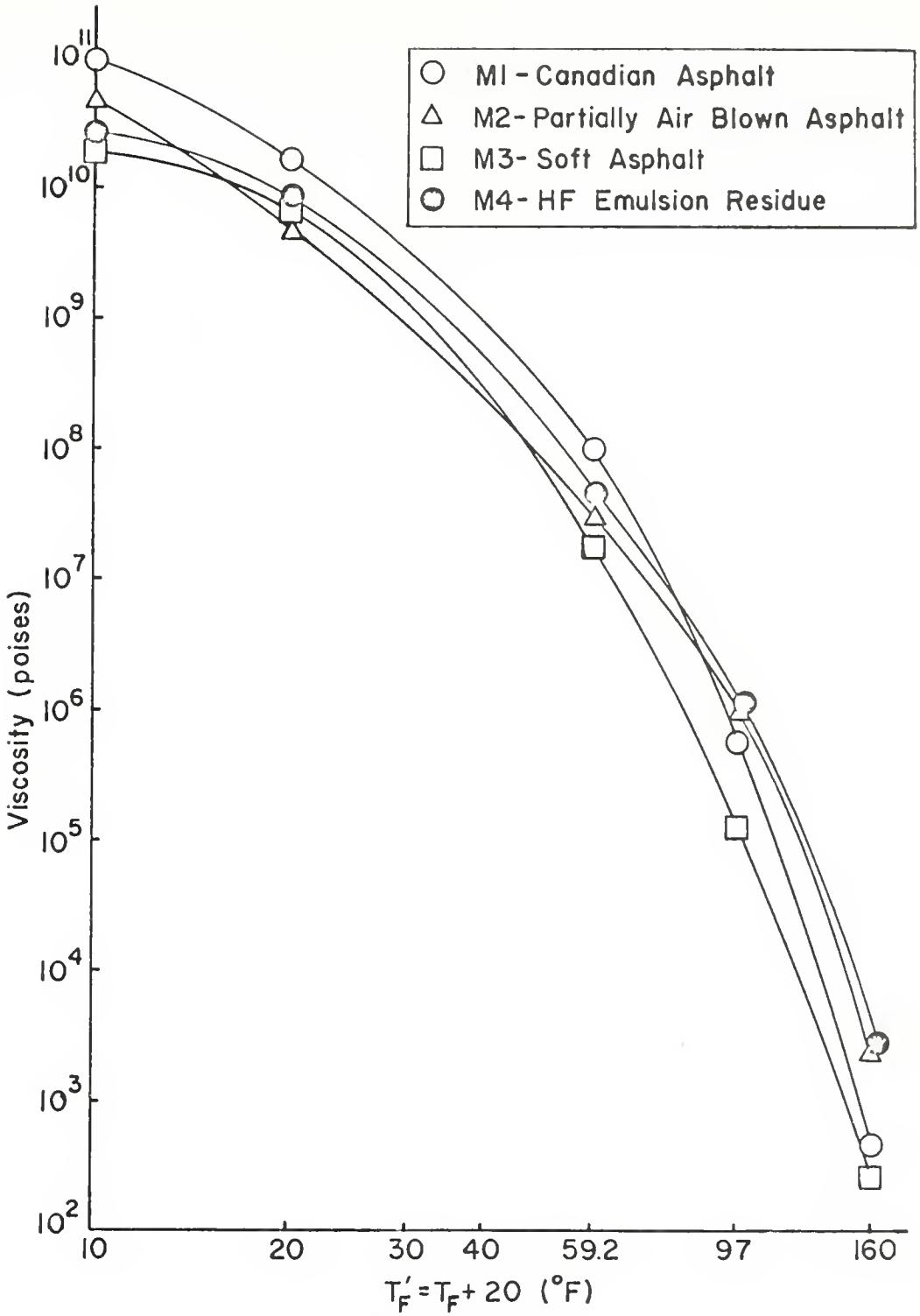

FIGURE 5 VISCOSITY VS. TEMPERATURE FOR BINDERS M1, M2, M3, M4

purpose. The absolute viscosities at 39.2°F and 77°F were calculated by converting penetration readings at recurring intervals using Pendleton equations (40). See Figures 6 and 7.

Mixtures and Mixture Design

One gradation was used with each of the four binders used in this study. The mixture gradation for the experiment and typical Indiana State Highway Commission and Asphalt Institute specifications for comparison are shown in Table 5. The gradation curve is shown in Figure 8. The mixtures were identified in keeping with the designations for binder types.

TABLE 5

Mixture Gradation

Sieve Size	Percent Passing		
	AI IVb	ISHC #9 Surface	Mix
3/4	100	100	100
1/2	80-100	76-92	91
3/8	70-90	46-77	76
4	50-70	32-53	54
8	35-50	24-47	46
16	-	16-40	37
30	18-29	6-26	25
50	13-23	2-17	16
100	8-16	0-7	7
200	4-10	0-4	4

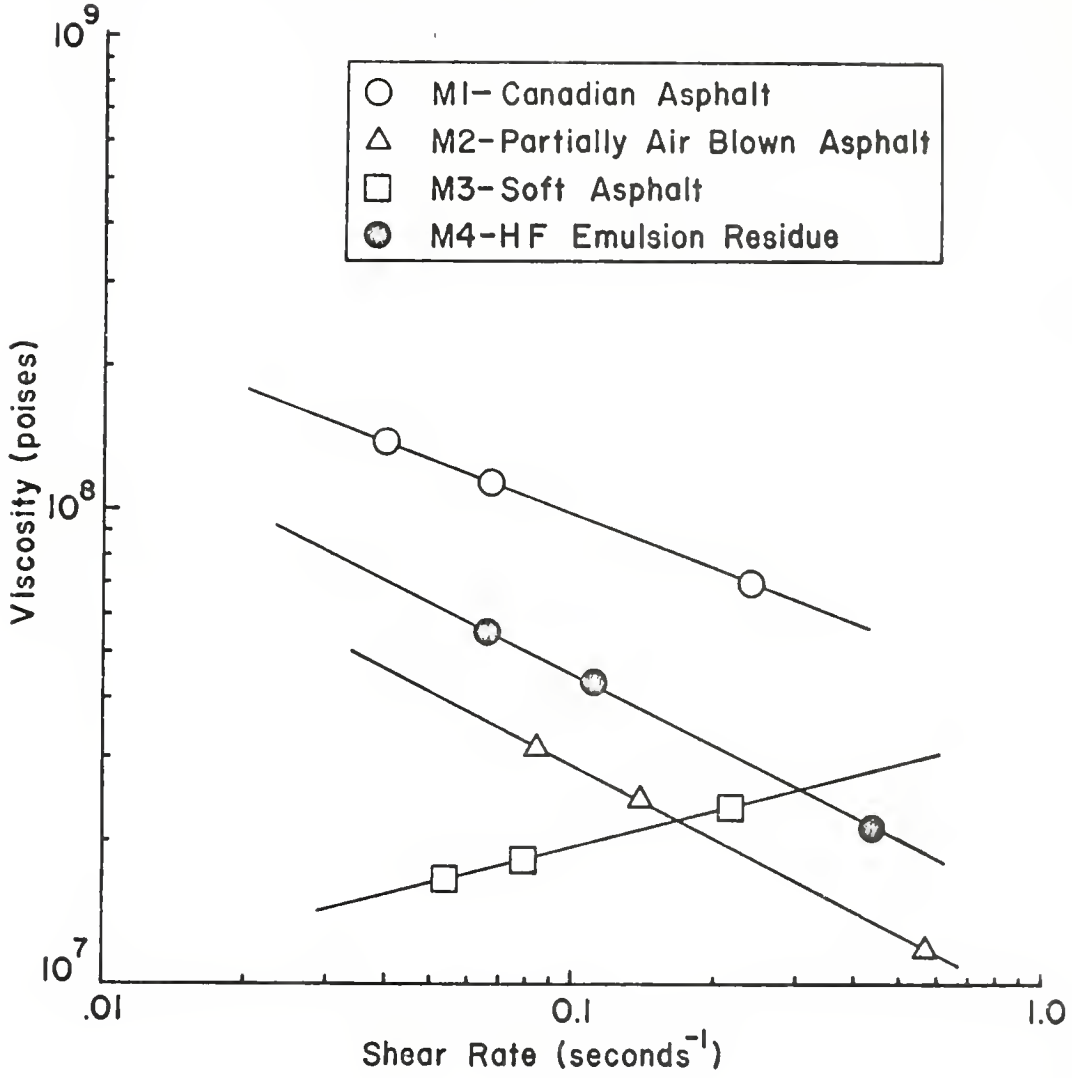

FIGURE 6 VISCOSITY VS. SHEAR RATE AT 39.2°F FOR BINDERS M1, M2, M3, M4

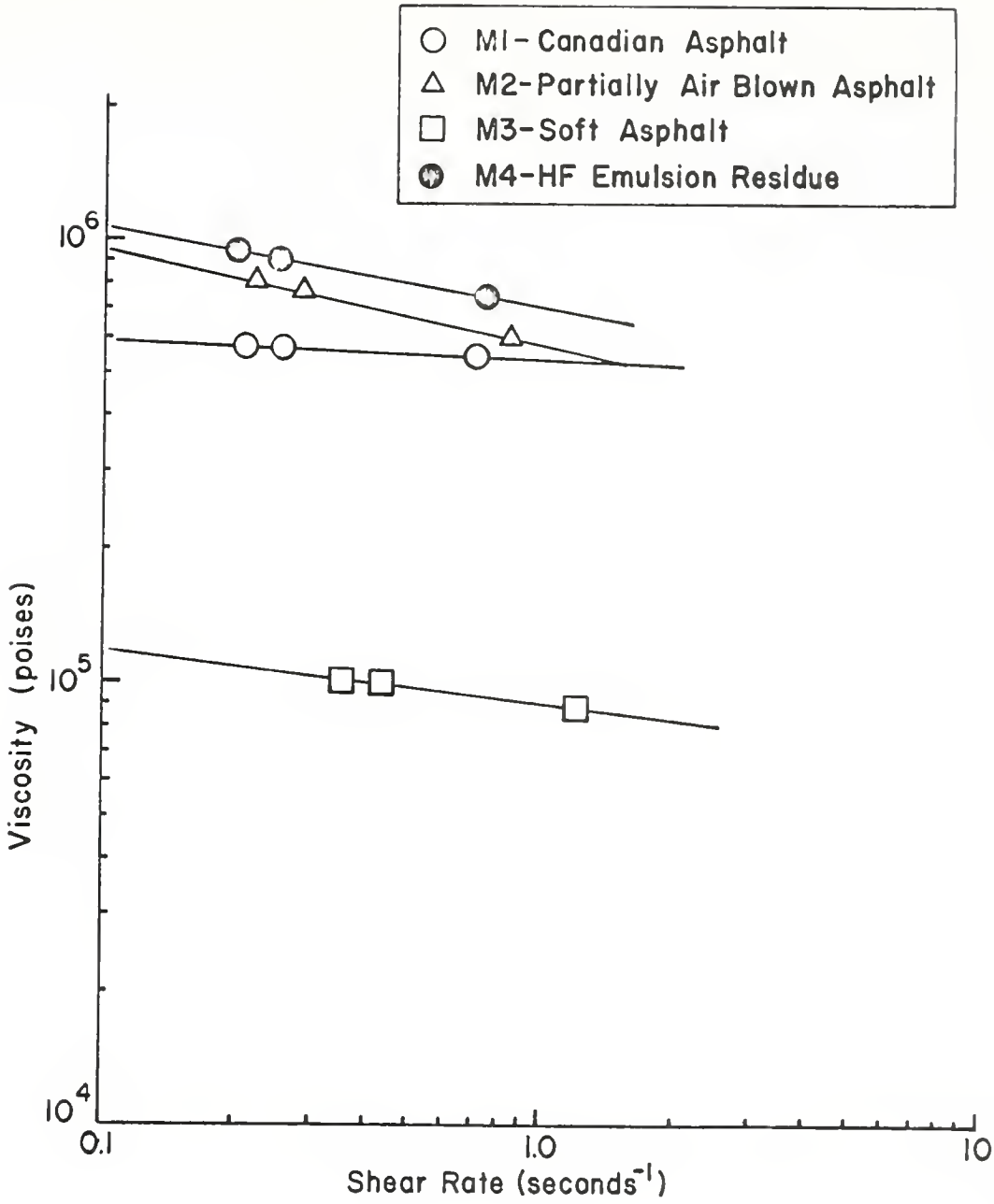

FIGURE 7 VISCOSITY VS. SHEAR RATE AT 77°F FOR BINDERS M1, M2, M3, M4

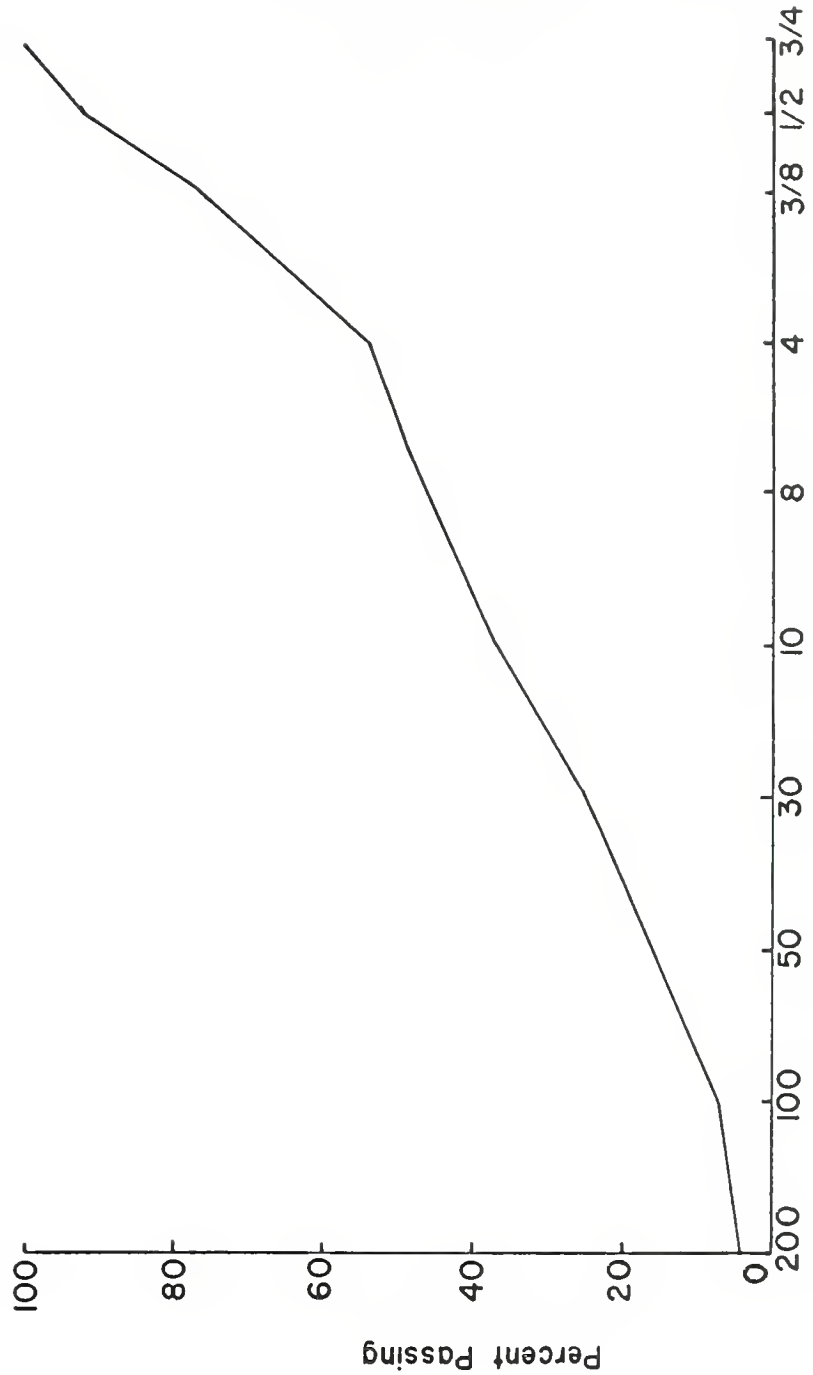

FIGURE 8 MIXTURE GRADATION

Specific gravity and absorption values of coarse as well as fine fractions of the gradation are given in the "aggregate" section. The values of bulk specific gravity and apparent specific gravity for the blended fractions to produce the mixture gradation are 2.670 and 2.772 respectively.

Surface area of the aggregate was calculated using the California surface area factors (42). This method multiplies a factor for each sieve size by the percentage by weight passing the sieve to give the surface in square feet per pound of material of that fraction. The sum of the surface areas of the fractions is the surface area of the blend of fractions used in the mixture. Surface area of the gradation used for this study was calculated to be 26.78 square feet per pound.

Design binder content was determined by the Hveem (California) method as described by The Asphalt Institute (42). Pertinent data for entering the mix design charts (42, 43) and design constants from the charts are shown in Table 6.

TABLE 6

Hveem Mixture Design Values

Factor	Design Value
Corr. CKE	3.10
Oil. Ret.	3.20
K_c	1.40
K_f	0.75
K_m	0.93
Oil Ratio	3.8
Bit. Ratio	5.25

Mixtures were prepared using the estimated asphalt content (5.25 percent) and specimens were fabricated for stability and cohesiometer and density-voids analysis. For this asphalt content, stability and cohesiometer values were adequate for heavy traffic but air voids in the compacted mixture were 7.7 percent and thus exceeded the desirable level of 2-5 percent. Two alternatives are available to adjust mixture components to reduce air voids to an acceptable level; these are:

1. Change aggregate gradation usually by increasing the finer portion.

2. Increase the asphalt content.

Because calculated voids in the mineral aggregate was very close to minimum acceptable values and since the gradation of the trial mixture was approaching the fine limit

of the Indiana State Highway Commission specifications for these types of mixtures, the first alternative was rejected and the second was chosen for trial. Specimens were fabricated and tested at increased asphalt contents. The asphalt content which satisfied all the design criteria was chosen as the design asphalt content. The emulsion mixtures were prepared by using the same binder content (emulsion residue) as for the asphalt mixtures. The summary of mixture properties is included in Table 7.

Bulk density values for the test specimens were determined by ASTM Method D2726. The specimens were then broken and the measurements for maximum theoretical specific gravity and absorbed asphalt were made using the Yale Pycnometer method (44). Basic principles applied in this method are the same as in Rice Method (ASTM D2041) but the Yale Pycnometer method leads to quick and efficient determination of parameter values of interest.

TABLE 7

Summary of Mixture Properties

Property/Mixture	M1	M2	M3	M4
% Asphalt by wt. aggregate	6.25	6.25	6.25	6.25
% Asphalt by wt. mixture	5.882	5.882	5.882	5.882
% Aggregate	94.118	94.118	94.118	94.118
Mix bulk Sp. Gr.	2.418	2.414	2.407	-
Absorbed asphalt (%)	1.408	1.408	1.408	-
Aggregate bulk Sp. Gr.	2.67	2.67	2.67	2.67
Asphalt Sp. Gr.	1.012	1.020	1.018	-
VMA (%)	14.765	14.765	14.765	14.765
Air voids (%)	3.88	3.89	3.88	3.89
Stabilometer Value	40	43	38	45
Cohesiometer Value	289	321	300	311

EXPERIMENTAL WORK

In this section, layout of the design of the experiment, specimen fabrication, experimental set-up and testing procedures are described.

Design of the Experiment

The experiment was designed and carried out in two phases. The indirect tension testing for the first phase was conducted at a testing speed of 50 MI per second and at temperatures of -10^0F, 5^0F, 20^0F and 35^0F. For the second phase, a testing speed of 1000 MI per second and temperatures of 35^oF, 70^0F, 105^oF and 140^oF were employed. The rationale for selection of these conditions is presented as a part of the following discussion.

Variables

Response or dependent variables to be evaluated by this study were limiting strain and limiting stiffness. Limiting strain is defined as strain at failure or the strain that is associated with the maximum load. Limiting stiffness is defined as limiting strength divided by limiting strain at failure.

Variables that were intended to be completely controlled during this study were mixture type, testing speed, and

temperature. Mixture type was controlled at four levels. A single gradation was used for each of the four binders (M1, M2, M3 and M4). Each mixture was tested at one binder content as determined to be optimum by the Hveem method of mixture design. Temperature was controlled at eight levels. The upper level was 140°F (60°C) which is approximately the highest ambient temperature that a pavement will experience and is also the standard test temperature for stability measurements for mixture design. The lower limit of test temperature was -10°F (-23.3°C). This was considered to be the level of the temperature which may simulate a reasonably low temperature that would occur in the field and which would also place the binders in the glassy region. While maintaining orthogonality in the experiment, the first phase of the experiment was carried out at test temperatures of -10°F (-23.3°C), 5°F (-15°C), 20°F (-6.7°C) and 35°F (1.7°C) and the second phase involved test temperatures of 35°F (1.7°C), 70°F (21.1°C), 105°F (40.6°C), and 140°F (60°C).

Type of Design

A completely randomized design was considered to be too time consuming and thus uneconomical. At first, it was contemplated to block the temperatures with three replications for each treatment combination. The general model for the analysis would have been the following:

$$Y_{ijk} = \mu + T_i + \delta_{(i)} + M_j + TM_{ij} + \varepsilon_{(ij)k}$$

As is evident from the model, there was no test for temperature and also, there was no possible way to formulate the regression of the effect of temperature on the response variables. These difficulties made the use of a randomized complete block design undesirable.

After detailed discussion, it was decided to use a nested factorial design. The general model for the analysis culminated in the following form:

$$Y_{ijk} = \mu + T_i + D_{(i)j} + \delta_{(ij)} + M_k + TM_{ik} + DM_{(i)jk} + \varepsilon_{(ijk)}$$

$$i = 1,2,3,4 \quad j = 1,2,3 \quad k = 1,2,3,4$$

where

Y_{ijk} = response variable

μ = overall mean

T_i = effect of i^{th} temperature (fixed)

$D_{(i)j}$ = effect of j^{th} occurrence (days) in the i^{th} temperature

$\delta_{(ij)}$ = restriction error caused by the four mixture specimens being run in the j^{th} occurrence of the i^{th} temperature. This has zero degrees of freedom and no sum of squares

M_k = effect of k^{th} mixture type (fixed)

TM_{ik} = effect of the interaction of the i^{th} temperature with k^{th} mixture type

$DM_{(i)jk}$ = effect of the interaction of the j^{th} occurrence in i^{th} temperature by k^{th} mixture type

$\varepsilon_{(ijk)}$ = within error and since there is only one observation within j^{th} occurrence of i^{th} temperature and k^{th} mixture type, there are zero degrees of freedom

A schematic of the arrangement of data from the nested factorial experiment is shown in Table 8.

TABLE 8

Arrangement of Data from
Nested Factorial Experiment

Temperature	1			2			3			4		
Days	1	2	3	4	5	6	7	8	9	10	11	12
Mixture type												
1												
2												
3												
4												

Steps involved in carrying out the design of the experiment were:

1. Four specimens, one for each mixture type, were fabricated and cured at 140°F for 15 hours followed by air curing at room temperature for 7 days.

2. A day was selected at random and the four cured specimens, one for each mixture type, were tested.

3. The same testing procedure was repeated for other eleven days demanding that each temperature had three days which resulted in the form of a nested factorial design.

Specimen Fabrication

In this section, the procedures for mixing, compaction and curing of mixtures are described.

Mixing for Asphalt Cement Mixtures

In preparing the mixtures containing asphalt cements, 1200 gram batches of aggregate were weighed into individual pans and heated to the mixing temperature in a forced-draft oven while the asphalts were being heated in open beakers on electric hot plates with constant stirring. Mixing temperatures were set to give mixing viscosities between 150 and 300 centistrokes as recommended by The Asphalt Institute (48). The weighed and heated aggregate was placed in a heated mixing bowl and placed on a balance where the required amount of asphalt was weighed into a crater in the aggregate. Mixing was accomplished with a planetary action mechanical mixer using a wire beater. Mixtures were mixed for 30 seconds after which the bowl sides were scraped down with a hot spoon. Mixing was then continued for a total elapsed time of 90 seconds. After mixing, each mixture was placed in a clean pan and placed in an oven maintained at 250° Fahrenheit for a few minutes until compacted.

Mixing for Emulsion Mixtures

In preparing the mixtures containing emulsion, 1200 gram batches of aggregate were weighed into individual pans and then transferred to bowls for heating and mixing. The bowls had flat bases so that uniform heat could be applied to the mixture during mixing. The required amount of emulsion was weighed into a crater in the aggregate. While the bowl was being heated on a thermostatically controlled electric hot plate, the mixture was handmixed until it attained the temperature of 250° Fahrenheit. The heating was then controlled so as to maintain the temperature of the mixture at 250° Fahrenheit for fifteen minutes. After this, each mixture was placed in a clean pan and placed in an oven maintained at 250° Fahrenheit for a few minutes until compacted.

Compaction

Although the binder content was determined by the Hveem Method of mix design, the compaction of the test specimens was achieved by use of the gyratory testing machine. The gyratory testing machine (GTM) (49), developed by Waterways Experiment Station, Vicksburg, Mississippi, is based on a compaction technique devised by the Texas Highway Department. The gyratory machine is a combination of compactor and testing machine. It has been demonstrated that as a compactor it produces specimens having stress-strain characteristics more representative of actual field conditions than those compacted by other means and that the simulation of field compaction

and traffic densification is both feasible and practical in the laboratory through the use of this machine (50). Moreover, gyratory compaction produces specimens with realistic orientation of the particles without appreciable degradation of the aggregate. It also produces specimens with more uniform density than the California kneading compactor. For these reasons, gyratory compaction was adapted for fabrication of the test specimens.

The machine was set for a gyratory angle of 1 degree and a vertical pressure of 200 psi. The GTM fixed roller was used. The above settings were based on the ASTM tentative testing method (51). It was ascertained that 60 gyratory revolutions produced specimens with the same magnitude of density as 150 tamping blows at 500 psi foot pressure of the California kneading compactor. In order to achieve uniformity of density during compaction, variable gyratory revolutions (60 ± 3) were employed.

The GTM heater was set at 140 ± 5F and was switched on one hour before starting the specimen compaction. To avoid loss of heat during compaction, the mold and the base plate were preheated to 250 ± 5F. The heated mold, base plate and a paper disc were placed on the carrying tray. The prepared bituminous mixture contained in the pan in the oven at 250^{o}F was then transferred into the mold with a spoon in a manner to avoid spading or tamping, and a paper disc was placed on the top of the mixture. With the help of the carrying tray, the

mold containing the mixture was placed in the GTM and the vertical pressure was applied. After clamping the mold in the mold chuck, the roller carriage was actuated. Each specimen was compacted with the desired number of gyratory revolutions (60±3). Immediately following the compaction, the specimen was levelled using the GTM leveling mechanism and a height reading taken.

Curing

Curing of the freshly laid bituminous mixture in the field takes place in the compacted state and, thus, it was considered reasonable and pragmatical to cure the laboratory specimens also in the compacted state. For hot emulsion mixes it was ascertained that curing at 140°F for 15 hours followed by air curing at room temperature for 7 days achieved a cured state wherein the curve of strength versus days of curing became flat, thus indicating that curing was complete. Hence, it was decided that all the mixtures prepared with asphalt as well as with emulsion would be cured at 140°F for 15 hours, extruded from the mold, and air cured at room temperature for 7 days.

Uniformity of Test Specimens

After the compacted specimen contained in the mold had been extruded, it was allowed to cool to room temperature, and then weighed. Fabrication uniformity was checked by comparing unit weight of the specimens. For all specimens made

from different binders, their respective average unit weight and standard deviation is shown in Table 9.

TABLE 9

Specimen Bulk Specific Gravity

Mix	No. Obs.	Average Unit Wt. (lbs/cu. ft.)	Std. Dev.
M1	24	150.32	0.25
M2	24	150.20	0.38
M3	24	150.36	0.25
M4	24	150.38	0.40

Experimental Set-Up

In this section, the temperature control system, loading system, and the instrumentation needed for testing of the specimens are described.

Temperature Control System

Specimens were tested in a small constant temperature chamber. This test chamber was supplied with conditioned air from a larger conditioning box. Inside dimensions of the test chamber are approximately two feet by two feet by three feet high. This temperature control system was fabricated as a part of a previous study and the reader is referred to this study (16) for a detailed description of the system. The temperature control system was found to be quite efficient and showed the capability of maintaining plus or minus one

degree Fahrenheit for extended periods (8 to 24 hours) and plus or minus one half degree for shorter periods of time.

Temperature Monitoring of Specimens

In order to sense the temperature at the geometrical center of the specimen, a calibrated thermistor was used. The thermistor was inserted in a drilled hole in a dummy specimen of the same size and shape as the test specimens and was enclosed snugly with insulation. The specimens to be tested were conditioned in the testing chamber along with the dummy specimen. The temperature equilibrium between the dummy specimen and that of the testing chamber indicated that test specimens were ready for testing.

Loading System

An MTS electro-hydraulic closed loop testing machine was used as the loading system. The closed loop operation (45) of the testing system is shown in Figure 9. The input may be load or stroke. This input is applied to the specimen, and the system then compares the polarity and the magnitude of the command signal with that given by the feedback transducer. If the difference between the command signal and that of the feedback transducer is not zero, the controller makes the necessary adjustment by signaling the loading system. The control system, through a servo valve, regulates the flow of the hydraulic fluid moving the piston. The movement of the piston provides the loading to the specimen. The system was calibrated and adjusted by a factory technician just prior to

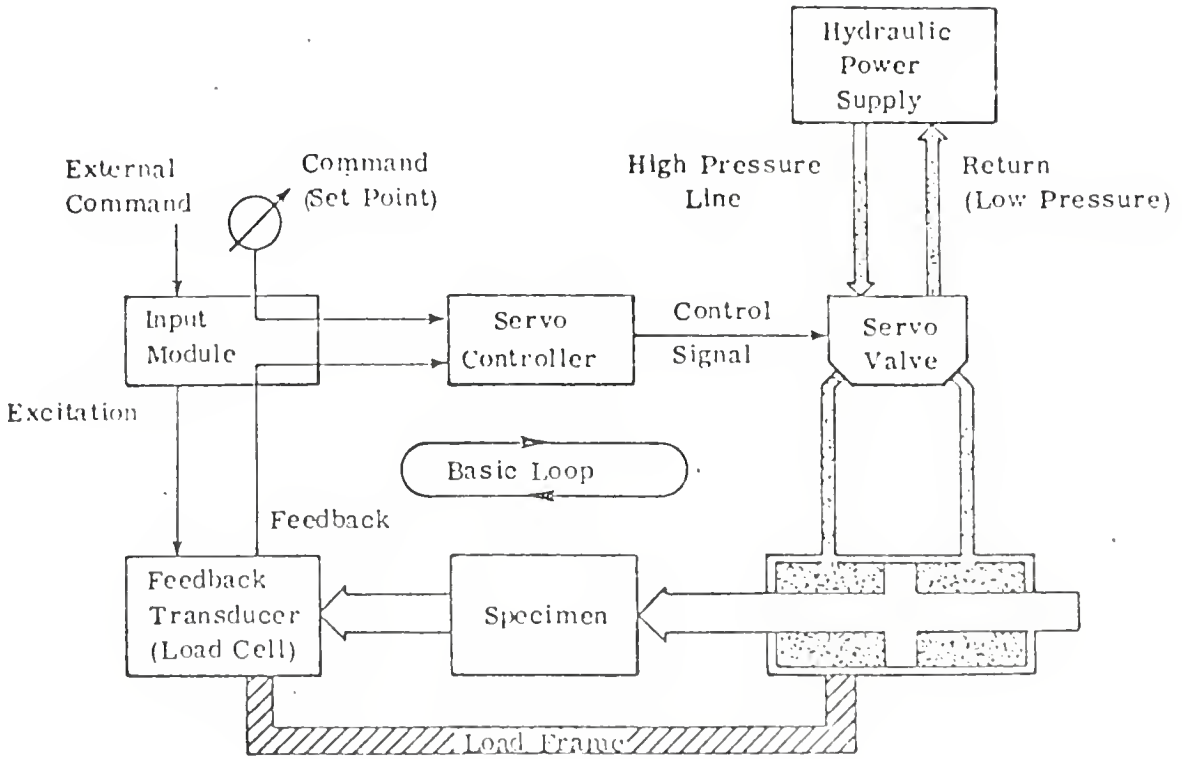

FIGURE 9 THE BASIC LOOP OF THE ELECTRO-HYDRAULIC TESTING SYSTEM

the experiment. A general view of the equipment is depicted in Figure 10.

In order to include a slow enough stroke rate to provide for slower crosshead speed necessary for this study, suitable electronic additions were made to the frequency control module of the function generator. Such a modification made the system capable of being operated at slower rates of ram movement and in compression as well as in tension mode. A schematic diagram of this analog converter and a calibration curve for capacitance versus head speed is given in Figures 11 and 12.

Strain Measurements

Two methods of strain or deformation measurement are available; direct strain measurement with electrical resistance strain gages and measurement with an extensometer. The usage of strain gages poses some problems. In all cases, fixing the gages to asphalt concrete is extremely difficult. Recommended adhesives would either soften the binder or simply would not adhere, particularly at the extreme temperatures necessary for the test. The difficulties in mounting, lack of reliability under the conditions of the experiment, and overall cost and time economy inhibit the direct measurement by strain gages and thus was eliminated as a measuring technique.

The alternative means of deformation measurement involved the use of an extensometer. Theoretical and physical aspects

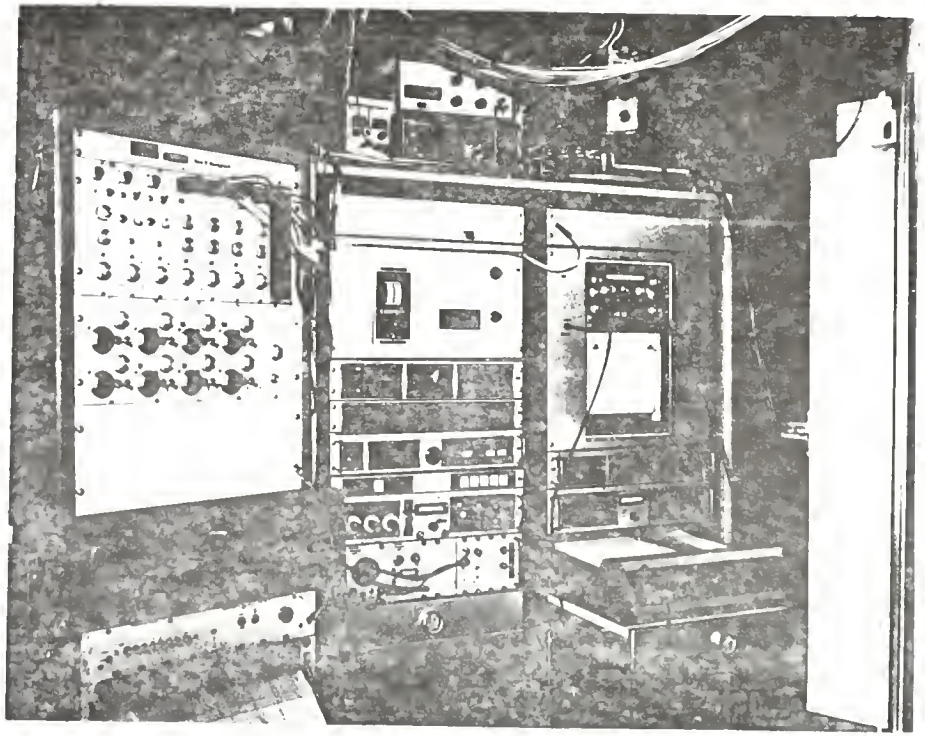

FIGURE 10 A GENERAL VIEW OF EQUIPMENT

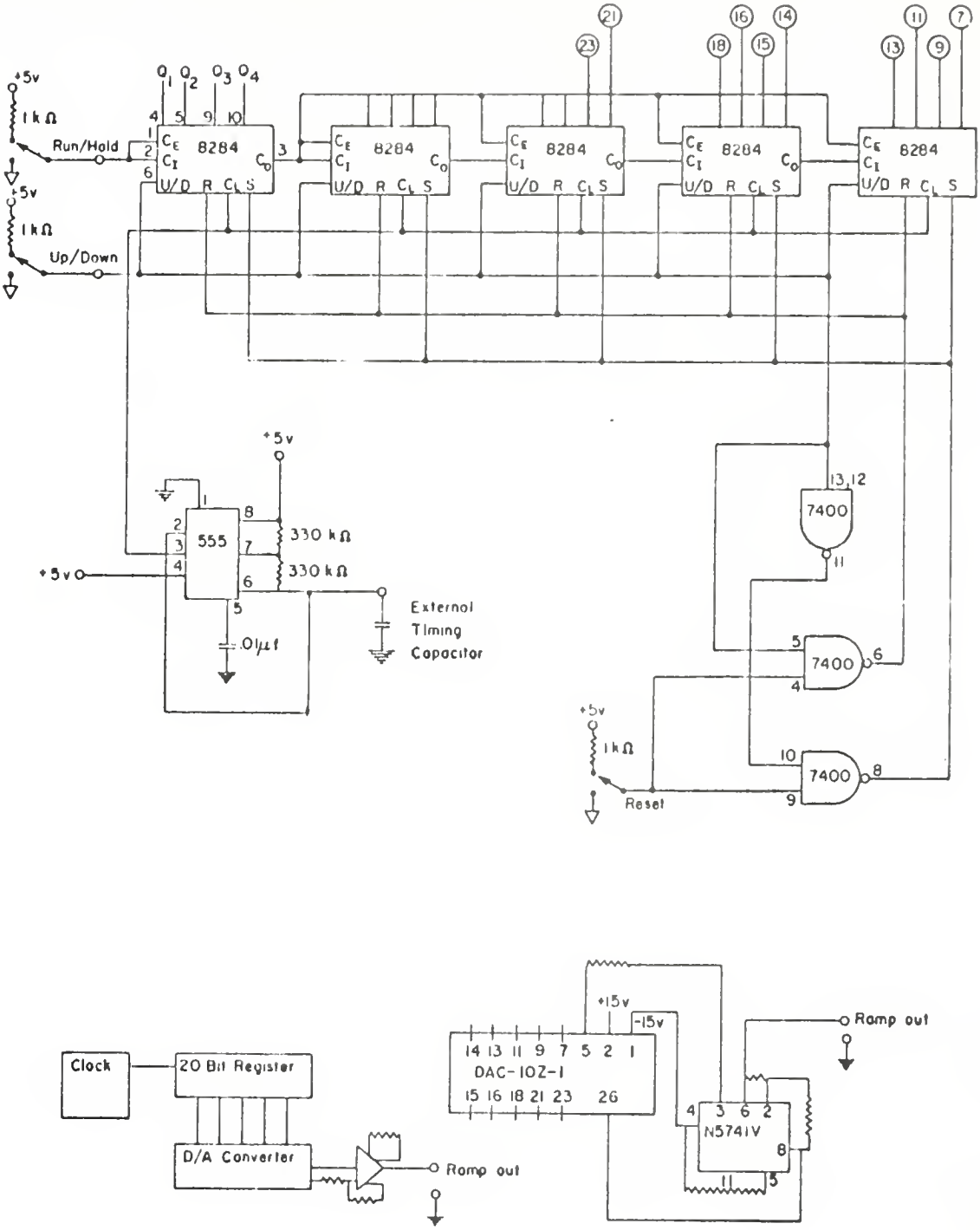

FIGURE 11 RAMP GENERATOR

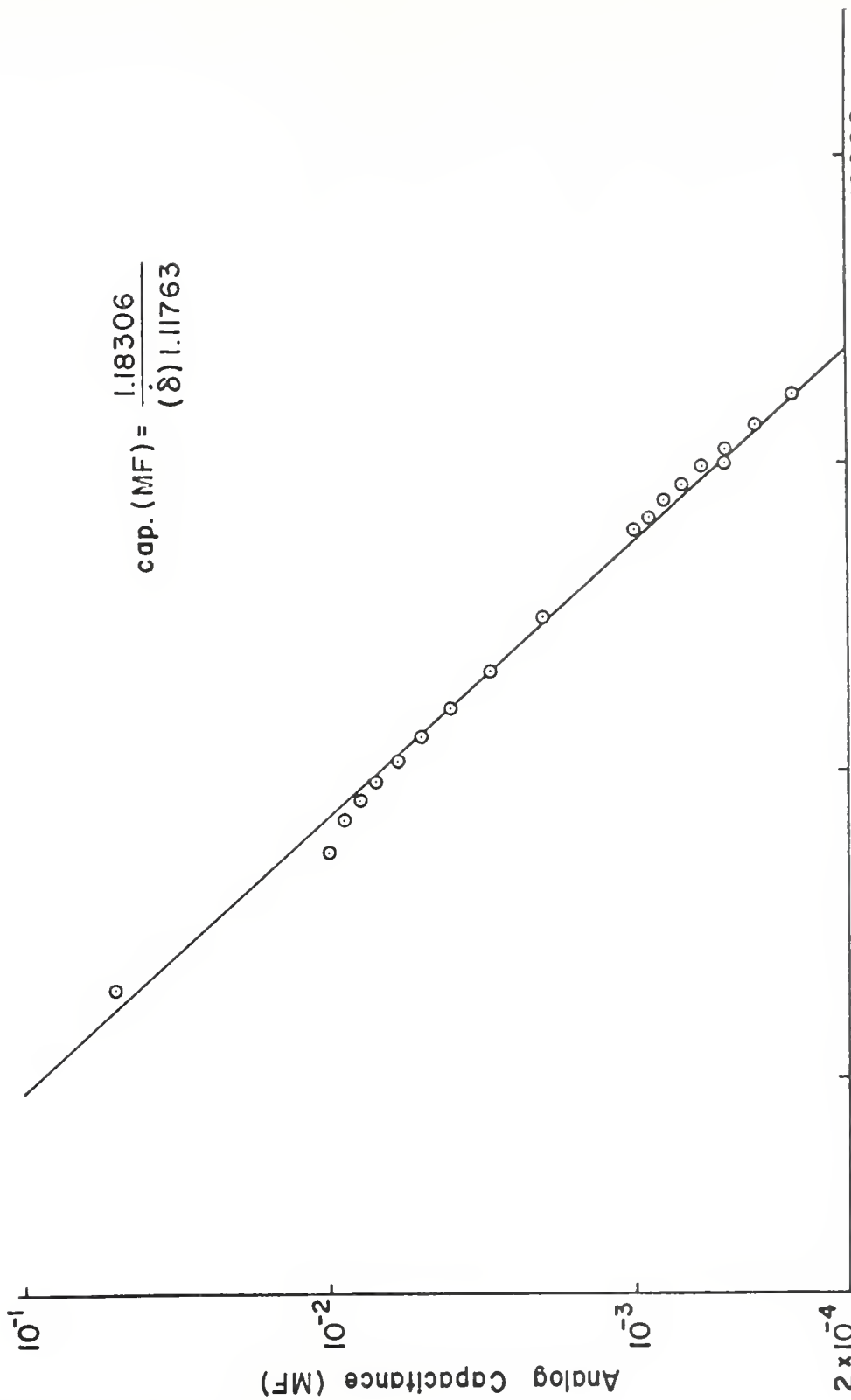

FIGURE 12 ANALOG CONTROLLER CALIBRATION

of these devices are discussed in references (46, 47). The conventional type of extensometer could not be used for the intended type of Indirect Tension test and, thus, a special kind of diametral extensometer was designed for this purpose. The details along with a general view of diametral extensometer are given in Figures 13 and 14.

The LVDT (linear variable differential transformer) used for this project was a Schaevitz model 100 HR-DC with serial number 1507. The device is direct current operated and is completely self contained inasmuch as the microcircuitry necessary for signal conditioning, modulation and demodulation are encapsulated within the housing itself. The only external electronics necessary for operation of this device is a 24 volt DC power supply and a device to measure and record output voltages that result from displacement of the LVDT core.

The LVDT was installed in the diametral extensometer as shown in Figure 13. A 0.0001 inch micrometer, in place of the test specimen, as aa' in Figure 13, was put in for the purpose of calibration. Output voltage of the LVDT versus displacement of micrometer were measured at different test temperatures. Thus, while testing the specimens at different temperatures, the corresponding calibration of the LVDT was used.

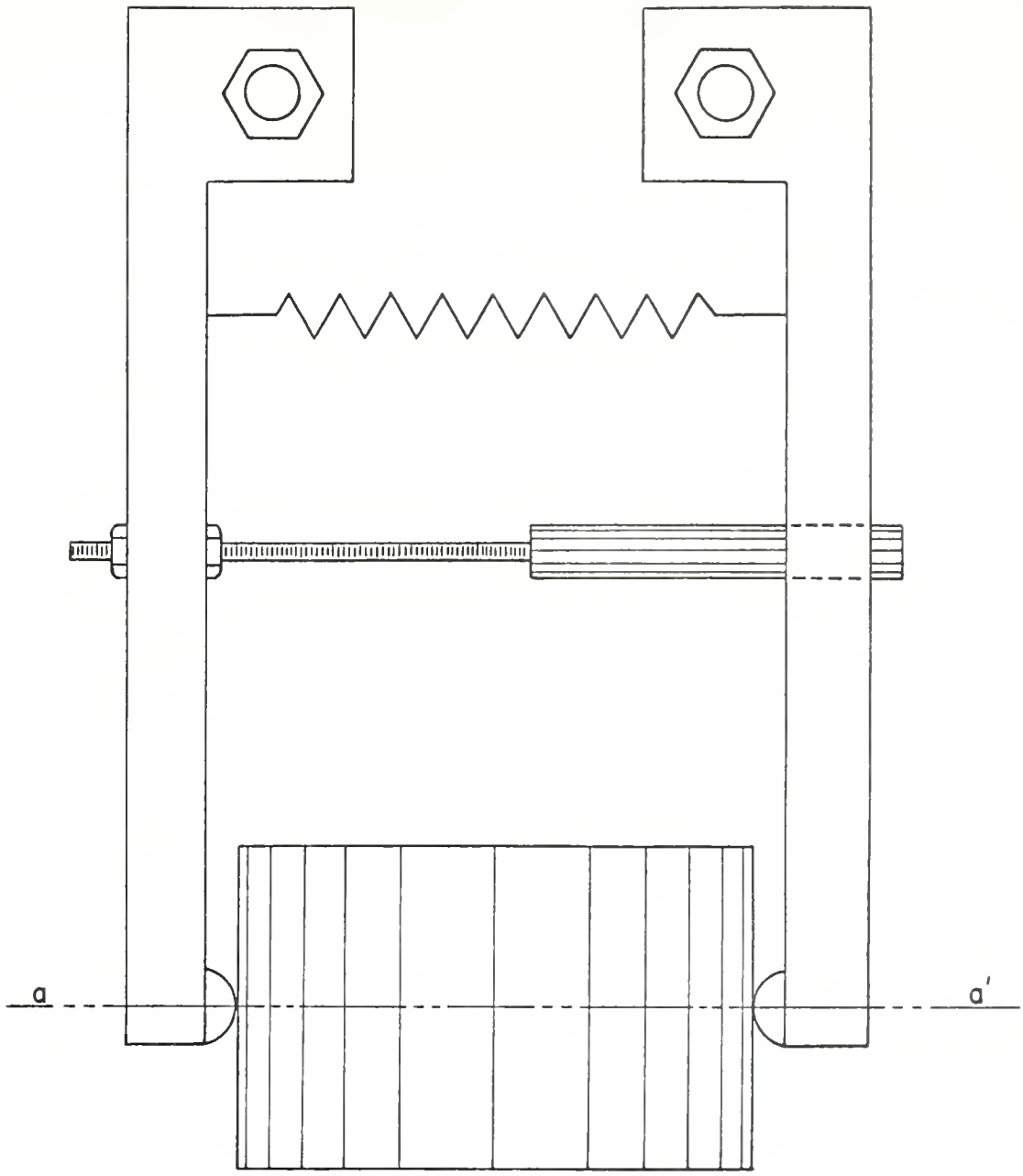

FIGURE 13 DIAMETRAL EXTENSOMETER

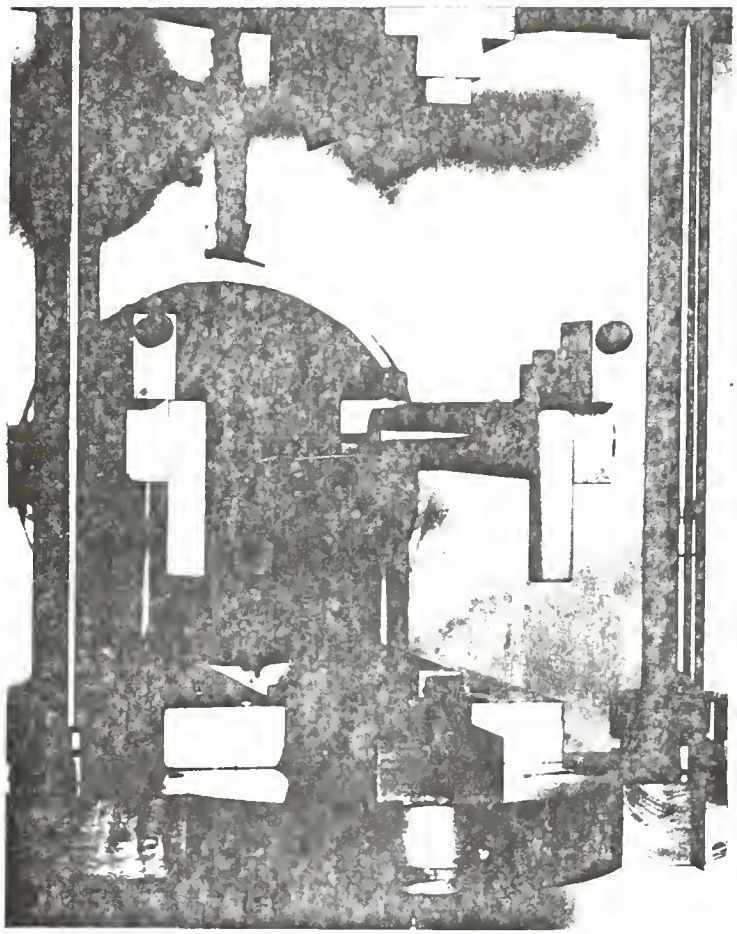

FIGURE 14 GENERAL VIEW OF DIAMETRAL EXTENSOMETER

Acoustic Emission Instrumentation

The objective of using the acoustic emission technique was to detect crack initiation and propagation at low temperatures.

The Dunegan Research Corporation acoustic emission equipment was used which consisted of the following pieces: S1403 transducer, S/D-60P preamplifier, PP-2 power module preamplifier, N5-1 totalizer, BC-677 audio monitor, CP-10 reset clock and CR-11 ramp generator. This equipment was fitted into the MTS Console. A high vacuum grease was used as the viscous coupling material between the transducer and the specimen to insure intimate contact. A rubber band was used to firmly secure the transducer to the specimen. A general view of the transducer attached to the specimen is shown in Figure 15.

Emission counts were recorded on one of the channels of an eight channel Dynograph-R recorder.

Principles of the technique are quite simple in that when the material is stretched enough that one of the bonds breaks, the energy that originally held it together is released in the form of an elastic wave. This wave is detected by a lead-zirconate-titanate (PZT) transducer that exhibits a piezoelectric effect in that deformation of the crystal causes the emission of an electric impulse. The impulse is conditioned, amplified, and stored digitally. A digital-to-analog converter provides a DC voltage output in

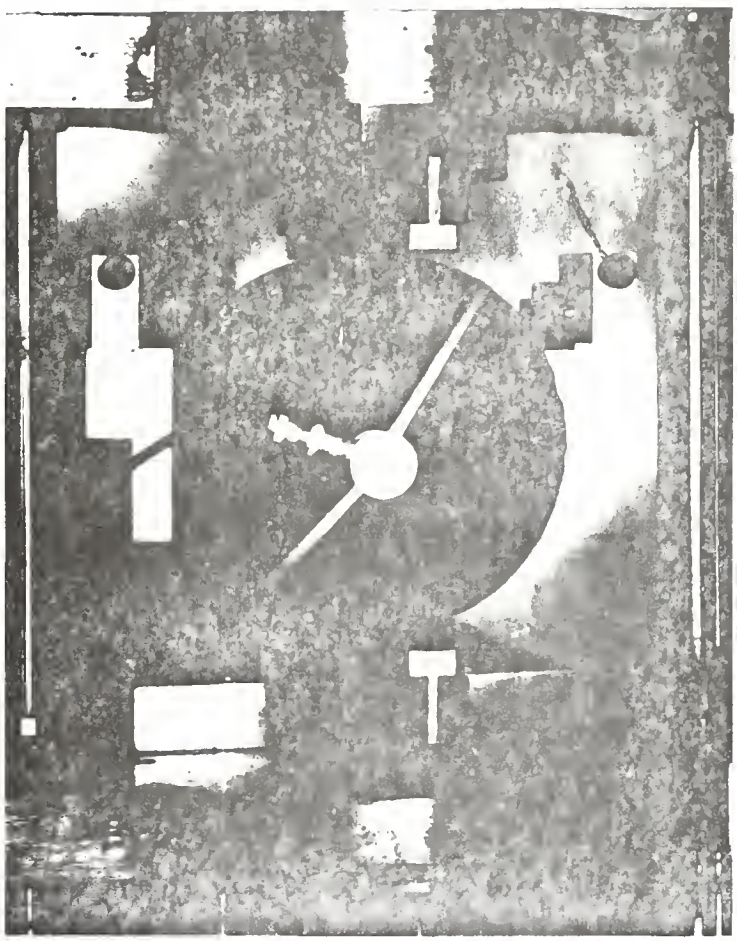

FIGURE 15 ACOUSTIC EMISSION TRANSDUCER ATTACHED TO THE SPECIMEN

real time corresponding to the acoustic emission rate and the counts accumulated. The signals can then be plotted on a recorder. Failure by fracture is indicated by a sharp increase in total or cumulative counts.

Readout Equipment

A Brush Recorder Mark 280 was used for recording load and stroke during the testing of the specimen. Besides this, for temperatures below 70 degree Fahrenheit, four channels of an eight channel Dynograph-R recorder were used for recording output of the load, stroke, displacement through LVDT and the acoustic emission count. For temperatures of 70 degree Fahrenheit and above, a Varian X-Y recorder of low sensitivity in conjunction with a Brush Recorder Mark 280 was used.

Indirect Tension Test

The Indirect Tension Test or Tensile Splitting Test was developed with a view towards simplicity of specimen preparation and testing procedure. The test specimen is loaded across a diameter in a compression testing frame. Tensile stresses induced in the direction of a diameter at right angles to the compressive loading eventually result in fracture of the specimen. A sketch of a specimen failing in tension under a compressive load is shown in Figure 16. Stainless steel curved loading strips were used in the test. The dimensions and configuration of the loading strips used are shown in Figure 17.

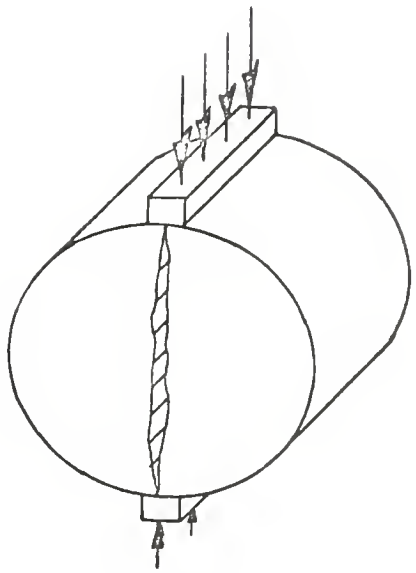

FIGURE 16 SPECIMEN FAILING IN TENSION UNDER COMPRESSIVE LOAD

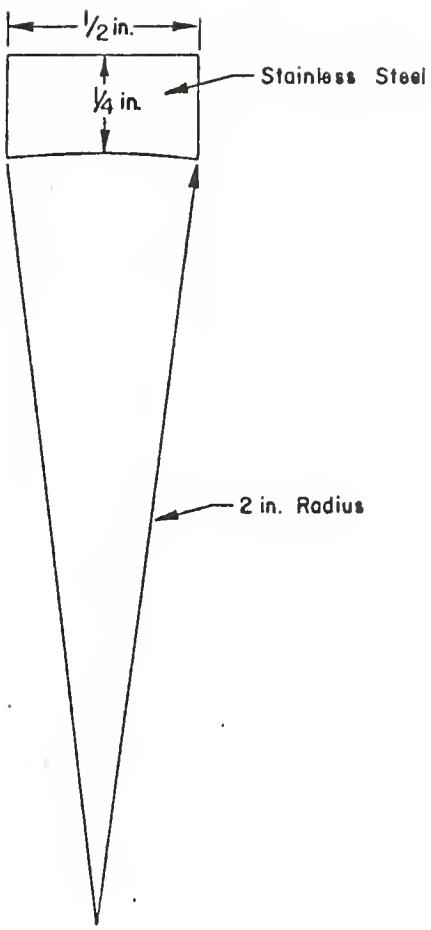

FIGURE 17 GENERAL CONFIGURATION OF THE LOADING STRIPS

The equations for tensile stress and strain at failure (52, 53, 54) for a circular element subjected to short strip loading are presented below. Stress components in a circular element are shown in Figure 18.

$$S_T = \frac{2P}{\pi a h} \left(\text{Sin } 2\alpha - \frac{a}{2R}\right) \qquad \text{(A)}$$

where

S_T = tensile strength

P = maximum load at failure

a = width of the loading strip

h = height of the specimen

α = angle in radians subtended by one-half the width of loading strip

For

a = 0.5 inch

$2\alpha = 14.291^{o}$

and α = 0.1247 radian

the equation (A) takes the following form.

$$S_T = 0.1556 \frac{P}{h} \qquad \text{(B)}$$

$$\varepsilon_T = \frac{X_{TF}}{\ell} \; \frac{\left[\int_{-\frac{\ell}{2}}^{+\frac{\ell}{2}} \frac{\sigma_{rx}}{P} - \nu \int_{-\frac{\ell}{2}}^{+\frac{\ell}{2}} \frac{\sigma_{\theta x}}{P} \right]}{\left[\int_{-r}^{+r} \frac{\sigma_{rx}}{P} - \nu \int_{-r}^{+r} \frac{\sigma_{\theta x}}{P} \right]} \qquad \text{(C)}$$

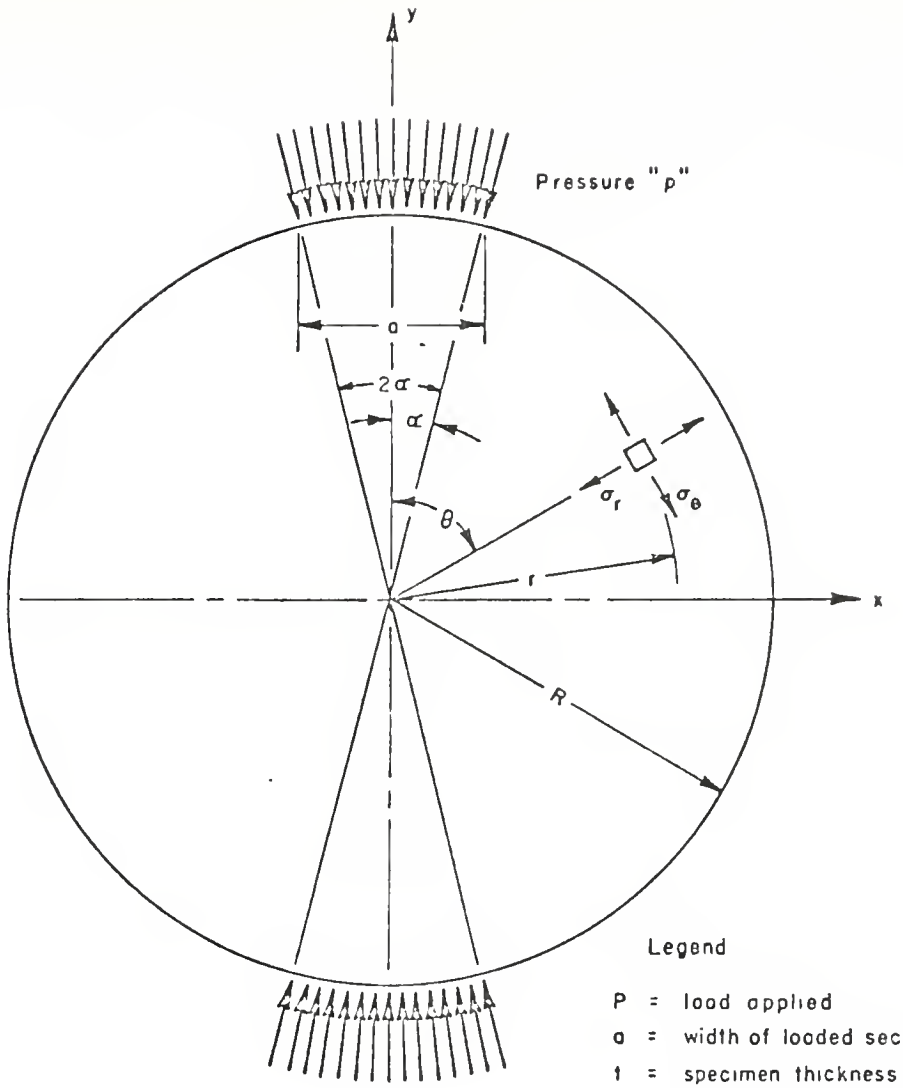

Legend

P = load applied
a = width of loaded section
t = specimen thickness
r = radial distance of a point from the origin
R = radius of circular element
2α = angle at origin subtended by width of loaded section
$p = \frac{P}{at}$ = applied load as a pressure
σ_r = radial stress
σ_θ = tangential stress
θ = angular displacement to a point from y-Axis

FIGURE 18 STRESS COMPONENTS IN A CIRCULAR ELEMENT

where

ε_T = tensile strain at failure

X_{TF} = total horizontal deformation at maximum load

ℓ = length over which strain is estimated

ν = estimated Poisson's ratio

For ℓ = 0.004, equation (C) takes the following form:

$$\varepsilon_T = \frac{X_{TF}}{.004}\left[\frac{6.234\times10^{-4} + 1.8966\times10^{-3}\nu}{0.2692 + 0.9976\nu}\right] \quad (D)$$

$$S_{mix(t,T)} = \frac{\sigma_{(t,T)}}{\varepsilon_{(t,T)}} \quad (E)$$

where

$S_{mix(t,T)}$ = mixture stiffness as a function of time of loading (t), and temperature (T)

$\sigma_{(t,T)}$ = tensile stress as a function of time of loading (t), and temperature (T)

$\varepsilon_{(t,T)}$ = tensile strain as a function of time of loading (t), and temperature (T)

The basic loading frame is shown in Figure 19. It was designed so that the guide posts constrained the upper and lower platens to remain parallel during testing. A general view of the test set-up, including the specimen and other fixtures in the testing chamber, is shown in Figure 20.

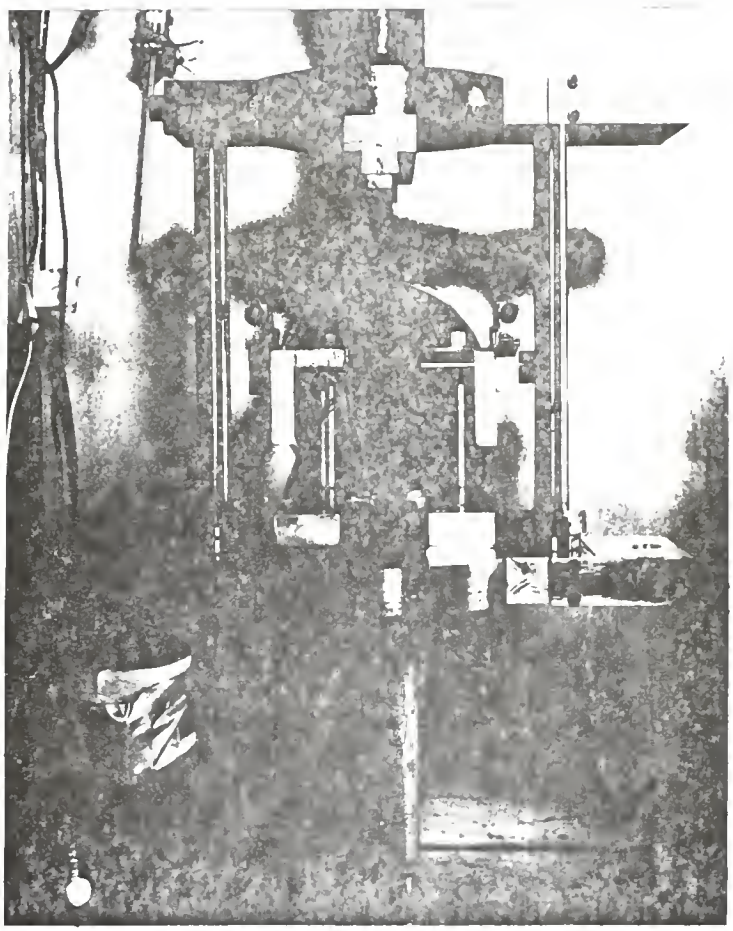

FIGURE 19 THE LOADING FRAME

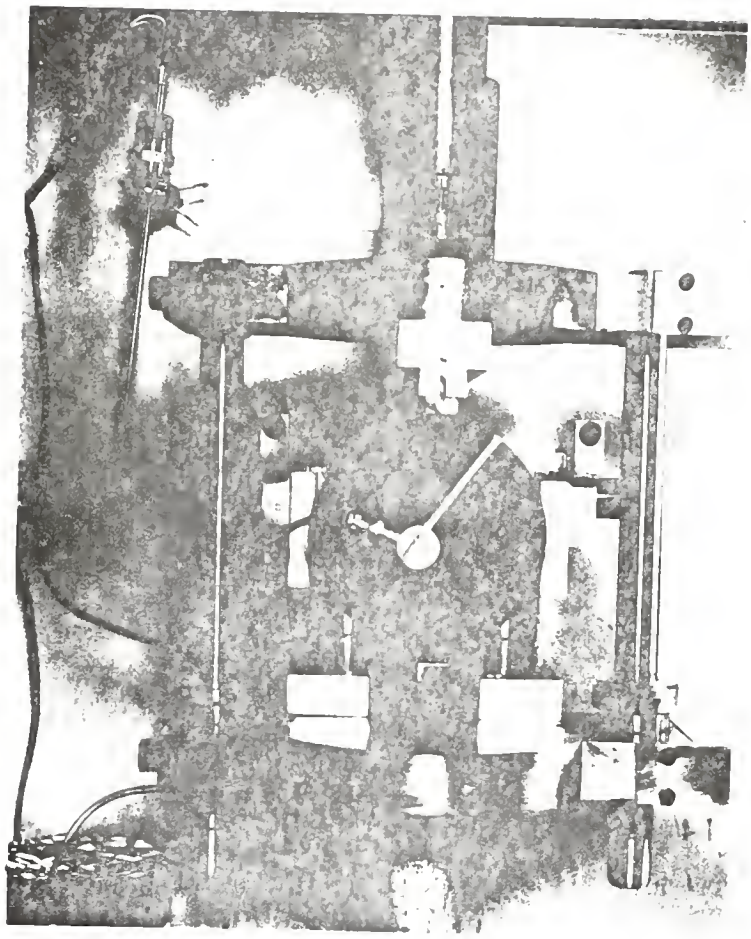

FIGURE 20 GENERAL VIEW OF TEST SET UP

EXPERIMENTAL RESULTS AND ANALYSIS

All values of limiting strain (strain at failure) are in microstrain units (MII). Microstrain is defined as 1 x 10^{-6} inches per inch. The values of limiting stiffness are expressed in PSI.

Limiting strain and limiting stiffness, referred to in this study, are as measured by the tensile splitting test (see "Experimental Work").

Reduced data for each test specimen are contained in Appendix C.

Analysis of Results at Low to Medium Temperatures

To examine the effect of mixture type at low to medium temperatures, an analysis of the data based on test results at $-10^{o}F$, $5^{o}F$, $20^{o}F$ and $35^{o}F$ was performed.

In this analysis and those to follow, it was assumed that the data satisfied the usual assumptions for analysis of variance. Guidelines of Anderson and McLean (55) were followed in the analysis of the data.

Analysis of variance for test results for limiting values of strain and stiffness are shown in Tables 10 and 11 respectively. From this analysis, it is evident that temperature, mixture type and interaction of mixture type and temperature are significant at 5 percent level. It means that the

TABLE 10

Analysis of Variance for Test Results of Limiting Strain at Low to Medium Temperatures

Source	Sum of Squares	Degrees of Freedom	Mean Square	F	F(.05) crit
Temperature (T_i)	7.63×10^7	3	2.5×10^7	1630*	4.07
Days in temperature ($D_{(i)j}$)	124611	8	15576	-	
Restriction error ($\delta_{(ij)}$)	-	0	-	-	
Mixture type (M_k)	1.04×10^7	3	3480360	716*	3.01
Interaction (TM_{ik})	5593167	9	621463	127*	2.30
Interaction ($DM_{(i)jk}$)	116583	24	4857	-	
Error ($\varepsilon_{(ijk)}$)	-	0	-	-	

*Significant at 5 percent level

TABLE 11

Analysis of Variance for Test Results of Limiting Stiffness at Low to Medium Temperatures

Source	Sum of Squares	Degrees of Freedom	Mean Square	F	F(.05) crit
Temperature (T_i)	4.30	3	1.43	1458*	4.07
Days in temperature ($D_{(i)j}$)	7.70×10^{-3}	8	9.62×10^{-4}	-	
Restriction error ($\delta_{(ij)}$)	-	0	-	-	
Mixture type (M_k)	0.605	3	0.201	51.24*	3.01
Interaction (TM_{ik})	0.370	9	4.11×10^{-2}	10.44*	2.30
Interaction ($DM_{(i)jk}$)	9.45×10^{-2}	24	3.93×10^{-3}	-	
Error ($\varepsilon_{(ijk)}$)	-	0	-	-	

*Significant at 5 percent level

mixtures are different from each other and also that they behave differently at different temperatures.

In order to examine the individual means the Newman Keuls Sequential Range Test was performed. The results are presented in Tables 12, 13, 14 and 15. The conclusions from NK test results for limiting strain are as follows:

1. The combinations (1,3), (1,2) and (2,1) are not distinguishable.

2. The combinations (1,2), (2,1) and (1,4) are not distinguishable.

3. The combinations (3,1) and (2,2) are not distinguishable.

4. The combinations (2,4) and (1,3) are not distinguishable.

5. The combinations (4,4) and (4,1) are not distinguishable.

6. All other combinations are significantly different from each other at 5 percent level.

The conclusions from NK test results for limiting stiffness are as follows:

1. The combinations (1,2), (2,1) and (1,4) are not distinguishable.

2. The combinations (1,4) and (1,3) are not distinguishable.

3. The combinations (2,4) and (2,3) are not distinguishable.

TABLE 12

Ranked Means for Limiting Strain
at Low to Medium Temperatures

Order of Original (i,k)	Means Ranked	Ranked Means
(4,3)	1	5144
(4,2)	2	3960
(3,3)	3	3179
(4,4)	4	3028
(4,1)	5	2972
(3,2)	6	2387
(3,4)	7	1752
(3,1)	8	1416
(2,2)	9	1378
(2,3)	10	1055
(2,4)	11	764
(1,3)	12	688
(1,2)	13	567
(2,1)	14	559
(1,4)	15	530
(1,1)	16	385

TABLE 13

Table of Differences Between Means for NK Test
for Limiting Strain at Low to Medium Temperatures

Rank	16	15	14	13	12	11	10	9	8
1	4759*	4614*	4585*	4577*	4456*	4380*	4089*	3766*	3728*
2	3575*	3430*	3401*	3393*	3272*	3196*	2905*	2582*	2544*
3	2794*	2649*	2620*	2612*	2491*	2415*	2124*	1801*	1763*
4	2643*	2498*	2469*	2461*	2340*	2264*	1973*	1650*	1612*
5	2587*	2442*	2413*	2405*	2284*	2208*	1917*	1594*	1556*
6	2002*	1857*	1828*	1820*	1699*	1623*	1332*	1009*	971*
7	1367*	1222*	1193*	1185*	1064*	988*	697*	374*	336*
8	1031*	886*	857*	849*	728*	652*	361*	38	
9	993*	848*	819*	811*	690*	614*	323*		
10	670*	525*	496*	488*	367*	291*			
11	379*	234*	205*	197*	76				
12	303*	158*	129	121					
13	182*	37	8						
14	174*	29							
15	145*								

Rank	7	6	5	4	3	2
1	3392*	2757*	2172*	2116*	1965*	1184*
2	2208*	1573*	988*	932*	781*	
3	1427*	792*	207*	151*		
4	1276*	641*	56			
5	1220*	585*				
6	635*					

*Significant at 5 percent level

TABLE 14

Ranked Means for Limiting Stiffness
at Low to Medium Temperatures

Order of Original (i,k)	Means Ranked	Ranked Means
(1,1)	1	1.14
(1,2)	2	0.78
(2,1)	3	0.78
(1,4)	4	0.68
(1,3)	5	0.65
(2,4)	6	0.47
(2,3)	7	0.38
(2,2)	8	0.25
(3,1)	9	0.25
(3,4)	10	0.16
(3,2)	11	0.09
(3,3)	12	0.08
(4,1)	13	0.07
(4,4)	14	0.07
(4,2)	15	0.04
(4,3)	16	0.03

TABLE 15

Table of Differences Between Means for NK Test
for Limiting Stiffness at Low to Medium Temperatures

Rank	16	15	14	13	12	11	10	9	8
1	1.11*	1.10*	1.07*	1.07*	1.06*	1.05*	0.98*	0.89*	0.89*
2	0.75*	0.74*	0.71*	0.71*	0.70*	0.69*	0.62*	0.53*	0.53*
3	0.75*	0.74*	0.71*	0.71*	0.70*	0.69*	0.62*	0.53*	0.53*
4	0.65*	0.64*	0.61*	0.61*	0.60*	0.59*	0.52*	0.43*	0.43*
5	0.62*	0.61*	0.58*	0.58*	0.57*	0.56*	0.49*	0.40*	0.40*
6	0.44*	0.43*	0.40*	0.40*	0.39*	0.38*	0.31*	0.22*	0.22*
7	0.35*	0.34*	0.31*	0.31*	0.30*	0.29*	0.22*	0.13*	0.13*
8	0.22*	0.21*	0.18*	0.18*	0.17*	0.16*	0.09	0.00	
9	0.22*	0.21*	0.18*	0.18*	0.17*	0.16*	0.09		
10	0.13	0.12	0.09	0.09	0.08	0.07			
11	0.06	0.05	0.02	0.02	0.01				
12	0.05	0.04	0.01	0.01					
13	0.04	0.03	0.00						
14	0.04	0.03							
15	0.01								

Rank	7	6	5	4	3	2
1	0.76*	0.67*	0.49*	0.46*	0.36*	0.36*
2	0.40*	0.31*	0.13*	0.10	0.00	
3	0.40*	0.31*	0.13*	0.10		
4	0.30*	0.21*	0.03			
5	0.27*	0.18*				
6	0.09					

*Significant at 5 percent level

4. The combinations (2,2), (3,1) and (3,4) are not distinguishable.

5. The combinations (3,4), (3,2), (3,3), (4,1), (4,4), (4,2) and (4,3) are not distinguishable.

6. All other combinations are significantly different from each other at 5 percent level.

Regression Equations

In order to estimate limiting strain and limiting stiffness as is generally necessary for analytical solutions, it was considered desirable to generate regression equations to provide these estimators. A review of the model (see section on Type of Design) indicates that the restriction error violates the assumption of only one error for regression analysis. Thus, a test was made to see if $\delta_{(ij)}$ is zero. The details for this test for the data on limiting strain and limiting stiffness are given in Tables 16 and 17 respectively.

TABLE 16

Test for $\delta_{(ij)}$ for Limiting Strain at Low to Medium Temperatures

Source	df	MS	F	F(0.25)
$D_{(i)j}$	8	15576	3.2*	1.39
$DM_{(i)jk}$	24	4857		

*Significant at 25 percent level

TABLE 17

Test for $\delta_{(ij)}$ for Limiting Stiffness
at Low to Medium Temperatures

Source	df	MS	F	F(0.25)
$D_{(i)j}$	8	9.62×10^{-4}	0.24	1.39
$DM_{(i)jk}$	24	3.93×10^{-3}		

It is clear from the analysis given in Tables 16 and 17 that $\delta_{(ij)}$ is not zero in the case of limiting strain data. Thus no regression equation could be generated for limiting strain data. However, a plot of the mean limiting strain values versus temperature is given in Figure 21.

Calculation of regression coefficients for regression equation relating limiting stiffness to temperature was done by Purdue CDC 6500 using SPSS 15 REGRESSION. The following model was used:

$$\hat{S}_M = \beta_0 + \beta_1 (T') + \beta_2 (T')^2 + \beta_3 (T')^3 + e$$

where

$\hat{S}_M$ = estimated limiting stiffness of mixture in 1×10^6 PSI

$T' = \frac{T + 25}{15}$ where T is the actual test temperature

β_i = regression coefficient

e = error term

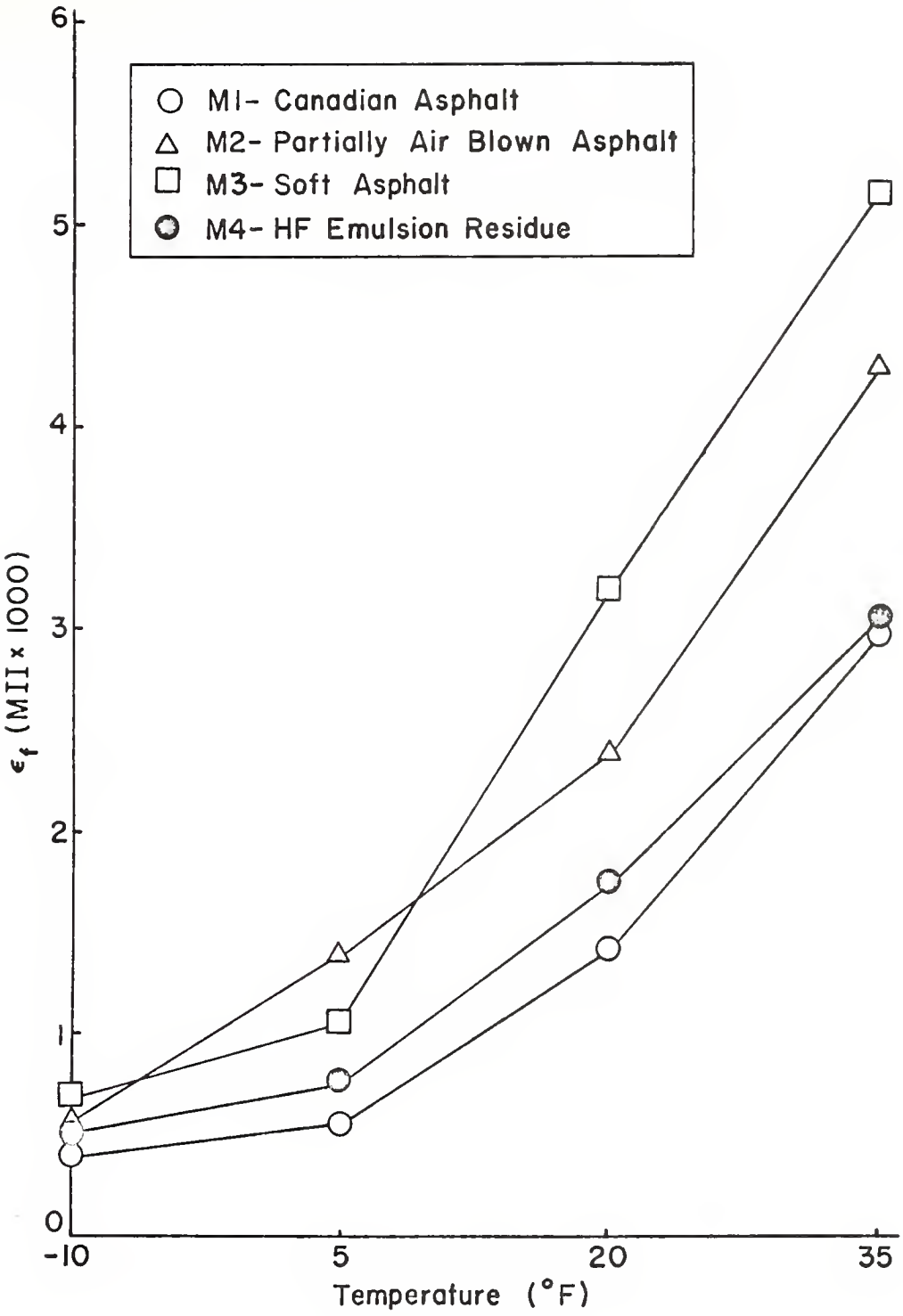

FIGURE 21 LIMITING STRAIN VS. TEMPERATURE FOR MIXTURES M1, M2, M3, M4

Three fits were made with this model. A "cubic" fit uses all terms of the model, a "quadratic" fit uses β_0, β_1 and β_2, and a "linear" fit uses β_0 and β_1. Calculated coefficients and R^2 values for each of these equations are shown in Tables 18, 19, 20 and 21.

TABLE 18

Regression Coefficients for "M1" at Low to Medium Temperatures

Fit	β_0	β_1	β_2	β_3	R^2
Linear	1.495	-0.374	0	0	0.940
Quadratic	1.720	-0.599	0.045	0	0.970
Cubic	0.848	0.086	-0.605	0.806	0.986

A plot of the cubic fit for each of these equations is shown on Figure 22.

Analysis of Results at Medium to High Temperatures

To examine the effect of mixture type at medium to high temperatures, the analysis of the data based on test results at 35°F, 70°F, 105°F and 140°F was performed.

Analysis of variance for test results for limiting values of strain and stiffness are shown in Tables 22 and 23 respectively. From this analysis, it is evident that temperature, mixture type and interaction of mixture type and temperature are significant at 5 percent level. It means that the mixtures are distinguishable from each other and their behavior is different at different temperatures.

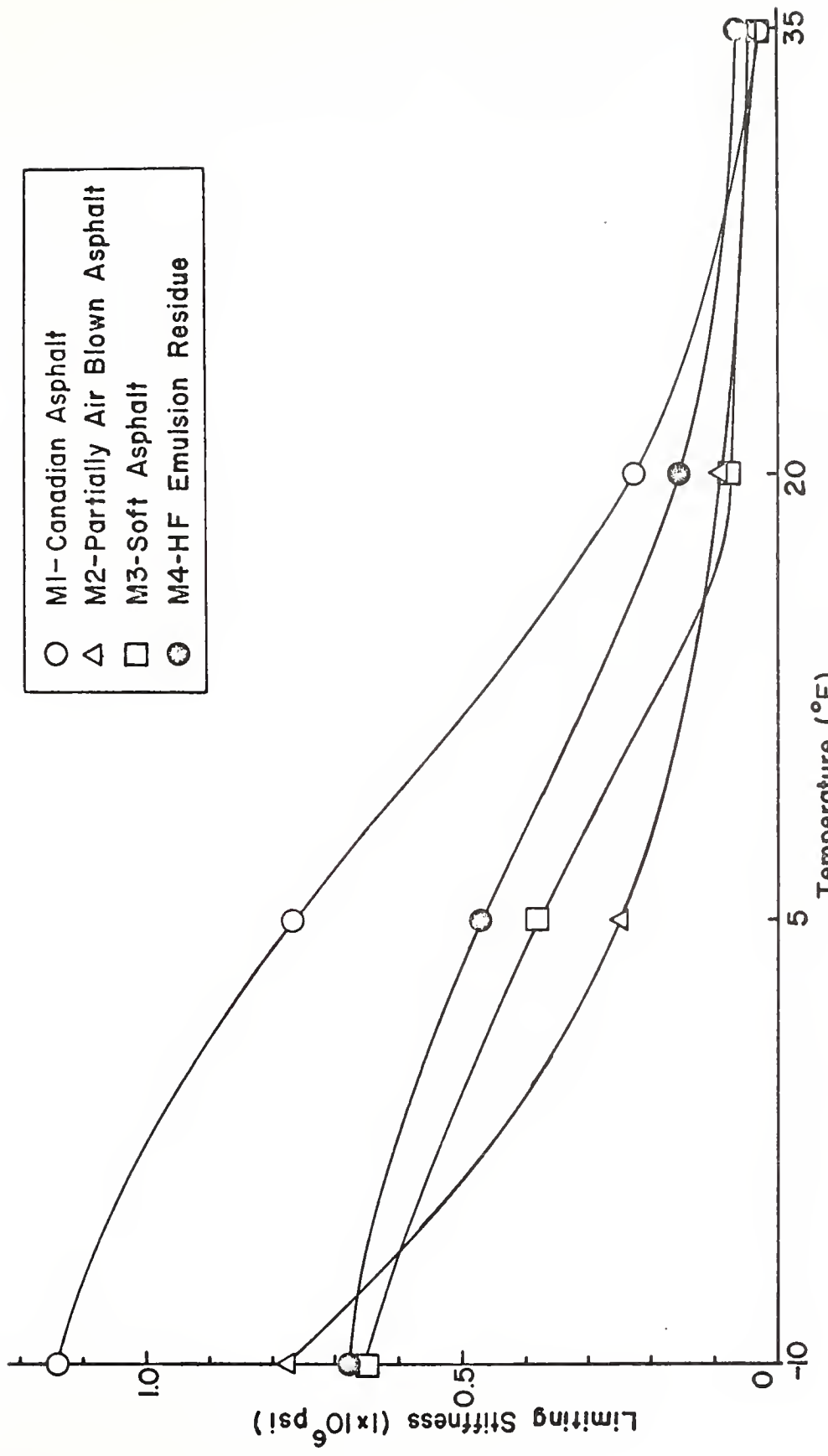

FIGURE 22 LIMITING STIFFNESS VS. TEMPERATURE FOR MIXTURES M1, M2, M3, M4

TABLE 19

Regression Coefficients for "M2"
at Low to Medium Temperatures

Fit	β_0	β_1	β_2	β_3	R^2
Linear	0.898	-0.239	0	0	0.81
Quadratic	1.492	-0.843	0.121	0	0.97
Cubic	1.953	-1.576	0.450	-0.044	0.994

TABLE 20

Regression Coefficients for "M3"
at Low to Medium Temperatures

Fit	β_0	β_1	β_2	β_3	R^2
Linear	0.821	-0.215	0	0	0.90
Quadratic	1.109	-0.502	0.575	0	0.95
Cubic	0.613	0.286	-0.296	0.472	0.98

TABLE 21

Regression Coefficients for "M4"
at Low to Medium Temperatures

Fit	β_0	β_1	β_2	β_3	R^2
Linear	0.881	-0.215	0	0	0.94
Quadratic	1.031	-0.365	0.300	0	0.96
Cubic	0.460	0.543	-0.378	0.054	0.99

TABLE 22

Analysis of Variance for Test Results of Limiting Strain at Medium to High Temperatures

Source	Sum of Squares	Degrees of Freedom	Mean Square	F	F(.05) crit
Temperature (T_i)	1.41×10^8	3	4.70×10^7	845*	4.07
Days in temperature ($D_{(i)j}$)	4.45×10^5	8	5.56×10^4	-	
Restriction error ($\delta_{(ij)}$)	-	0	-	-	
Mixture type (M_k)	1.06×10^7	3	3.53×10^6	118*	3.01
Interaction (TM_{ik})	5.67×10^6	9	6.30×10^5	21*	2.30
Interaction ($DM_{(i)jk}$)	7.16×10^5	24	2.98×10^4	-	
Error ($\varepsilon_{(ijk)}$)	-	0	-	-	

*Significant at 5 percent level

TABLE 23

Analysis of Variance for Test Results of Limiting Stiffness at Medium to High Temperatures

Source	Sum of Squares	Degrees of Freedom	Mean Square	F	F(.05) crit
Temperature (T_i)	6.33×10^4	3	2.11×10^4	1486*	4.07
Days in temperature ($D_{(i)j}$)	1.13×10^2	8	14.24	-	
Restriction error ($\delta_{(ij)}$)	-	0	-	-	
Mixture type (M_k)	4.44×10^3	3	1.48×10^3	100*	3.01
Interaction (TM_{ik})	1.18×10^4	9	1.31×10^3	88*	2.30
Interaction ($DM_{(i)jk}$)	3.54×10^2	24	14.76	-	
Error ($\varepsilon_{(ijk)}$)	-	0	-	-	

*Significant at 5 percent level

In order to examine the individual means the Newman Keuls Sequential Range Test was performed. The results are presented in Tables 24, 25, 26 and 27. The conclusions from NK test results for limiting strain are as follows:

1. The combinations (1,1) and (1,4) are not distinguishable.

2. The combinations (3,1) and (3,4) are not distinguishable.

3. The combinations (3,1), (3,2) and (3,4) are not distinguishable.

4. The combinations (3,3) and (4,1) are not distinguishable.

5. The combinations (3,3), (4,2) and (4,4) are not distinguishable.

6. All other combinations are significantly different from each other at 5 percent level.

The conclusions from NK test results for limiting stiffness are as follows:

1. The combinations (2,1), (2,2), (2,3) and (2,4) are not distinguishable.

2. The combinations (2,1), (2,2), (2,3), (3,2), (3,4), (3,1), (3,3), (4,2), (4,4), (4,1) and (4,3) are not distinguishable.

3. All other combinations are significantly different from each other at 5 percent level.

TABLE 24

Ranked Means for Limiting Strain
at Medium to High Temperatures

Order of Original (i,k)	Means Ranked	Ranked Means
(4,3)	1	8735
(4,1)	2	8424
(3,3)	3	8292
(4,4)	4	7993
(4,2)	5	7980
(3,1)	6	7495
(3,4)	7	7447
(3,2)	8	7149
(2,3)	9	6822
(2,4)	10	6207
(2,1)	11	6188
(2,2)	12	5847
(1,3)	13	5339
(1,2)	14	3913
(1,4)	15	3047
(1,1)	16	2870

TABLE 25

Table of Differences Between Means for NK Test
for Limiting Strain at Medium to High Temperatures

Rank	16	15	14	13	12	11	10	9	8
1	5865*	5688*	4822*	3396*	2888*	2547*	2528*	1913*	1586*
2	5554*	5377*	4511*	3085*	2577*	2236*	2217*	1602*	1275*
3	5422*	5245*	4379*	2953*	2445*	2104*	2085*	1470*	1143*
4	5123*	4946*	4080*	2654*	2146*	1805*	1786*	1171*	844*
5	5110*	4933*	4067*	2641*	2133*	1792*	1773*	1158*	831*
6	4625*	4448*	3582*	2156*	1648*	1307*	1288*	673*	346
7	4577*	4400*	3534*	2108*	1600*	1259*	1240*	625*	298
8	4279*	4102*	3236*	1810*	1302*	961*	942*	327*	
9	3952*	3775*	2909*	1483*	975*	634*	615*		
10	3337*	3160*	2294*	868*	360*	19			
11	3318*	3141*	2275*	849*	341*				
12	2977*	2800*	1934*	508*					
13	2469*	2292*	1426*						
14	1043*	866*							
15	177								

Rank	7	6	5	4	3	2
1	1288*	1240*	755*	742*	443*	311*
2	977*	929*	444*	431*	132	
3	845*	797*	312	299		
4	546*	498*	13			
5	533*	485*				
6	48					

*Significant at 5 percent level

TABLE 26

Ranked Means for Limiting Stiffness
at Medium to High Temperatures

Order of Original (i,k)	Means Ranked	Ranked Means
(1,1)	1	134.94
(1,4)	2	110.46
(1,2)	3	61.60
(1,3)	4	43.59
(2,4)	5	12.90
(2,2)	6	9.63
(2,1)	7	8.52
(2,3)	8	4.64
(3,2)	9	3.22
(3,4)	10	2.78
(3,1)	11	1.86
(3,3)	12	1.45
(4,2)	13	1.34
(4,4)	14	1.23
(4,1)	15	0.57
(4,3)	16	0.46

TABLE 27

Table of Differences Between Means for NK Test
for Limiting Stiffness at Medium to High Temperatures

Rank	16	15	14	13	12	11	10	9	8
1	134.48*	134.37*	133.71*	133.60*	133.49*	133.08*	132.16*	131.72*	130.30*
2	110.00*	109.89*	109.23*	109.12*	109.01*	108.60*	107.68*	107.24*	105.82*
3	61.14*	61.03*	60.37*	60.26*	60.15*	59.74*	58.82*	58.38*	56.96*
4	43.13*	43.02*	42.36*	42.25*	42.14*	41.73*	40.81*	40.37*	38.95*
5	12.44*	12.33*	11.67*	11.56*	11.45*	11.04*	10.12*	9.68*	8.26
6	9.17	9.06	8.40	8.29	8.18	7.77	6.85	6.41	4.99
7	8.06	7.95	7.29	7.18	7.07	6.66	5.74	5.30	3.88
8	4.18	4.07	3.41	3.30	3.19	2.78	1.86	1.42	
9	2.76	2.65	1.99	1.88	1.77	1.36	0.44		
10	2.32	2.21	1.55	1.40	1.33	0.92			
11	1.40	1.29	0.63	0.52	0.41				
12	0.99	0.88	0.22	0.11					
13	0.88	0.77	0.11						
14	0.77	0.66							
15	0.11								

Rank	7	6	5	4	3	2
1	126.42*	125.31*	122.04*	91.35*	73.34*	24.48*
2	101.94*	100.83*	97.56*	66.87*	48.86*	
3	53.08*	51.97*	48.70*	18.01*		
4	35.07*	33.96*	30.69*			
5	4.38	3.27				
6	1.11					

*Significant at 5 percent level

Regression Equations

As before, using the ANOVA results, a test was made to see if $\delta_{(ij)}$ is zero. The details for this test for the data on limiting strain and limiting stiffness are given in Tables 28 and 29 respectively.

TABLE 28

Test for $\delta_{(ij)}$ for Limiting Strain at Medium to High Temperatures

Source	df	MS	F	F(0.25)
$D_{(i)j}$	8	55655	1.87*	1.39
$DM_{(i)jk}$	24	29835		

*Significant at 25 percent level

TABLE 29

Test for $\delta_{(ij)}$ for Limiting Stiffness at Medium to High Temperatures

Source	df	MS	F	F(0.25)
$D_{(i)j}$	8	14.24	0.96	1.39
$DM_{(i)jk}$	24	14.76		

It is clear from the analysis in Tables 28 and 29 that $\delta_{(ij)}$ is not zero in case of limiting strain data. Thus no regression equation could be generated for limiting strain data. However, a plot of the mean limiting strain values

versus temperature is given in Figure 23.

Calculation of regression coefficients for regression equation relating limiting stiffness to temperature was done using the following model:

$$\hat{S}_M = \beta_0 + \beta_1(T') + \beta_2(T')^2 + \beta_3(T')^3 + e$$

where

$\hat{S}_M$ = estimated limiting stiffness of mixture in $1x10^3$ PSI

$T' = \frac{T}{35}$ where T is the actual test temperature

β_i = regression coefficient

e = error term

Three fits were made with this model. A "cubic" fit uses all terms of the model, a "quadratic" fit uses β_0, β_1 and β_2, and a linear fit uses only β_0 and β_1. Calculated coefficients and R^2 values for each of these equations are shown in Tables 30, 31, 32 and 33.

A plot of the cubic fit for each of these equations is shown on Figure 24.

Stiffness-Loading Time Relationships

The low temperature cracking phenomenon is a function of ambient air temperature and thermal loading time. Loading times in the range of a half-hour to several hours are considered reasonable. McLeod (22) has suggested a loading time of 20,000 seconds as the rate at which the pavement is stressed due to chilling to low temperature.

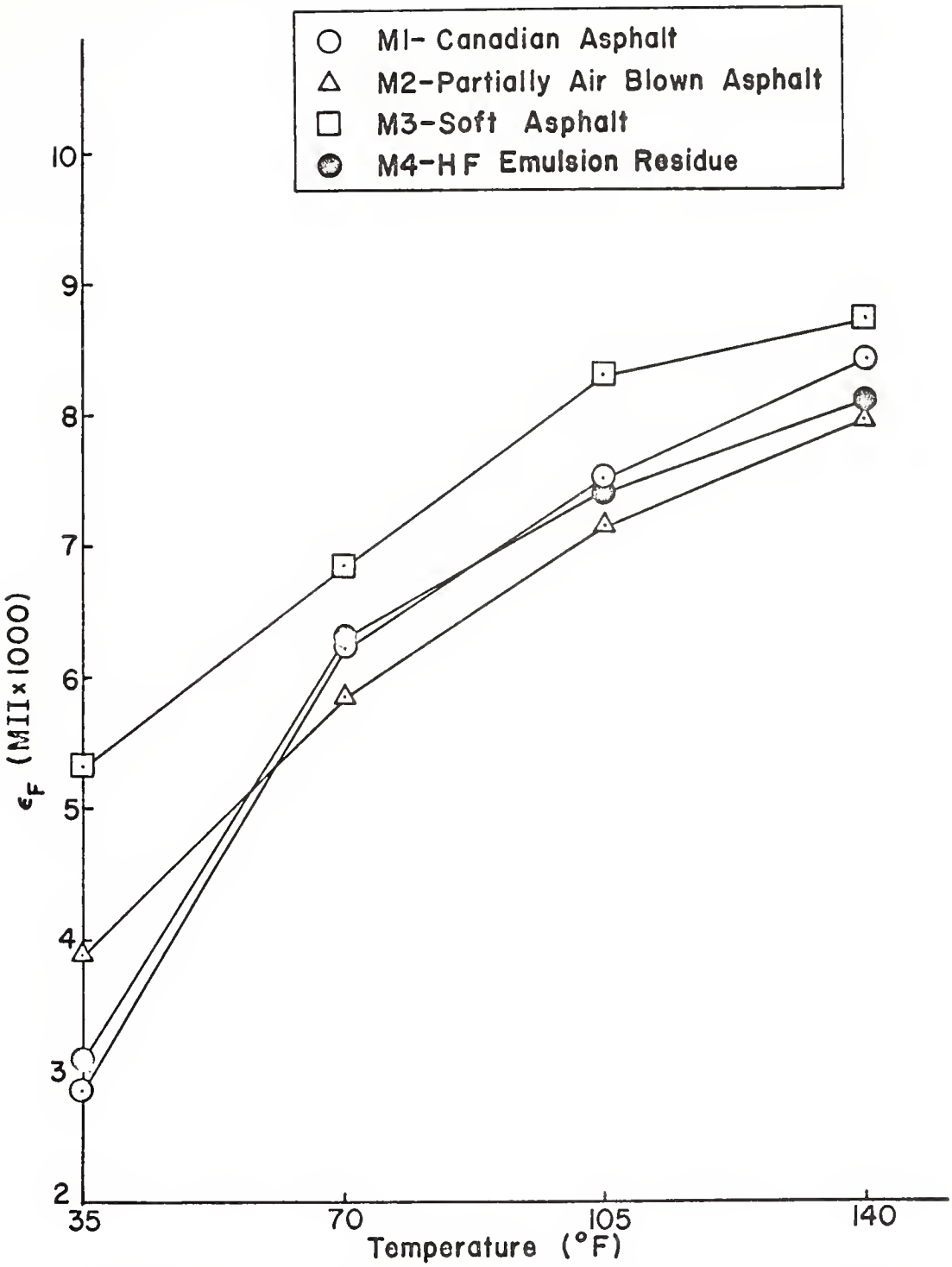

FIGURE 23 LIMITING STRAIN VS. TEMPERATURE FOR MIXTURES M1, M2, M3, M4

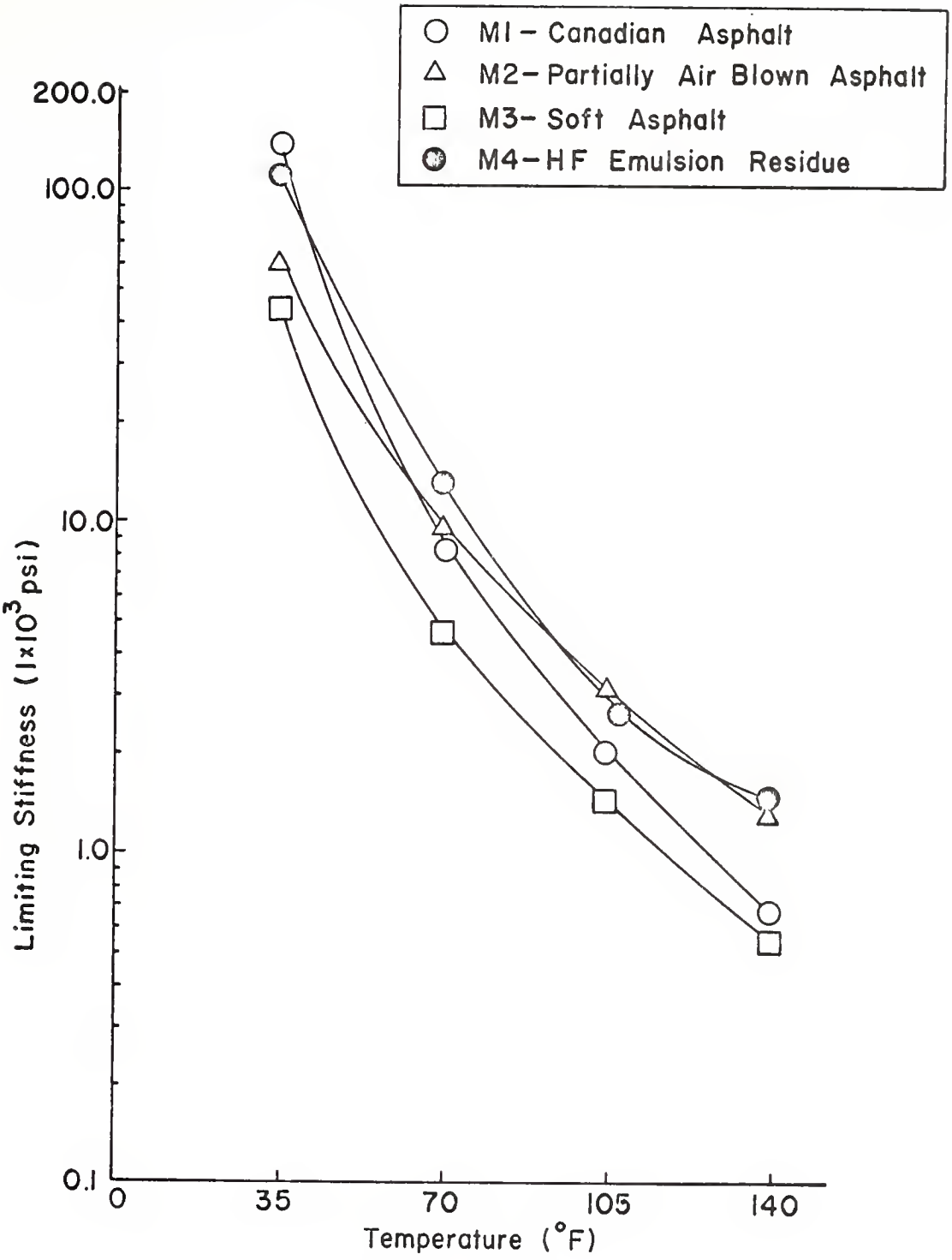

FIGURE 24 LIMITING STIFFNESS VS. TEMPERATURE FOR MIXTURES M1, M2, M3, M4

TABLE 30

Regression Coefficients for "M1"
at Medium to High Temperatures

Fit	β_0	β_1	β_2	β_3	R^2
Linear	138.908	-40.974	0	0	0.64
Quadratic	295.32	-197.38	31.28	0	0.94
Cubic	495.52	-515.80	174.28	-19.06	0.99

TABLE 31

Regression Coefficients for "M2"
at Medium to High Temperatures

Fit	β_0	β_1	β_2	β_3	R^2
Linear	65.74	-18.72	0	0	0.70
Quadratic	128.37	-81.34	12.52	0	0.96
Cubic	200.18	-195.56	63.82	-6.84	0.99

TABLE 32

Regression Coefficients for "M3"
at Medium to High Temperatures

Fit	β_0	β_1	β_2	β_3	R^2
Linear	45.68	-13.26	0	0	0.67
Quadratic	93.14	-60.71	9.49	0	0.95
Cubic	151.86	-154.11	51.43	-5.59	0.997

TABLE 33

Regression Coefficients for "M4"
at Medium to High Temperatures

Fit	β_0	β_1	β_2	β_3	R^2
Linear	116.29	-33.78	0	0	0.68
Quadratic	236.32	-153.80	24.00	0	0.96
Cubic	374.33	-373.30	122.58	-13.14	0.999

The experimental stiffnesses at low to medium temperatures, in this study, were measured up to the loading time of roughly 700 seconds. In order to extend the data to the loading time of 20,000 seconds at low temperatures, use was made of time-temperature superposition techniques. This involved moving the experimental stiffness curves along the loading time axis until each of the experimental curves superimposed as one single master curve. These master curves for stiffness vs. reduced loading time for each mixture type along with the corresponding shift factor (a_t) vs. temperature curve, shown as an inset, are presented in Figures 25, 26, 27 and 28. These master curves permit the stiffness at any temperature or time of loading to be determined. For the loading time of 20,000 seconds, the stiffness values at $-10^{\circ}F$ are calculated and reported in Table 34.

TABLE 34

Stiffness Values at $-10^{\circ}F$ and Loading Time of 20,000 Seconds

Mixture Type	Stiffness (psi)
M1	5.2×10^5
M2	1.9×10^5
M3	9×10^4
M4	2×10^5

In order to eliminate transverse pavement cracking, McLeod (22) has suggested a limiting stiffness value of

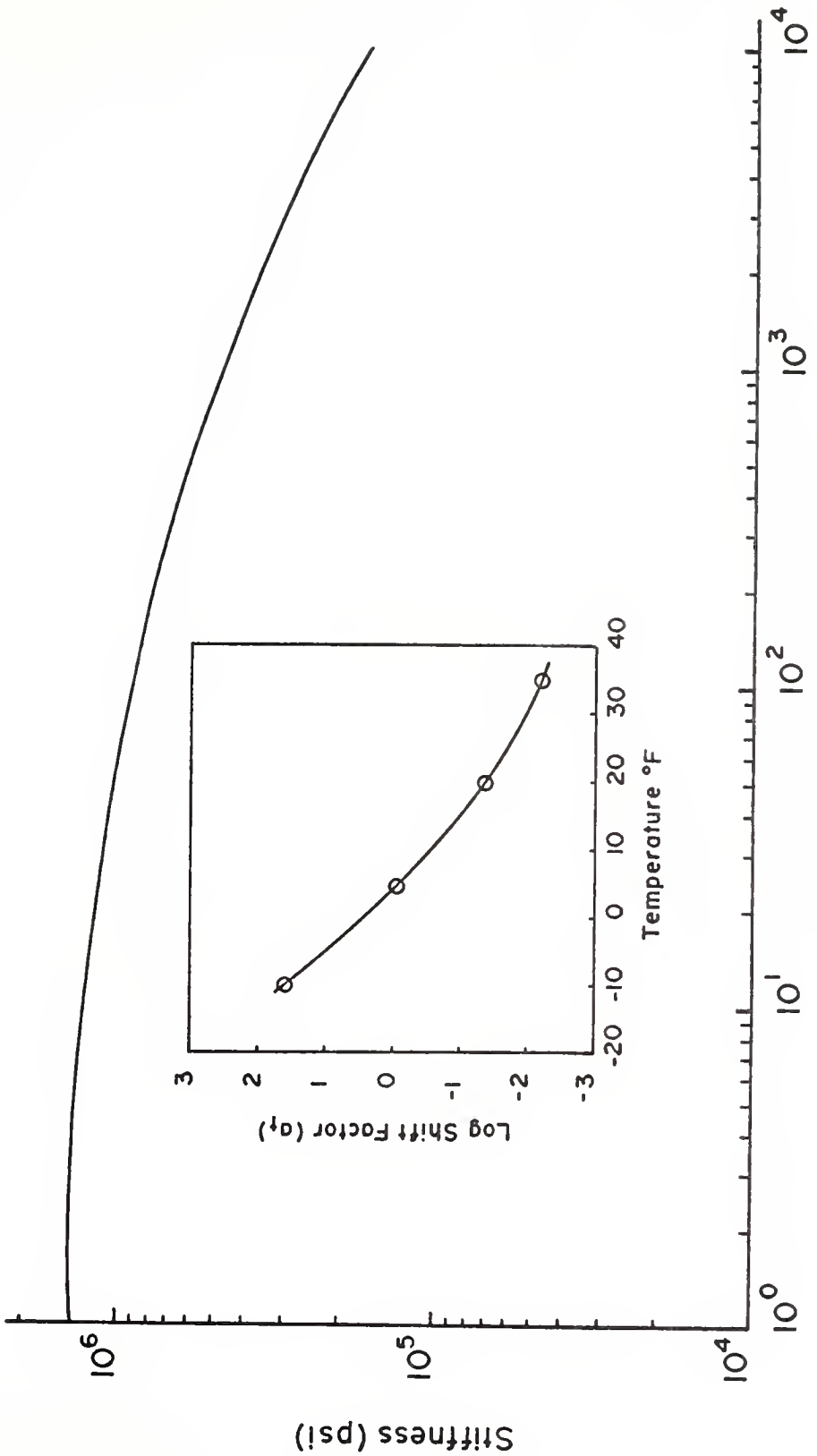

FIGURE 25 MASTER CURVE FOR MI

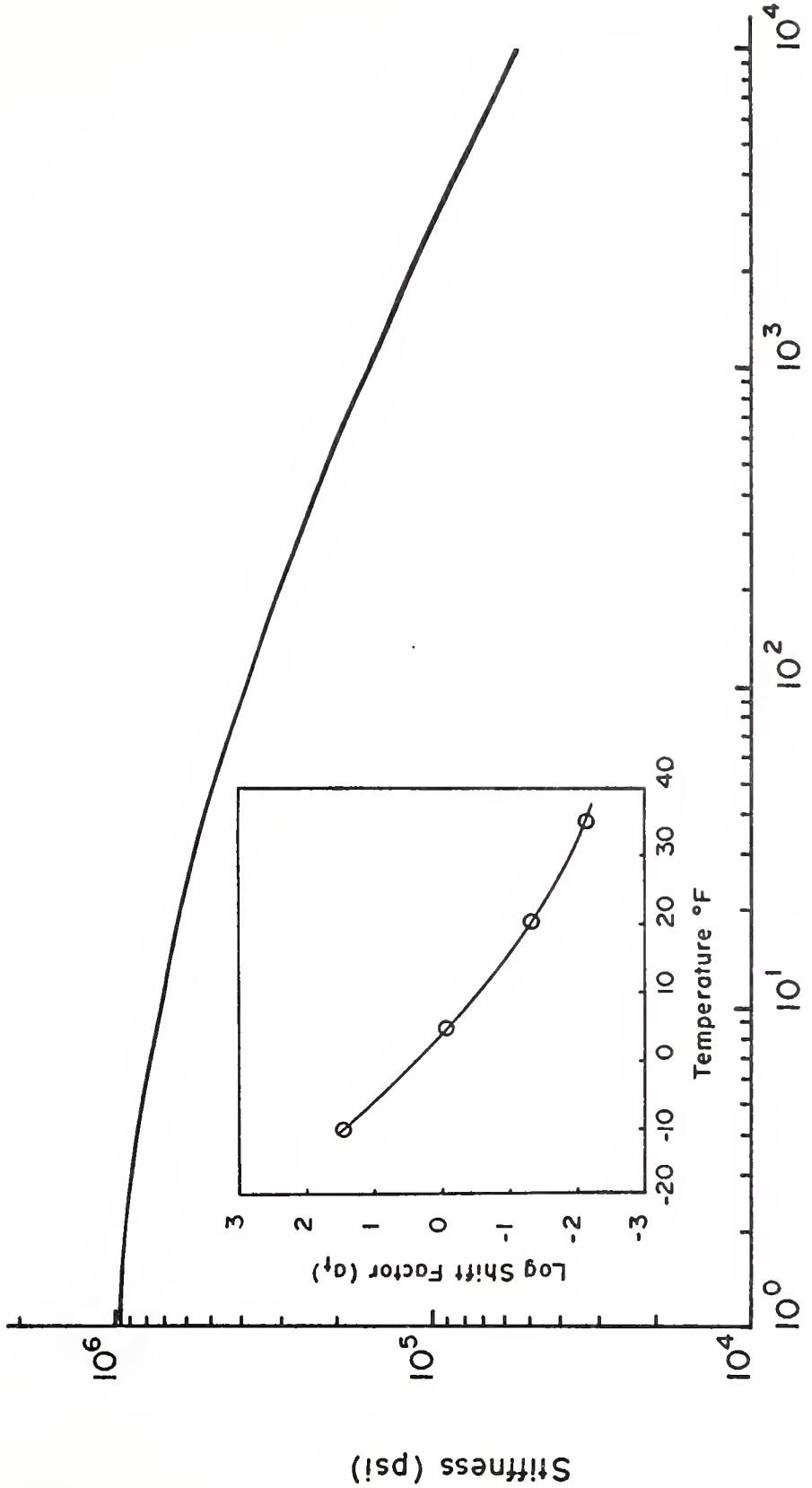

FIGURE 26 MASTER CURVE FOR M2

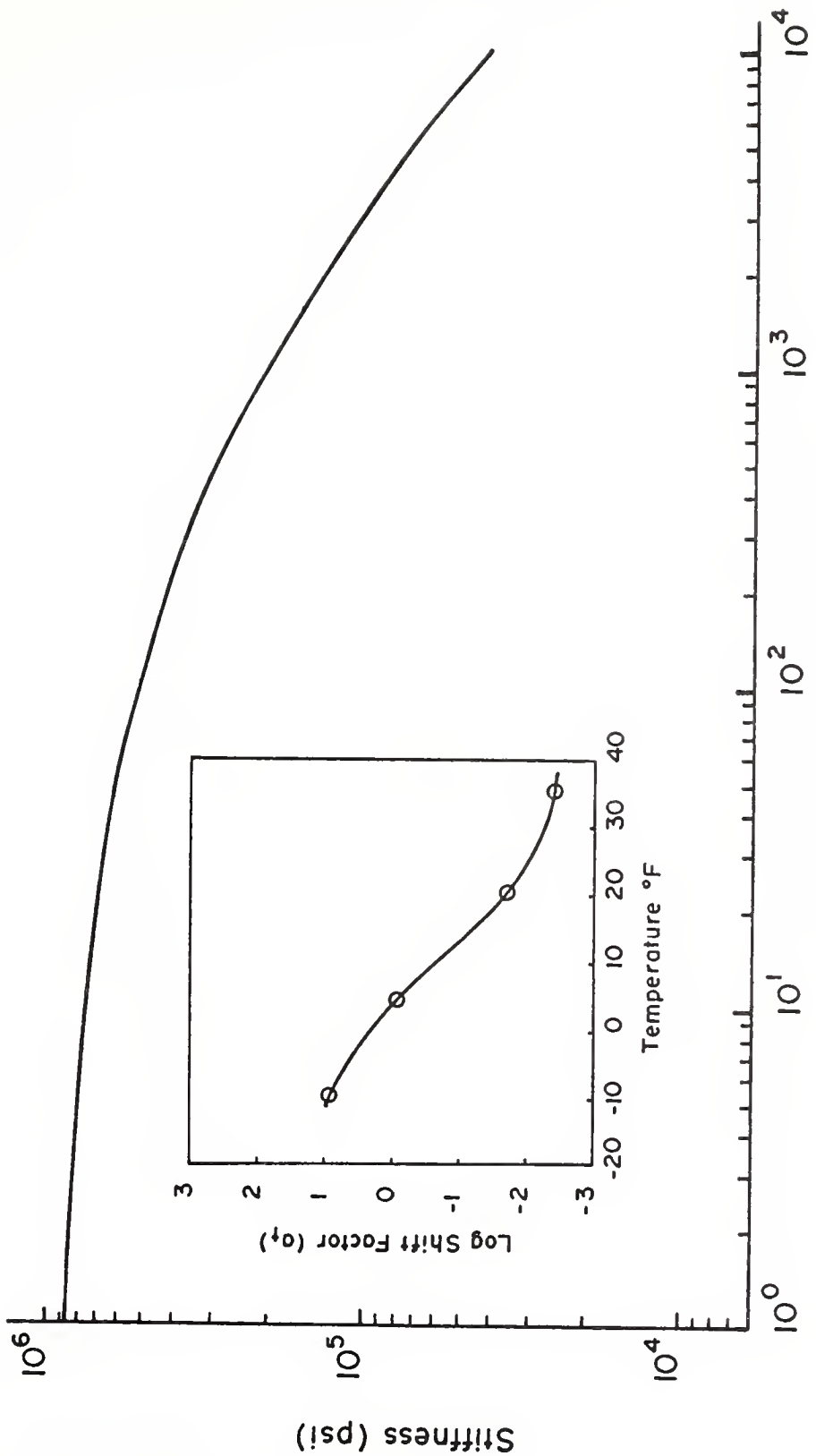

FIGURE 27 MASTER CURVE FOR M3

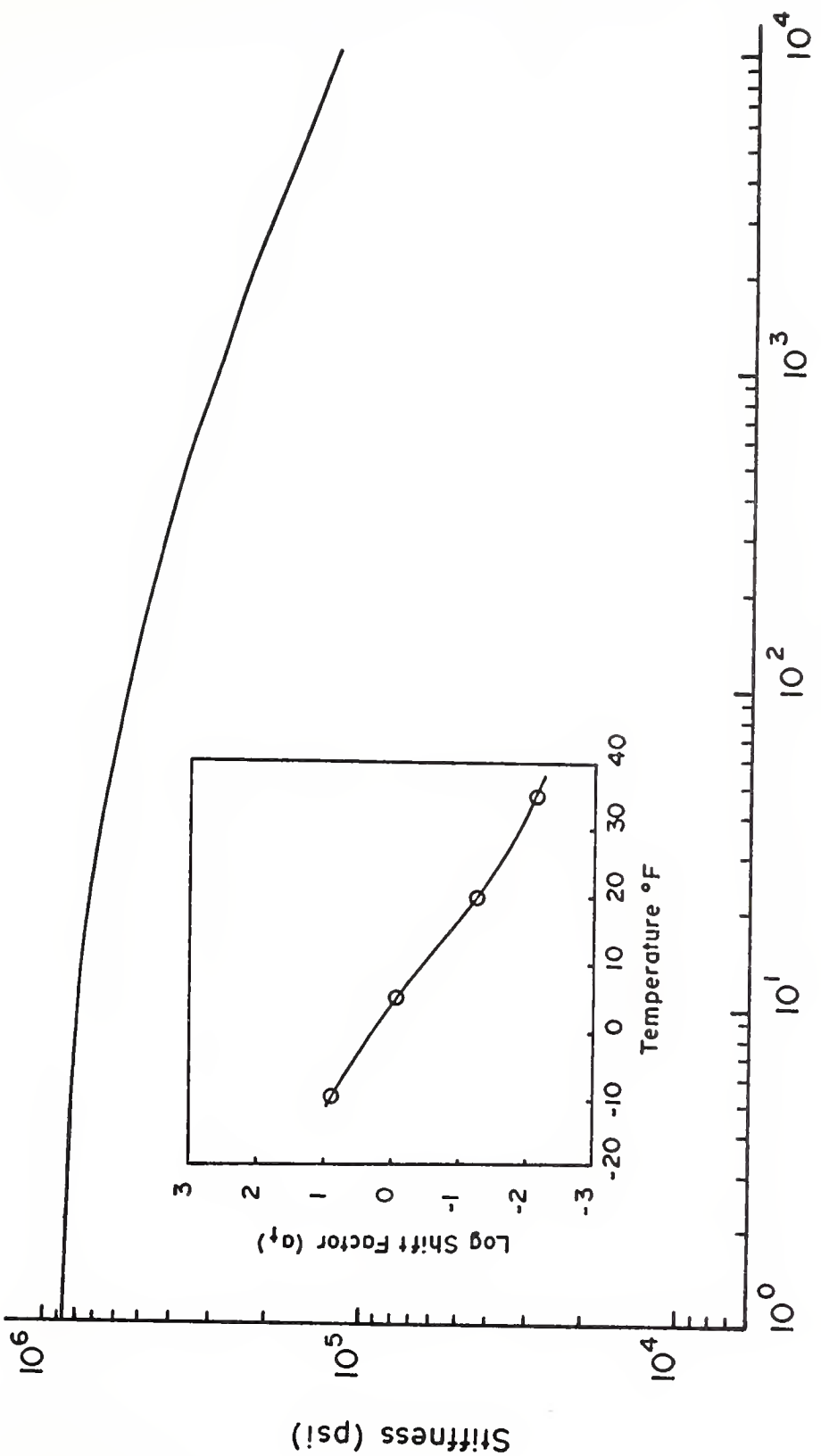

FIGURE 28 MASTER CURVE FOR M 4

2×10^5 psi at $-10^{\circ}F$ and 20,000 seconds loading time. In this regard, the stiffness values for the mixtures in Table 34 suggest that the mixture M1, containing Canadian asphalt, would not be able to mitigate transverse pavement cracking. On the other hand, the mixtures containing emulsion residue, M4, partially air blown asphalt, M2 and soft asphalt, M3 would be resistant to low temperature transverse pavement cracking under these criteria.

Effect of Testing Speed

The nature of bituminous concrete is such that as loads are increased, the strain rate also increases. To control strain rate under this situation requires constant monitoring of deformation rate and adjustment of stroke rate to compensate for this increase. This compensation can be performed manually only if reduced strain data are produced as real time output during the test. This problem can be conveniently handled by electronically comparing the output signal of the displacement transducer with programmed external references; adjustment signals from this process controller then become the feedback for the existing function generator of the test system. Units that perform these functions are recently commercially available, but the estimated costs of the equipment for this control were too high to consider their acquisition as part of this study. Thus, rather than controlling the strain rate, the crosshead speed was maintained constant during the test.

As mentioned before (see "Experimental Work") the testing for the first phase of the experiment was conducted at testing speed of 50 MI per second and that for the second phase at 1000 MI per second. These crosshead speeds were chosen primarily on the basis of practical considerations for testing time. At the temperature of 35°F, the mixtures were tested at both crosshead speeds to evaluate the effect, if any, on the tensile characteristics.

Figures 29 and 30 show the comparison of limiting values of strain and stiffness for low and high testing speeds. As is evident from these Figures, there is no appreciable difference in limiting strain values but a noticeable difference is exhibited for the limiting stiffness values for a given mixture. Since stiffness is a ratio of stress to strain for the given conditions of time and temperature, it means that the tensile characteristic more predominantly affected by the change of crosshead speed is the stress at failure. Higher the testing speed, higher is the resistance offered by the mixture which culminates in higher value of strength. Although all the four types of mixtures seem to be susceptible to the testing speed, the one with Canadian asphalt as the binder seems to be affected the most. This may be due to the reason that the Canadian asphalt is the most temperature susceptible and the most viscous at 35°F (see Figure 3) out of all the binders.

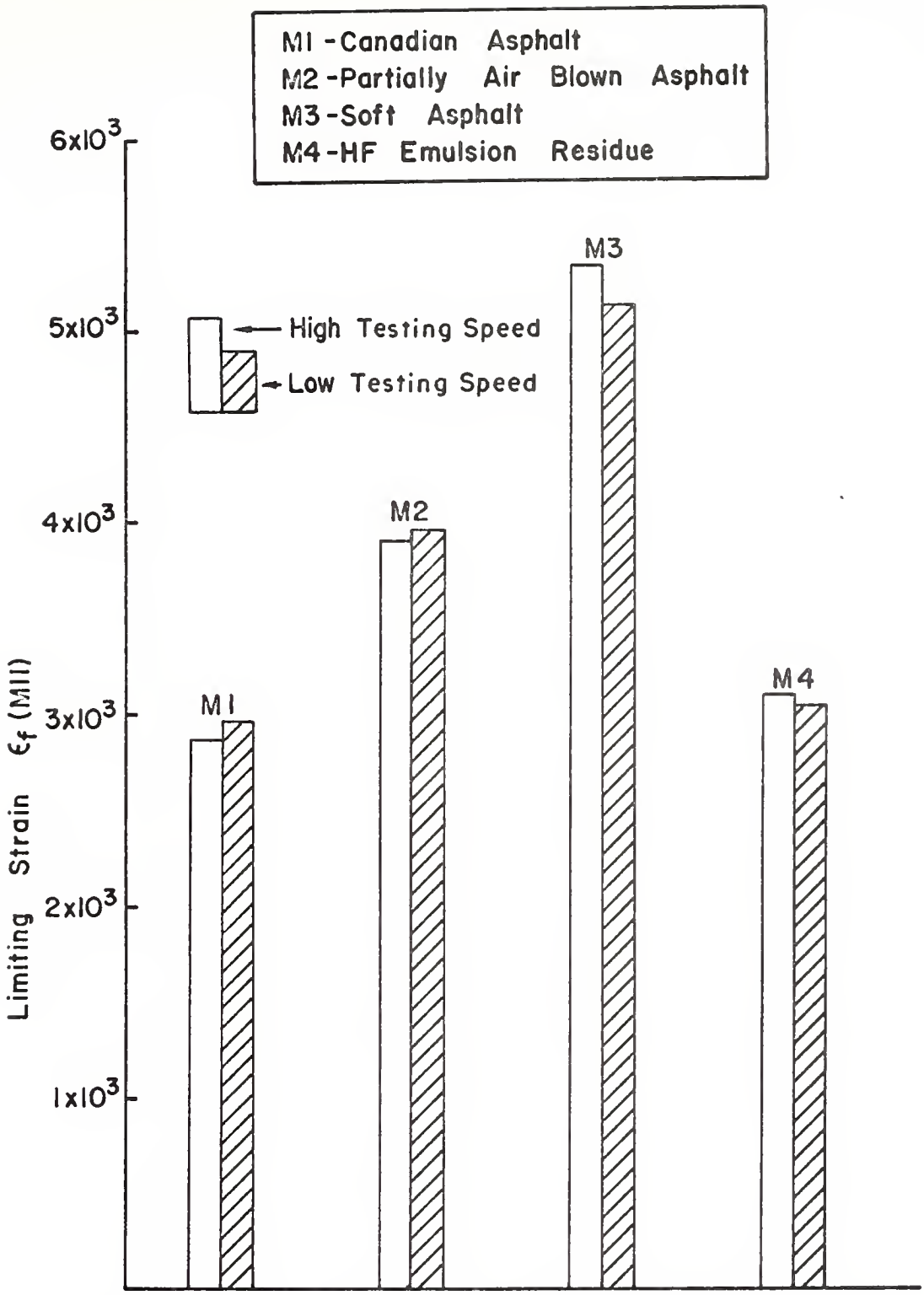

FIGURE 29 COMPARISON OF LIMITING STRAIN OF MIXTURES AT 35 °F

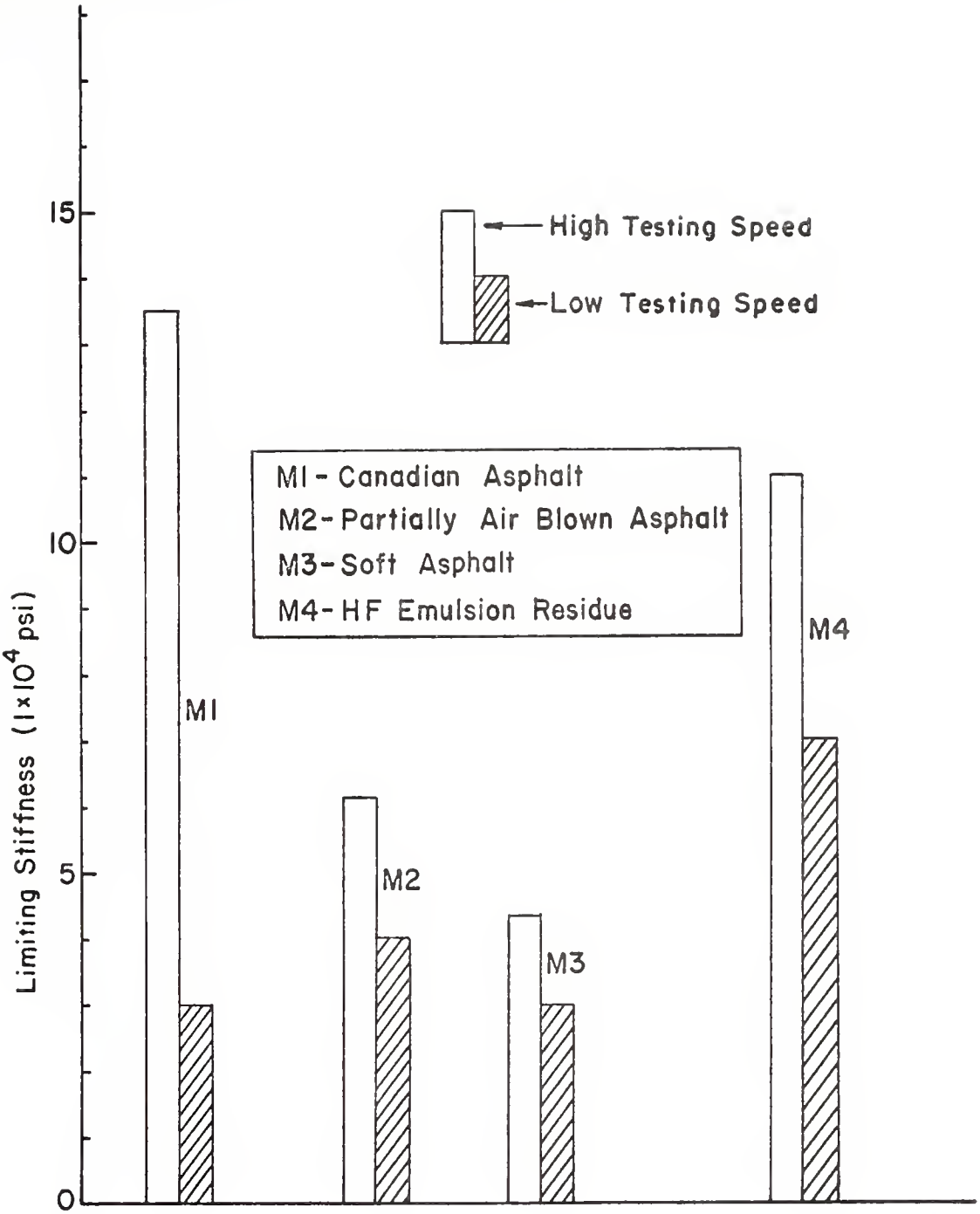

FIGURE 30 COMPARISON OF LIMITING STIFFNESS OF MIXTURES AT 35 °F

Stiffness Comparison

The mixture stiffness value was calculated as follows:

$$S_{mix(t,T)} = \frac{\sigma_{(t,T)}}{\varepsilon_{(t,T)}}$$

where

$S_{mix(t,T)}$ = mixture stiffness as a function of time of loading (t), and temperature (T)

$\sigma_{(t,T)}$ = tensile stress as a function of time of loading (t), and temperature (T)

$\varepsilon_{(t,T)}$ = tensile strain as a function of time of loading (t), and temperature (T)

These values were compared with theoretical stiffness which is calculated as follows:

$$\frac{S_{mix}}{S_{bit}} = \left[1 + \frac{2.5}{\eta} \frac{C_v}{1-C_v} \right]^{\eta}$$

where

S_{bit} = bitumen stiffness which is obtained from McLeod's nomograph and is a function of time of loading, temperature and Pen-Vis number of the bitumen

$$\eta = 0.83 \log_{10} \frac{4x(10)^5}{S_{bit}}$$

C_v = volume concentration of aggregate and is defined as

$$= \frac{\text{Volume of Compacted Aggregate}}{\text{Volume of (Aggregate + Asphalt)}}$$

The equation was originally developed for well-compacted mixtures with about 3% air voids and C_v values between about 0.7 and 0.9. For mixtures with air voids greater than 3%, a "corrected" C_v value, developed by Van Draat and Somer (28) should be substituted. Volume concentration of aggregates for this study is approximately 0.81.

Results of comparison are shown in Table 35. Comparison of theoretical and calculated values are reasonably good considering that bitumen stiffness nomograph to be accurate within a factor of 2.

Acoustic Emission Technique for Crack Detection

The objective of using acoustic emission technique was to detect cracking and thus to better define the failure point in bituminous mixtures. The cumulative count rate curve was used to define more precisely the limiting load and deformation values at which failure occurred. Figure 31 shows total counts and load as a function of time for a test at $-10^{\circ}F$. Cumulative counts (and hence count rate) begin to increase at about 80 percent of ultimate strength and later, at about 95 percent of ultimate strength there is a dramatic increase in cumulative counts and count rate.

In general, at temperatures below normal room temperature, the same trend and the same type of output appeared for almost all test specimens. At temperatures above room temperature, count sensitivity was quickly lost and output was totally due to background noise. When output gain was increased to full

TABLE 35

Comparison of Measured (S_M) and Theoretical (S_T) Mixture Stiffness

Mix	Temp (^oF)	Avg. S_M/S_T
M1	-10	0.81
"	5	1.73
"	20	1.67
"	35	1.85
"	70	1.74
"	105	1.96
"	140	2.28
M2	-10	1.73
"	5	1.79
"	20	1.70
"	35	1.71
"	70	0.65
"	105	0.54
"	140	1.34
M3	-10	1.44
"	5	1.36
"	20	1.60
"	35	1.70
"	70	1.53
"	105	1.45
"	140	1.50
M4	-10	1.51
"	5	1.62
"	20	2.00
"	35	1.90
"	70	1.43
"	105	1.39
"	140	1.76

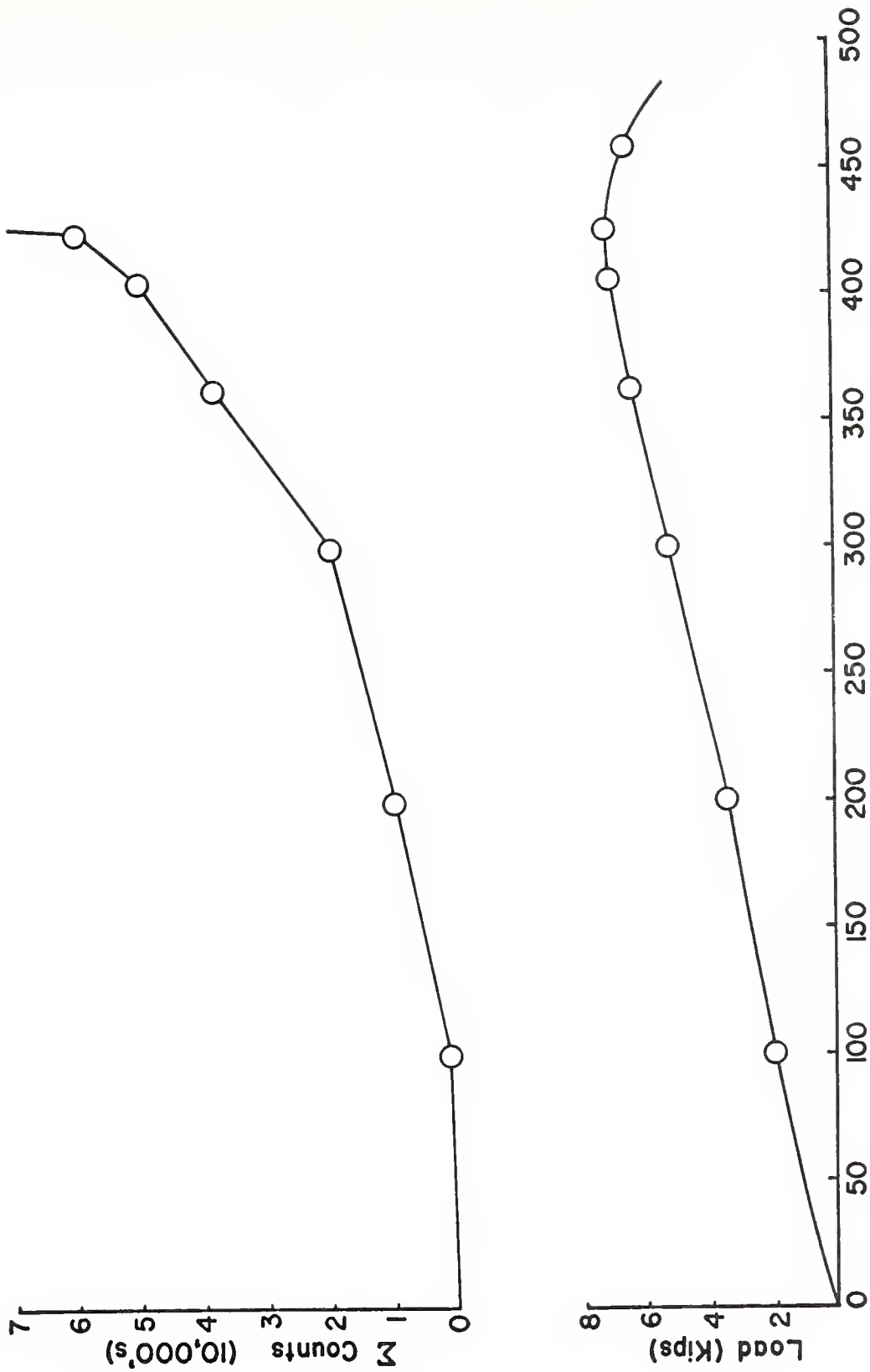

FIGURE 31 TOTAL COUNTS FOR MI AT −10°F

equipment capacity and sensitivity increased to provide fewer counts per unit scale, recorder flutter was so great that output became meaningless. It is possible that either of the following or some combination may be occurring: Fracture may be taking place in the aggregate and perhaps even to some degree in the asphalt binder, but at these elevated temperatures the binder is less brittle than at low temperatures and due to its high damping factor the transmitted wave is of so low a strength that it can not activate the transducer.

Since failure mechanisms are not within the scope of this study, no further experiments were conducted to investigate reasons for loss of signal output at temperatures above normal room temperature.

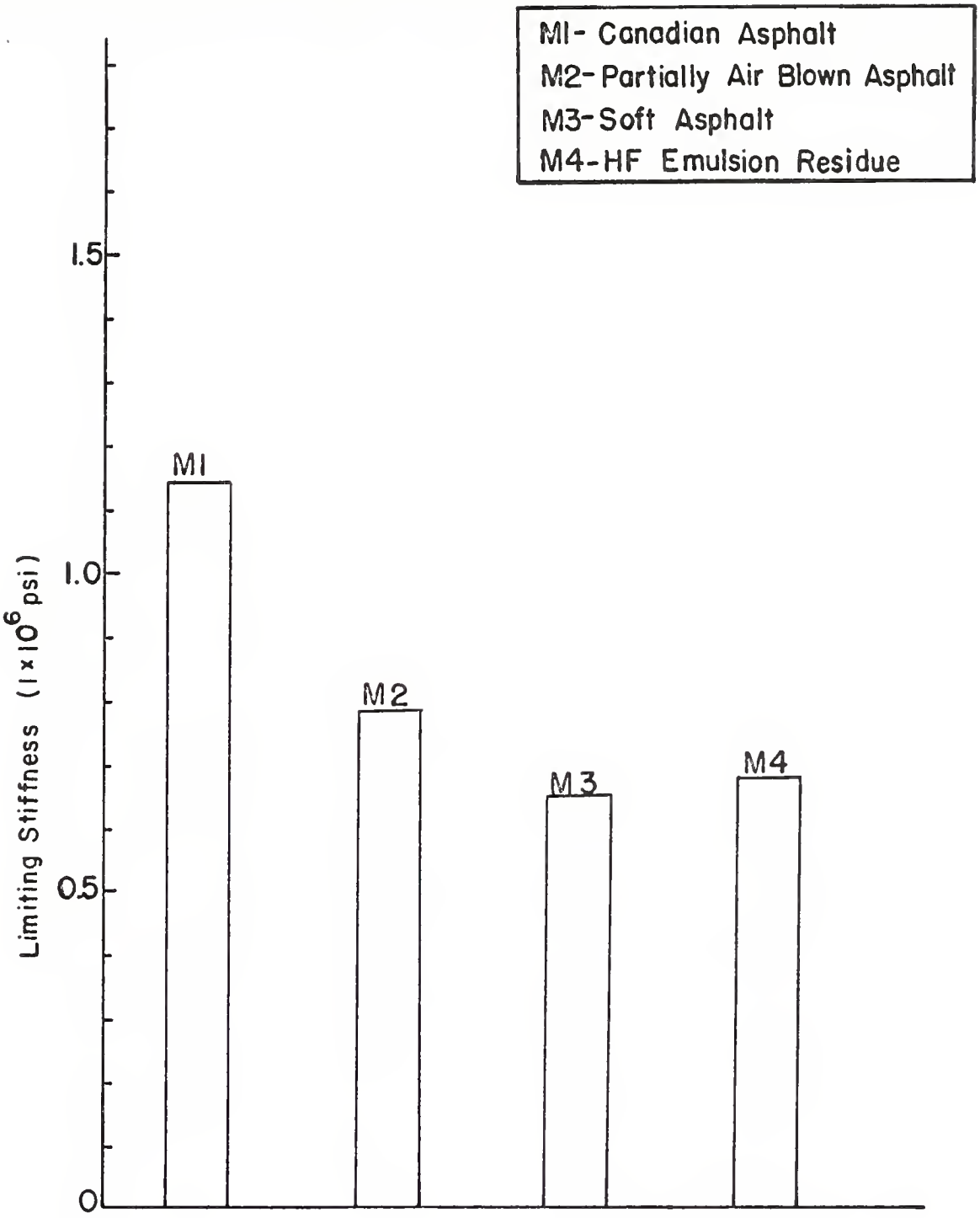

FIGURE 32 COMPARISON OF LIMITING STIFFNESS OF MIXTURES AT -10 °F

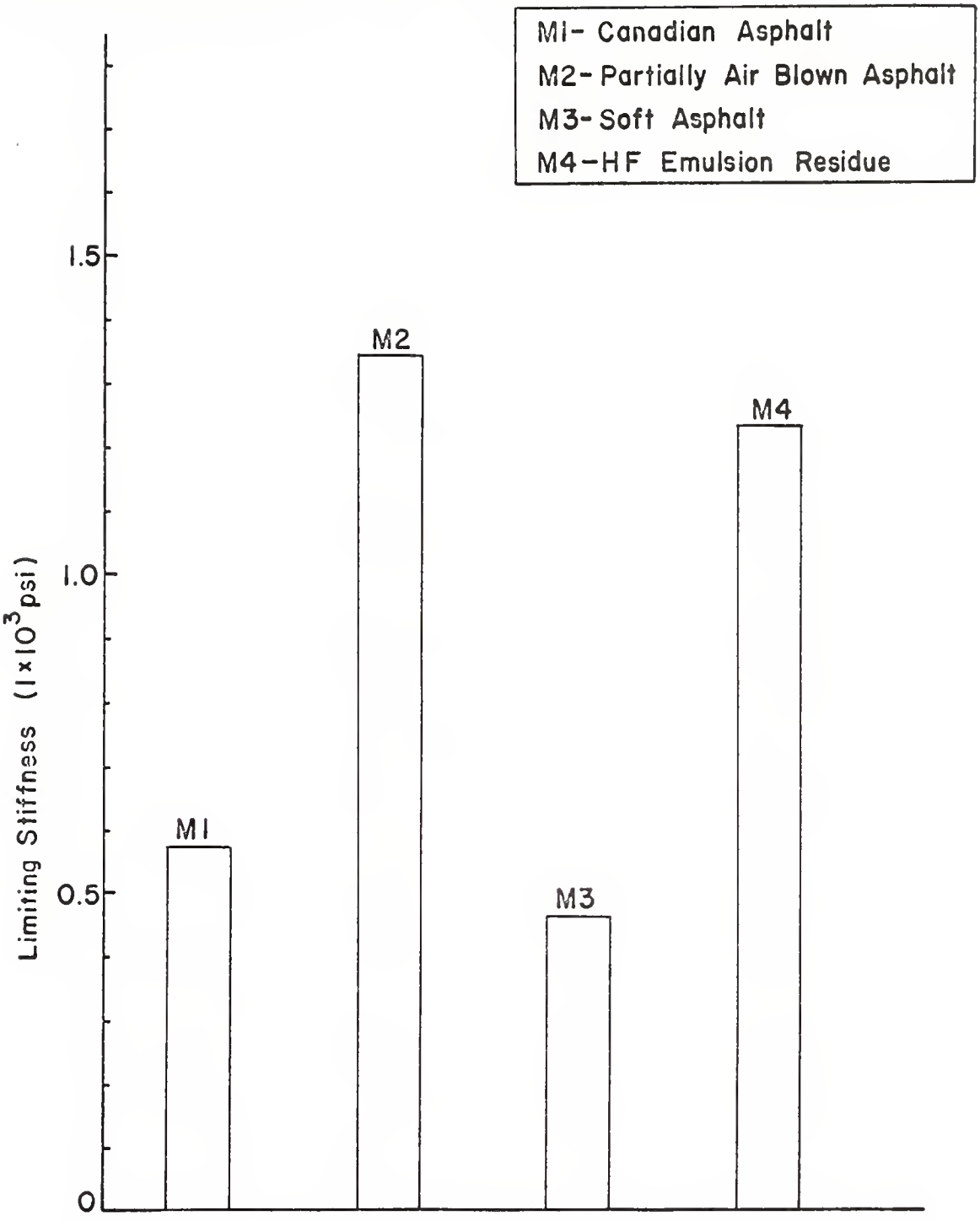

FIGURE 33 COMPARISON OF LIMITING STIFFNESS OF MIXTURES AT 140 °F

SUMMARY OF RESULTS AND CONCLUSIONS

These conclusions are based on the results obtained in this laboratory study and their discussion as presented. It should be noted that they are applicable to the materials and testing procedures of this specific study and may not be extended beyond these limits without appropriate verification.

Limiting strain and limiting stiffness values of bituminous concretes in indirect tension were measured and reported. Regression equations that relate limiting stiffness values to temperature were developed. Parameters in the experiment included a single aggregate of 100 percent crushed limestone at one gradation, four binder types, eight temperatures and variable testing speed. Based on these tests, the following results and conclusions are presented.

Temperature is, by far, the most significant factor of the parameters studied affecting the failure strain and stiffness. A small increase in temperature increases the limiting strain and decreases the limiting stiffness much more than a similar change in any other parameter.

Testing speed, as should be expected for a viscoelastic material, has an effect on a mixture's limiting stiffness. Based on tests at $35^{o}F$, there was no appreciable difference in the limiting strain value of a given mixture with a

change in testing speed, but the limiting stiffness, on the contrary, was affected by a change in testing speed. Since stiffness is a ratio of stress to strain for given conditions of time and temperature, it follows that the tensile characteristic predominantly affected by a change of testing speed is the stress at failure.

This study utilized three binders with nominal penetration grade of 85-100 and a soft binder with nominal penetration grade of 200-250. The three 85-100 penetration grade binders included a highly temperature susceptible asphalt, high float emulsion residue and a partially air blown asphalt. It has been contended for some time that, softer penetration grades of asphalt should be used for pavements in regions that experience lower ambient temperatures, presumably to eliminate or to at least mitigate brittle cracking, and that harder grades should be used in regions of higher ambient temperatures to provide increased stability and less deformation from wheel loads.

Within this context, findings of this study indicate that even though soft asphalt at low temperatures provides for higher limiting strain and lower limiting stiffness values for the mixtures, it results in lower values of limiting stiffness at high temperatures. See Figures 32 and 33. For mixtures made with the three asphalts of the same penetration grade, the use of the most temperature susceptible binder resulted in mixtures with the lowest limiting strain and the highest limiting stiffness at low

temperatures and with the lowest limiting stiffness at high temperatures, but the use of the same binder in emulsified form resulted in a reverse picture of performance. The use of the partially air blown asphalt produced results similar to those of the high float emulsion residue. Also, for long thermal loading times, the mixtures containing emulsion residue and partially air blown asphalt had considerably lower stiffness values than the mixture containing the temperature susceptible Canadian asphalt. Thus it is concluded that emulsification and air blowing can definitely reduce the temperature susceptibility of the binder and provide for mixtures that will perform well at low as well as at high ambient temperatures.

At low temperatures, the differences in strain at failure for the various mixtures were more pronounced than the differences in tensile strength. At high temperatures, however, the reverse was true. Consequently, the parameter of stiffness at failure, combining the responses of tensile strength and failure strain, is considered a better indicator of the behavior of mixtures at both ends of the temperature scale than either tensile strength or limiting strain.

Stiffness values that relate stress to strain for a given binder, temperature, loading time and aggregate volume as determined by McLeod's nomograph were reasonably well verified.

Finally, based on the experiments conducted on bituminous concrete, it is concluded that acoustic emission techniques

are useful in detecting and registering crack initiation in brittle particulate materials and thus aid in better definition of the failure point.

The principal conclusions of this study can be summarized as follows:

1. The tensile characteristics of bituminous mixtures are strongly influenced by the characteristics of the binder.

2. Both the low and high temperature characteristics of a bituminous binder can be modified by the emulsification process as well as by the air blowing process.

3. The tensile behavior of a bituminous mixture is better characterized by the parameter of stiffness than by either of the stress or strain parameters themselves.

4. Temperature is the most significant factor of the parameters studied affecting the tensile characteristics of the bituminous mixtures.

5. The testing speed has a more pronounced effect on values of limiting stress than on values of limiting strain.

6. Acoustic emission techniques are useful in better defining the failure point of bituminous mixtures tested at temperatures below room temperature.

RECOMMENDATIONS FOR FURTHER RESEARCH

In practice there is a strong correlation between mix stiffness and the stiffness of the asphalt the mixture contains and consequently pavement cracking can be related directly to asphalt stiffness at low temperatures. This study indicates that viscosity is an important property of the binder contributing to the stiffness of the mixture. However, since viscosity is shear rate dependent and stiffness of the mixture is time dependent, a quantitative prediction of the stiffness value from a given value of viscosity is difficult. Consequently, the development of asphalt specifications designed to reduce or eliminate low temperature pavement cracking can best be carried out on the basis of low temperature asphalt stiffness. Moreover, the stiffness is expressed in simple engineering units (psi), and can be incorporated directly into many design calculations. The most accurate evaluation of low temperature asphalt stiffness requires that it be measured directly, rather than predicted from other asphalt test data. The shell modified sliding-plate rheometer (56) seems to be a promising instrument to measure asphalt stiffness at the required low temperatures. Thus, it appears that asphalts can be characterized in a more meaningful way by a measure of stiffness than by viscosity.

Other modifications, besides air blowing and emulsifications, may also be studied. The use of sulfur-asphalt emulsion to improve the properties of asphalt and asphaltic mixtures has recently been demonstrated (57). Economic benefit using sulfur-asphalt materials may also be expected because, although the total volume of the material will not be reduced, less asphalt will be required. The addition of carbon-oil pellets called microfillers (58) in the asphalt is believed to decrease its temperature susceptibility and improve its impact strength and the studded wheel abrasion resistance of asphalt pavement mixtures. With regard to modification by the use of filled asphalts, Gussasphalt and Natural asphalt mastic (Trinidad asphalt blended with petroleum asphalt) may be considered. It is believed that mastic concrete has high resistance to tractive forces which may cause tensile cracks in thin layers.

This study was limited to a single gradation of 100 percent crushed limestone of a single source. Other studies should include: coarse and fine gradations to study their role in the tensile characteristics of bituminous mixtures; pit run sand and gravel to find the effect of rounded rather than crushed particles; and other crushed materials that are noncarbonate to determine if mineralogical characteristics have an effect.

The effect of variations in binder content and degree of compaction should be investigated in order to determine as to what tolerances can be accommodated in the field.

The limiting strain as affected by the age hardening of binders should be studied to see if it could be an index of durability.

LIST OF REFERENCES

LIST OF REFERENCES

(1) Shields, B.P. and Anderson, K.O., "Some Aspects of Transverse Cracking in Asphalt Pavements", Proc., CTAA, 1964.

(2) Shields, B.P., Anderson, K.O., and Dacyszyn, J.M., Proc. AAPT, 1966.

(3) Culley, R.W., "Transverse Cracking of Flexible Pavements in Sakatchewan", Sakatchewan Department of Highways, Technical Report 3, 1966.

(4) Lamb, D.R., Pavlovich, R.D., and Scott, W.G., "Roadway Failure Study No. 1, Final Report", Highway Engineering Research Publication H-15, Natural Resources Research Institute, University of Wyoming, 1966.

(5) Breen, J.J., and Stephens, J.E., "Fatigue and Tensile Characteristics of Bituminous Pavements at Low Temperatures", Report No. J.H.K. 66-3, School of Engineering, University of Connecticut, 1966.

(6) Campen, W.H., Prepared Discussion, "Symposium-Non-Traffic Load Associated Cracking of Asphalt Pavements", Proc. AAPT, Vol. 35, 1966.

(7) Symposium on Non-Traffic Load Associated Cracking of Asphalt Pavements, Proc. AAPT, 35, 1966.

(8) Western Summer Meeting, HRB, Denver, Colorado, 1968.

(9) Young, F.D., Deme, I., Burgess, R.A., and Kopnillem, "A Field Study of Transverse Crack Development in Asphalt Pavements", CTAA, 1969.

(10) Haas, R.C.G., "Thermal Shrinkage Cracking of Some Ontario Pavements", Ontario Joint Highway Research Programme, D.H.O. Report No. RR 161, 1970.

(11) Van der Poel, C., "A General System Describing the Visco-Elastic Properties of Bitumens and its Relation to Routine Test Data", Journal of Applied Chemistry, May, 1954.

(12) Van der Poel, C., "Presentation of Rheological Properties of Bitumen Over a Wide Range of Temperatures and Loading

Times", Proc. Second International Conference on Rheology, 1954.

(13) Ashton, J.E. and Moavenzadeh, F., "Analysis of Stresses and Displacements in a Three-Layered Visco-Elastic System", Second International Conference on the Structural Design of Asphalt Pavements, University of Michigan, 1967.

(14) Perloff, W.H., and Moavenzadeh, F., "Deflection of Viscoelastic Medium Due to a Moving Load", Ann Arbor Conference, 1967.

(15) Barksdale, R.D., and Leonards, G.A., "Predicting Performance of Bituminous Surfaced Pavements", Ann Arbor Conference, 1967.

(16) Pavlovich, R.D., "Limiting Strain as a Failure Criterion for Bituminous Mixtures", Ph.D. Thesis, Purdue University, 1975.

(17) Rader, L.F., "Investigation of the Physical Properties of Asphaltic Mixtures at Low Temperatures", Proc. AAPT, 1935.

(18) Brown, J.D., and Steinbaugh, V.B., "A Study of Asphalt Recovery Tests and their Value as a Criterion of Service Behavior", Proc. AAPT, Vol. 9, 1937.

(19) Busby, E.O., and Rader, L.F., "Flexture Stiffness Properties of Asphalt Concrete at Low Temperatures, Proc. AAPT, 1972.

(20) Abson, G., in a Discussion of a Paper by Skidmore, H.W., "Basic Criteria for the Design and Control of Asphalt Paving Mixtures", Proc. AAPT, 1949.

(21) Fromm, H.J., and Phang, W.A., "A Study of Transverse Cracking of Bituminous Pavements", Proc. AAPT, 1972.

(22) McLeod, N.W., "A 4-Year Survey of Low Temperature Transverse Pavement Cracking on Three Ontario Test Roads", Proc. AAPT, 1972.

(23) Hughes, E.C., and Faris, R.B., "Low Temperature Maximum Deformability of Asphalts", Proc. AAPT, 1950.

(24) Vallerga, B.A., "On Asphalt Pavement Performance, Proc. AAPT, 1955.

(25) Haas, R.C.G., and Anderson, K.O., "A Design Subsystem for the Response of Flexible Pavements at Low Temperatures", Proc. AAPT, 1969.

(26) Heukelom, W., and Klomp, J.G., "Road Design and Dynamic Loading", Proc. AAPT, 1964.

(27) Heukelom, W., "Observations on the Rheology and Fracture of Bitumens and Asphalt Mixes", Proc. AAPT, 1965.

(28) Van Draat, W.E.F., and Sommer, P., "An Instrument for Determination of the Dynamic Modulii of Elasticity of Asphalts", Strasse and Autobohn, Vol. 35, 1966.

(29) Lefebvre, J.A., "A Modified P.I. for Canadian Asphalts", Proc. AAPT, 1970.

(30) Clark, M.F., and Culley, R.W., "Evaluation of Air-Blown Asphalts to Reduce Thermal Cracking of Asphalt Pavements", Proc. AAPT, Vol. 45, 1976.

(31) Dunegan, H.L., Harris, D.O., and Tatro, C.A., "Fracture Analysis by Use of Acoustic Emissions", National Symposium on Fracture Mechanics, Lehigh University, 1967.

(32) Green, A.T., "Detection of Incipient Failures in Pressure Vessels by Stress Wave Emissions", Nuclear Safety, Vol. 10, No. 1, 1969.

(33) Dunegan, H.L., and Harris, D.O., "Acoustic Emission - A New Nondestructive Testing Tool", Ultrasonics, Vol. 7, No. 3, 1969.

(34) Dunegan, H.L., Harris, D.O., and Tetelman, A.S., "Detection of Fatigue Crack Growth by Acoustic Emission Techniques", Materials Evaluation, Vol. XXV III, No. 10, 1969.

(35) "Index of Aggregate Producers for Aggregate Source Map", Indiana State Highway Commission, January, 1970.

(36) Ault, C.H., and Carr, D.C., "Directory of Crushed Stone, Ground Limestone, Cement, and Lime Producers in Indiana", Indiana Geological Survey, 1970.

(37) Pfeiffer, J.P., "The Properties of Asphaltic Bitumen", Elsevier Press, Inc., Houston, Texas, 1950.

(38) Rhodes, E.O., Volkman, E.W., and Barker, C.T., Eng. News-Record, 115, 714, 1935.

(39) Schweyer, H.E., Smith, L.L., and Fish, G.W., "A Constant Stress Rheometer for Asphalt Cements", Proc. AAPT, Vol. 45, 1976.

(40) Pendleton, W.W., "The Penetrometer Method for Determining the Flow Properties of High Viscosity Fluids", J. Applied Physics, 14, 170, 1943.

(41) Cox, S.M., "A Method of Viscosity Measurement", J. Sci. Instr., 20, 113 (1943).

(42) "Mix Design Methods for Asphalt Concrete and Other Hot Mix Types", The Asphalt Institute, Manual Series No. 2, Fourth Edition, March, 1974.

(43) Test Method No. Calif. 303-E (October 3, 1966), "Method of Test for Centrifugal Kerosene Equivalent Including K Factor", Materials Manual, Vol. I, State of California, Department of Public Works, Division of Highways.

(44) Warden, W.B., "The Yale Vacuum Pycnometer", International Road Federation, 1973.

(45) "An Introduction to MTS Closed-Loop Testing Systems", Published by Materials Testing Systems Corporation.

(46) Cook, N.H., and Rabinowicz, E., "Physical Measurement and Analysis", Addison-Wesley, 1963.

(47) Herceg, E.E., "Handbook of Measurement and Control", Schaevitz Engineering, Pennsanken, N.J., 1972.

(48) "The Asphalt Handbook", The Asphalt Institute, Manual Series No. 4, 1970.

(49) McRae, J.L., "Gyratory Testing Machine Technical Manual", Engineering Developments Company, Inc., Vicksburg, Mississippi, 1965, Revised, September, 1970.

(50) Kumar, A., and Goetz, W.H., "The Gyratory Testing Machine as a Design Tool and as an Instrument for Bituminous Mixture Evaluation", Proc. AAPT, Vol. 43, 1974.

(51) Tentative Method of Test for Compaction and Shear Strain Properties of Hot Bituminous Mixtures by Means of the U.S. Corps of Engineers Gyratory Testing Machine Using Fixed Roller, ASTM Designation D 3387-74T, 1975 Annual Book of ASTM Standards, Part 15.

(52) Hondros, G., "The Evaluation of Poisson's Ratio and the Modulus of Materials of a Low Tensile Resistance by the Brazilian Test with Particular Reference to Concrete", Australian Journal of Applied Science, Vol. 10, 1959.

(53) Handley, W.O., Hudson, W.R., and Kennedy, T.W., "A Method of Estimating Tensile Properties of Materials Tested in Indirect Tension", Research Report No. 98-1, Center for Highway Research, The University of Texas at Austin, 1970.

(54) Hadley, W.O., Hudson, W.R., and Kennedy, T.W., "Evaluation and Prediction of the Tensile Properties of Asphalt Treated Materials", Research Report No. 98-9, Center for Highway Research, The University of Texas at Austin, 1971.

(55) Anderson, V.L., and McLean, R.A., "Design of Experiments", Marcel-Dekker, Inc., 1974.

(56) Gaw, W.J., "The Measurement and Prediction of Asphalt Stiffnesses at Low and Intermediate Pavement Service Temperatures", Proc. AAPT, 1978.

(57) Shrive, N.G., and Ward, M.A., "Some Low Temperature Aging and Durability Aspects of Sulfur-asphalt Concretes", ASTM Special Technical Publication 628, 1976.

(58) Rostler, F.S., White, R.M., and Dannenberg, E.M., "Carbon Black as a Reinforcing Agent for Asphalt", Proc. AAPT, 1977.

APPENDICES

APPENDIX A

PROCEDURE FOR CONVERTING PENETRATION TO VISCOSITY

PROCEDURE FOR CONVERTING PENETRATION TO VISCOSITY

The four basic equations (40) used to arrive at the rate of shear, shearing stress and viscosity are the following:

$$P = K_2 t^{1/n+1} \tag{1}$$

$$\tau = \frac{M}{P-K'} \times 3.12 \times 10^5 \text{ dynes/cm}^2 \tag{2}$$

$$\dot{\gamma} = \frac{(n-1)P}{5(n+1)t} \left[\frac{1}{1-(a/b)^{n-1}}\right] \text{sec}^{-1} \tag{3}$$

and

$$\eta = \frac{Mt(n+1)}{P(P-K')(n-1)} \left[1-(a/b)^{n-1}\right] 1.56\times10^6 \text{ poises} \tag{4}$$

where

K_2 = a constant

P = depth of penetration in decimillimeters

t = time of penetration in seconds

n = the exponent of the power function for the general speed law

τ = shearing stress in dynes/cm^2

M = mass of the needle and spindle assembly in grams

K' = length correction which is P(0.849-0.00788P) - 0.0562 dmm for penetrations less than 54 dmm and is 23 dmm for penetrations greater than 54 dmm

$\dot{\gamma}$ = rate of shear sec^{-1}

a = radius of needle (0.05 cm for A.S.T.M. needle)

b = inner radius of cup (2.75 cm for A.S.T.M. cup)

and η = viscosity in poises

Procedure

1. The test sample, in the conventional tin, was conditioned to the desired test temperature.

2. The penetrations of the needle were noted for three successive time intervals.

3. The value of exponent 'n' was calculated from equation (1).

4. Knowing all other quantities in equations (2), (3) and (4), the values of shearing stress, rate of shear and the corresponding viscosity were calculated.

5. Values of viscosity and corresponding rate of shear were plotted as shown in Figures 6 and 7.

Sample of Calculations

A. Data:

M = 200 grams Test temperature = 39.2^{o}F

P_1 = 14 dmm; t_1 = 5 sec.; K'_1 = 10.28 dmm

P_2 = 24 dmm; t_2 = 30 sec.; K'_2 = 15.78 dmm

P_3 = 29 dmm; t_3 = 60 sec.; K'_3 = 17.93 dmm

B. Calculations:

Solving equation (1) for values of P_1, t_1 and P_3, t_3 we get

n = 2.484

and solving equations (2), (3) and (4) for the other given data, we get

$$\tau_1 = \frac{200}{14-10.28} \times 3.12 \times 10^5 = 1.679 \times 10^7 \text{ dynes/cm}^2$$

$$\tau_2 = \frac{200}{24-15.78} \times 3.12 \times 10^5 = 75.92 \times 10^5 \text{ dynes/cm}^2$$

$$\tau_3 = \frac{200}{29-17.93} \times 3.12 \times 10^5 = 5.64 \times 10^6 \text{ dynes/cm}^2$$

$$\dot{\gamma}_1 = \frac{(2.484-1)14}{5(3.484)5} \left[\frac{1}{1-\left(\frac{.05}{2.75}\right)^{1.484}}\right] = 0.239 \text{ sec}^{-1}$$

$$\dot{\gamma}_2 = \frac{(2.484-1)24}{5(3.484)30} \left[\frac{1}{1-\left(\frac{.05}{2.75}\right)^{1.484}}\right] = 0.068 \text{ sec}^{-1}$$

$$\dot{\gamma}_3 = \frac{(2.484-1)29}{5(3.484)60} \left[\frac{1}{1-\left(\frac{.05}{2.75}\right)^{1.484}}\right] = 0.041 \text{ sec}^{-1}$$

Thus,

$$\eta_1 = 7.02 \times 10^7 \text{ poises}$$

$$\eta_2 = 1.11 \times 10^8 \text{ poises}$$

and $\eta_3 = 1.37 \times 10^8$ poises

APPENDIX B

BALL PENETRATION TEST FOR VISCOSITY MEASUREMENT

BALL PENETRATION TEST FOR VISCOSITY MEASUREMENT

The method consists of measuring the viscosity with the aid of spherical imprint of a ball under a dead load. The formula giving the viscosity is as follows:

$$\eta = \frac{9PRT}{16a^3} \qquad (1)$$

where

η = viscosity in lb. sec/in^2

P = compressive load

R = radius of the sphere

T = time in seconds

a = radius of imprint

The device illustrated in Figures B1 and B2 was designed to measure the surface penetration of a smooth rigid steel sphere (1/4 inch in diameter) resting on a sample of the viscoelastic material. The advantages of such a device are: simplicity, low cost of manufacture, versatility for viscosity measurement at low temperatures, and portability of the device.

Experimental Procedure

1. The test sample, in the conventional penetration tin, was conditioned to the desired test temperature.

2. A smooth ball of 1/4 inch diameter was also conditioned to the test temperature. The device was placed

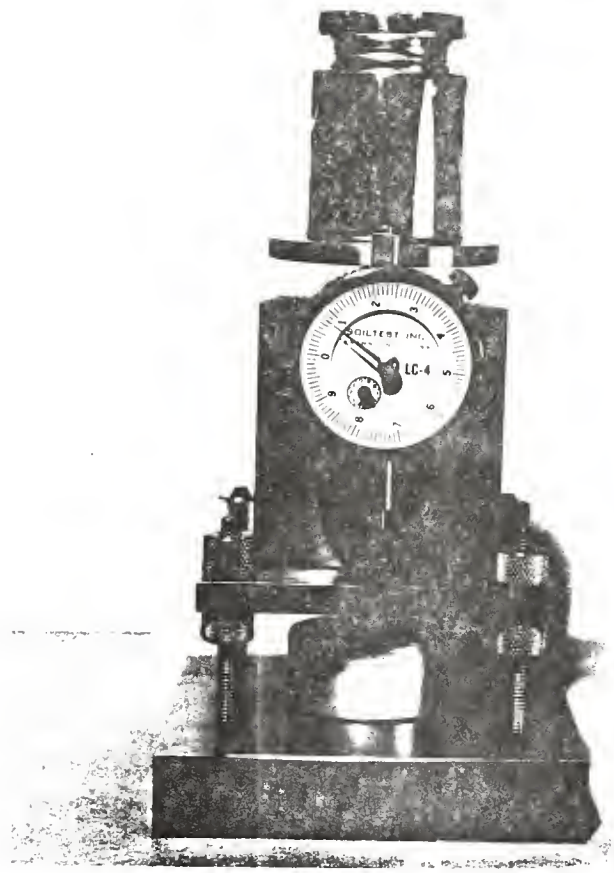

FIGURE B1 A VIEW OF BALL PENETRATION TEST

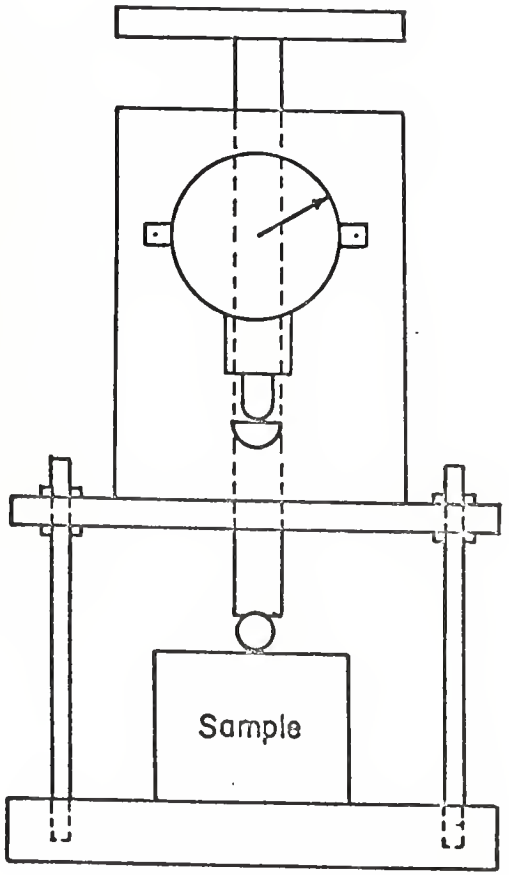

Front View

Not Drawn To Scale

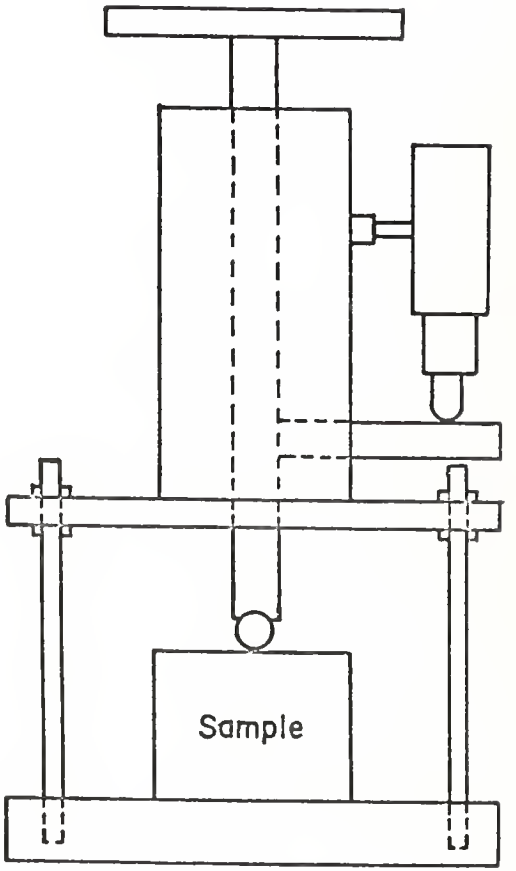

Side View

FIGURE B2 DETAILS OF BALL PENETRATION DEVICE

in the testing chamber and the ball was then made to rest on the surface of the material.

3. A dead weight of 2 Kg. was selected for the test. This weight was chosen by applying various weights on the device, observing the rate of penetration of the sphere, and selecting a rate that would allow transient measurements with as little error as possible.

4. The load was applied and the penetration of the ball was recorded after an interval of 15 minutes. This time interval was chosen so as to allow sufficient penetration of the ball.

5. Knowing the ball penetration, the viscosity of the material can be calculated by using the equation 1.

Sample of Calculations

A. Data:

Test temperature = $-10^{\circ}F$

Size of sphere = 1/4 inch in diameter

Load = 2 Kg. = 4.4 lbs.

Sample = Soft asphalt with penetration of 231 at $77^{\circ}F$

Time of test = 900 seconds

Penetration = 538.5×10^{-4} inch

B. Calculations:

For a spherical segment

$$2\pi Rb = 1/4\pi(4b^2 + c^2)$$

or $$8\,Rb = 4\,b^2 + c^2$$

$$8(0.125)\ (538.5\times10^{-4}) = 4(.05385)^2 + c^2$$

or $$c = 0.2055$$

or $$\frac{c}{2} = a = 0.1028$$

Hence,

$$\eta = \frac{9(4.4)(0.125)(900)}{16(0.1028)^3} = 2.56\times10^5 \ \frac{lb.sec}{in^2}$$

or $$2.56\times10^5(6.895\times10^4) = 1.76\times10^{10} \text{ poises}$$

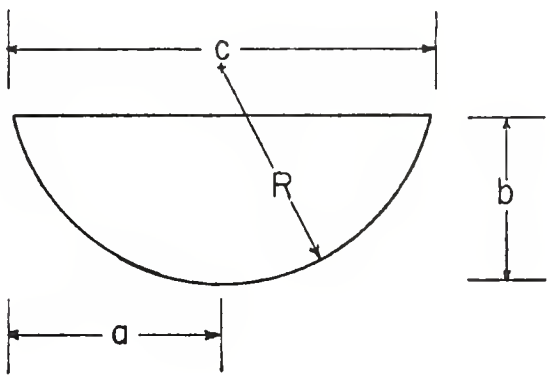

APPENDIX C

INDIRECT TENSION TEST DATA

TABLE C1

Specimen Test Data

Temperature -10°F
Rate of Loading 50 MI per second

Mixture	Limiting Stress (PSI)	Limiting Strain (MII)	Limiting Stiffness (PSI)	Time (Seconds)
M1	442	398	1.11E06	400
M1	431	434	0.99E06	425
M1	430	325	1.32E06	390
M2	419	507	0.83E06	430
M2	445	543	0.82E06	430
M2	454	652	0.70E06	400
M3	425	760	0.56E06	450
M3	445	688	0.65E06	430
M3	455	616	0.74E06	420
M4	361	543	0.66E06	390
M4	354	470	0.75E06	350
M4	366	579	0.63E06	380

TABLE C2

Specimen Test Data

Temperature 5°F
Rate of Loading 50 MI per second

Mixture	Limiting Stress (PSI)	Limiting Strain (MII)	Limiting Stiffness (PSI)	Time (Seconds)
M1	430	516	0.83E06	450
M1	425	549	0.77E06	470
M1	452	613	0.74E06	490
M2	354	1453	0.24E06	525
M2	340	1292	0.26E06	505
M2	346	1389	0.25E06	505
M3	402	1130	0.36E06	475
M3	403	969	0.42E06	490
M3	374	1066	0.35E06	490
M4	378	840	0.45E06	475
M4	340	775	0.44E06	470
M4	351	678	0.52E06	490

TABLE C3

Specimen Test Data

Temperature 20°F
Rate of Loading 50 MI per second

Mixture	Limiting Stress (PSI)	Limiting Strain (MII	Limiting Stiffness (PSI)	Time (Seconds)
M1	341	1485	0.23E06	610
M1	348	1337	0.26E06	625
M1	365	1426	0.26E06	600
M2	219	2377	0.09E06	610
M2	212	2288	0.09E06	615
M2	231	2496	0.09E06	590
M3	259	3090	0.08E06	630
M3	243	3268	0.07E06	650
M3	244	3179	0.08E06	660
M4	275	1782	0.15E06	580
M4	258	1664	0.16E06	605
M4	281	1812	0.16E06	595

TABLE C4

Specimen Test Data

Temperature 35°F
Rate of Loading 50 MI per second

Mixture	Limiting Stress (PSI)	Limiting Strain (MII)	Limiting Stiffness (PSI)	Time (Seconds)
M1	232	3103	0.07E06	680
M1	207	2935	0.07E06	670
M1	201	2879	0.07E06	690
M2	165	4081	0.04E06	710
M2	140	3914	0.04E06	720
M2	146	3886	0.04E06	735
M3	195	5284	0.04E06	740
M3	159	5032	0.03E06	700
M3	165	5116	0.03E06	710
M4	229	3131	0.07E06	665
M4	186	2935	0.06E06	700
M4	207	3019	0.07E06	685

TABLE C5

Specimen Test Data

Temperature 35°F
Rate of Loading 1000 MI per second

Mixture	Limiting Stress (PSI)	Limiting Strain (MII)	Limiting Stiffness (PSI)	Time (Seconds)
M1	391	2600	150E03	47
M1	385	2935	131E03	50
M1	379	3075	123E03	50
M2	239	3914	61E03	55
M2	251	3774	66E03	50
M2	232	4053	57E03	47
M3	229	5256	43E03	55
M3	225	5451	41E03	49
M3	244	5312	45E03	52
M4	342	3131	109E03	45
M4	351	3075	114E03	44
M4	317	2935	108E03	45

TABLE C6

Specimen Test Data

Temperature 70°F
Rate of Loading 1000 MI per second

Mixture	Limiting Stress (PSI)	Limiting Strain (MII)	Limiting Stiffness (PSI)	Time (Seconds)
M1	51	6297	8E03	25
M1	50	6072	8E03	18
M1	57	6185	9E03	21
M2	55	5735	9E03	24
M2	61	5960	10E03	21
M2	53	5847	9E03	29
M3	28	6635	4E03	19
M3	34	6747	5E03	22
M3	33	7084	4E03	27
M4	84	6117	14E03	28
M4	81	6185	13E03	30
M4	75	6320	12E03	30

TABLE C7

Specimen Test Data

Temperature 105°F
Rate of Loading 1000 MI per second

Mixture	Limiting Stress (PSI)	Limiting Strain (MII)	Limiting Stiffness (PSI)	Time (Seconds)
M1	16	7689	2E03	15
M1	14	7523	1.8E03	11
M1	12	7274	1.6E03	12
M2	24	7378	3.2E03	9
M2	22	6858	3.2E03	11
M2	23	7211	3.2E03	13
M3	13	8458	1.5E03	11
M3	12	8313	1.4E03	8
M3	11	8105	1.3E03	14
M4	22	7648	2.9E03	10
M4	20	7461	2.7E03	11
M4	20	7232	2.8E03	14

TABLE C8

Specimen Test Data

Temperature 140^{o}F
Rate of Loading 1000 MI per second

Mixture	Limiting Stress (PSI)	Limiting Strain (MII)	Limiting Stiffness (PSI)	Time (Seconds)
M1	5	8216	0.61E03	7
M1	4	8424	0.47E03	6
M1	5.5	8632	0.64E03	8
M2	11	7924	1.39E03	5
M2	11	8216	1.34E03	7
M2	10	7800	1.28E03	9
M3	3	8548	0.35E03	4
M3	4	8715	0.46E03	6
M3	5	8944	0.56E03	8
M4	10	8008	1.25E03	5
M4	9	7716	1.17E03	7
M4	10.5	8257	1.27E03	5

COVER DESIGN BY ALDO GIORGINI